UNIVERSITÀ DEGLI STUDI DI TRIESTE

XXIV CICLO DEL DOTTORATO DI RICERCA IN

SCIENZE E TECNOLOGIE CHIMICHE E FARMACEUTICHE

CHARACTERIZATION OF THE RISK OF PALYTOXIN AND ANALOGUES AS SEAFOOD CONTAMINANTS

Settore scientifico-disciplinare: BIO/15

DOTTORANDA: Giorgia Del Favero

DIRETTORE DELLA SCUOLA: Prof. Enzo Alessio

RELATORE: Prof. ssa Aurelia Tubaro

CORRELATORE: Prof. ssa Paola Lorenzon

ANNO ACCADEMICO 2010/2011

UNIVERSITÀ DEGLI STUDI DI TRIESTE

XXIV CICLO DEL DOTTORATO DI RICERCA IN

SCIENZE E TECNOLOGIE CHIMICHE E FARMACEUTICHE

CHARACTERIZATION OF THE RISK OF PALYTOXIN AND ANALOGUES AS SEAFOOD CONTAMINANTS

Settore scientifico-disciplinare: BIO/15

DOTTORANDA: Giorgia Del Favero

DIRETTORE DELLA SCUOLA: Prof. Enzo Alessio

RELATORE: Prof. ssa Aurelia Tubaro

CORRELATORE: Prof. ssa Paola Lorenzon

ANNO ACCADEMICO 2010/2011

INDEX

ABSTRACT

RIASSUNTO

Characterization of the risk of Palytoxin and analogues as seafood contaminants

The present thesis was developed for the characterization of the risk associated to palytoxins as seafood contaminants. To this aim, an integrated approach between *in vitro* and *in vivo* studies was chosen. Palytoxin and its analogues are known seafood contaminants that can accumulate in several edible species of shellfish, fish, crustaceans and echinoderms. Generally, primary symptoms associated to the ingestion of contaminated food involve the gastro-intestinal apparatus and later develop with the involvement of the muscular tissue. For a better comprehension of the mechanism of action of this family of biotoxins, the effects of PLTX have been studied on primary culture of mouse skeletal muscle cells. The myotoxic insult triggered by PLTX was described in detail with the definition of the cytotoxicity together with the description of the morphologic alterations and functional impairment caused by the toxin. Moreover, the influence of the ionic composition of the extracellular medium on the effects of the toxin was elucidated. Primary cultures of skeletal muscle cells, that presents *in vitro* many of the peculiarities of the adult muscle fiber, allowed the investigation of the membrane mechanisms that regulate the intracellular calcium increase triggered by the toxin. It was possible to discriminate the difference between calcium release from intracellular stores and the calcium entrance from extracellular compartment both elicited by the toxin, and to understand the importance of the latter in relation to the toxic event. Moreover, the involvement of the main

membrane channels and transporters that may be related to the entrance of calcium was investigated and the crucial role of stretch-activated channels in the mechanism of toxicity was demonstrated. Once defined the crucial molecular mechanisms of action of PLTX, experiments were also performed with two of its analogue: the 42-hydroxyl-palytoxin and the ostreocin-D.

In parallel to *in vitro* studies, the effects of repeated oral administration of PLTX in mice were also investigated. In fact, *in vitro* studies are not sufficient for the complete comprehension of the real hazard associated to a food contaminant, since molecules once in contact with the body may undergo adsorption, distribution and metabolism before reaching the target tissue. Short-term (7 days) administration of the toxin revealed toxicity at all the doses tested and lethality was recorded in the treated animals already from the dose of 30 μg/kg. Histological analysis highlighted alterations in several tissues: severe inflammatory processes and even foci of necrosis were observed in lungs. Alteration of the muscular tissues was visible as fiber separation and degeneration in the heart and increased cellularity between fibers in skeletal muscle. Moreover, depletion of glycogen content of hepatocytes and moderate alterations of the spleen were also observed. Data collected in the present project revealed, for the first time, toxicity of PLTX at doses much lower than that currently used by European Food Safety Authority (EFSA) for the estimation of limit values for presence of these compounds in seafood. For this reason, these results are likely to have a considerable impact at regulatory level and to have crucial importance for the protection of the consumers.

Caratterizzazione del rischio da palitossina e composti analoghi quali contaminati dei prodotti ittici destinati ad uso alimentare

Il presente lavoro di tesi è stato sviluppato con lo scopo di caratterizzare il rischio associato alla presenza delle palitossine quali contaminanti dei prodotti ittici destinati ad uso alimentare. A tal fine, è stato scelto un approccio integrato tra studi in vitro *e* in vivo. *La palitossina e i suoi analoghi sono noti contaminanti dei prodotti ittici e possono accumularsi in diverse specie edibili di molluschi, pesci, crostacei ed echinodermi. Generalmente, i primi sintomi associati all'ingestione di cibo contaminato coinvolgono l'apparato gastro-intestinale e poi si sviluppano con l'interessamento del tessuto muscolare. Per una migliore comprensione del meccanismo d'azione di questa famiglia di biotossine, gli effetti della PLTX sono stati studiati mediante colture primarie murine di cellule muscolari scheletriche. L'insulto miotossico indotto dalla PLTX è stato descritto nel dettaglio con la definizione della citotossicità assieme alla descrizione delle modifiche morfologiche e delle alterazioni funzionali causate dalla tossina. Inoltre, è stata caratterizzata l'influenza della composizione ionica dell'ambiente extracellulare negli effetti della tossina. Le colture primarie di cellule muscolari scheletriche, che presentano molte delle caratteristiche peculiari della fibra muscolare adulta, hanno permesso l'indagine dei meccanismi che regolano l'aumento intracellulare di calcio indotto dalla tossina. E' stato possibile discriminare la differenza tra il rilascio di calcio dai depositi intracellulari e l'entrata di calcio dai compartimenti extracellulari, entrambi effetti indotti dalla tossina, e comprendere l'importanza del secondo meccanismo in*

relazione agli eventi tossici. E' stato indagato il coinvolgimento dei canali e trasportatori di membrana in relazione all'ingresso di calcio ed è stato dimostrato il ruolo cruciale dei canali attivati da stiramento nel meccanismo di tossicità. Una volta definiti i meccanismi d'azione cruciali per la PLTX, esperimenti sono stati condotti anche con due dei suoi analoghi, la 42-idrossi-palitossina e l'ostreocina-D.

Parallelamente agli studi in vitro, *sono stati studiati gli effetti della somministrazione orale ripetuta della PLTX nel topo. Infatti, gli studi* in vitro *non sono sufficienti alla comprensione del reale pericolo associato ad un contaminate alimentare, dal momento che, le molecole, una volta a contatto con l'organismo, possono subire assorbimento, distribuzione e metabolismo prima di raggiungere il tessuto bersaglio. La somministrazione a breve termine della tossina (7 giorni) ha rivelato tossicità a tutte le dosi somministrate, e letalità è stata registrata negli animali trattati già alla dose di 30 µg/kg. Le analisi istologiche hanno evidenziato alterazioni a carico di diversi tessuti: a livello polmonare sono stati osservati severi processi infiammatori associati anche a focolai di necrosi. Le alterazioni del tessuto muscolare erano visibili come degenerazione e separazione delle fibre nel cuore e aumento degli elementi cellulari tra le fibre del muscolo scheletrico. Inoltre sono stai osservati, deplezione del contenuto di glicogeno negli epatociti e moderate alterazioni della milza. I dati raccolti nel presente elaborato hanno rivelato, per la prima volta, la tossicità della palitossina a dosi molto inferiori rispetto a quelle correntemente utilizzate della European Food Safety Authority (EFSA) per la stima di valori limite per la presenza di questi composti nei prodotti ittici destinati ad uso alimentare. Per questo motivo, i*

risultati avranno probabilmente un considerevole impatto a livello legislativo e un'importanza cruciale per la protezione dei consumatori.

1. INTRODUCTION

Risk characterization is a complex procedure that is aimed at the evaluation of the balance between the intrinsic hazard represented by the molecule, in our study palytoxin, and the likelihood of exposure, thus the probability of a person to come into contact with it. The evaluation of the data present in literature will develop in three major area: hazard identification, exposure assessment and toxicity assessment.

1.1. Hazard identification

Hazard identification is the first step of risk characterization and risk assessment; this procedure is aimed at description of the target molecule, giving all information necessary for the comprehension of the chemical properties, mechanism of action and ultimately to toxicity.

1.1.1. Chemical structure and properties

The molecule that gave origin to the group of biotoxins, nowadays called “palytoxins”, was discovered in 1971 from the research group of Prof. Moore, in Hawaii (Moore and Scheuer, 1971). Palytoxin was isolated from soft-corals of the genus *Palythoa* and, from the chemical point of view, as well as from biological properties, differed from any other biotoxin discovered up to that moment. Initially, molecular weight was estimated to be 3300 Dalton, but at the beginning of the ’80 it was finally determined, for PLTX and analogues in a range between 2659 and 2680 Da, depending on the source of toxin extraction (Moore and Bartolini, 1981; Riobò and Franco, 2011). The elucidation of the

planar structure of the molecule (Figure 1) was achieved only ten years after its discovery, in 1981. The challenge was carried out independently by two research groups, nearly simultaneously, at the Nagoya University in Japan (Uemura et al., 1981), and in United States (Moore and Bartolini, 1981). Later in the decade, chemical studies on palytoxin went on, leading initially to the definition of the stereochemistry of the 64 chiral centers (Fujioka et al., 1982; Cha et al., 1982; Shimizu, 1983) and, later, to its complete synthesis (Kishi, 1989).

Ultra Violet spectrum of PLTX shows bands at 233 nm and 263 nm, corresponding to the two chromophores of the toxin; in particular the first signal refers to the conjugated double bonds and the other describes the group 3-amido-N-(3-hydroxypropil)-acrylamidic. The importance of the latter for the toxicity of the molecule was identified already during the first characterization of PLTX published in 1971. In fact, Moore and Scheuer (1971) demonstrated that to a loss of the amidic group corresponded a reduction of biological properties of the molecule.

In accordance with its structure, rich in hydroxyl groups, PLTX is soluble in polar solvents such as ethanol, methanol, water and pyridine (Moore and Scheuer, 1971). In aqueous solution PLTX was found to exist as a dimer with two molecules overlapping each other to give a figure "∞" shape. For the formation of the dimer, the presence of a free amino group is crucial and any modification in this respect alters toxin behavior (Inuzuka et al., 2007). For instance, the acetylation of the amino group stabilizes the formation of a monomer in aqueous solution, with a peculiar "∩" shape (Uemura, 2006; Inuzuka et al., 2007). Moreover, the functionalization of the amino group not only

makes impossible the formation of the dimer, but seems to reduce toxicity of the molecule as well (Hirata et al., 1979; Ohizumi and Shibata, 1980; Kudo and Shibata 1980). Thus, the free amino group, that accounts for one of the three nitrogen ions present in the molecule, seems to be of crucial importance, not only for the physical-chemical behavior of the toxin, but also for its biological activity.

The apparent degradation of the toxin in alkaline or acidic environment described by Wiles et al. (1974) has been an insidious matter of discussion, especially during the performance of oral toxicity studies. Loss of activity after intra-peritoneal (i.p.) administration of toxin pre-incubated with acids or bases, as described in 1974, should assure a similar loss of function also after administration of the molecule in the gastro-intestinal tract. In spite of that, this loss or reduction of potency was not clearly visible in the studies conducted so far (Sosa et al., 2009).

Palytoxin, in addition to the peculiar behavior in aqueous solution, is also known for its specific affinity for the plastic surfaces. In particular, it was already observed, at the beginning of the ’90s, that biological effects i.e. alteration of blood pressure induced by the toxin, were highly variable after the passage through a polyethylene plastic tubes (Taylor et al., 1991).

1.1.2. Palytoxin and analogues

The discovery of palytoxin was followed by the chemical characterization of other molecules similar in structure, that, on the whole, finally constituted the so-called “palytoxin group”. The

discovery of palytoxin analogues began from the analysis of different species of soft corals of the genus of *Palythoa*. Minor constituents of Okinawan *Palythoa tubercolosa* revealed to be slightly different from the parent PLTX and were named homopalytoxin, bishomopalytoxin, neopalytoxin and deoxypalytoxin (Uemura et al., 1985). Many years later, in 2009, another molecule was chemically characterized from samples of *Palythoa toxica* and was named 42-hydroxyl-palytoxin (42-OH-PLTX) for the presence of an additional hydroxyl group in position 42 of the aliphatic backbone (Ciminiello et al., 2009).

Palytoxin analogues, discovered in samples of corals, were soon followed by other molecules, isolated from microalgae of the genus *Ostreopsis*. In this respect, the first molecule identified was Ostreocin-D (OST-D) from the unicellular benthonic microalgae of *Ostreopsis siamensis* (Usami et al., 1995; Ukena et al., 2001). This result, not only widened the number of molecules belonging to the "family" of palytoxins, but also led to the comprehension that these molecules are part of the so-called "algal toxins". From the discovery of OST-D, the analysis of different species of *Ostreopsis* revealed many other PLTX-analogues, distributed all over the world. Mascarenotoxin-A, B and C (Lenoir et al., 2004; Rossi et al., 2010) were isolated from *O. mascarenensis* collected in the Indian Ocean and *Ostreopsis* cf. *ovata* of the Mediterranean Sea. Along the Italian coast the first palytoxin-like compound isolated was Ovatoxin-A. Ovatoxin-A resulted to be very similar to parent palytoxin, with similar fragmentation pattern and chromatographic behavior, but slightly different, for the absence 3 of hydroxyl groups in position 17, 44, 64 and the presence of the –OH group in position 42 of the aliphatic backbone (Ciminiello et al., 2008;

Ciminiello et al., 2012a). This compound resulted to be the major product of *Ostreopsis ovata* collected along the Ligurian coasts during the toxic outbreak of 2005-6 (Durando et al., 2007) and also the major toxin constituent detected in *Ostreopsis* cf. *ovata* that we collected in autumn 2009 in the Gulf of Trieste (Honsell et al., 2011).

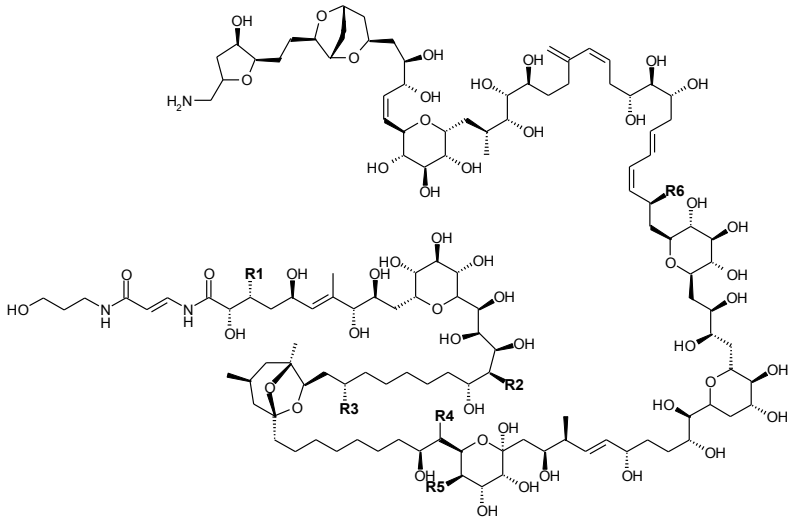

	R1	R2	R3	R4	R5	R6
Palytoxin	CH_3	OH	CH_3	H	OH	OH
42-hydroxypalytoxin	CH_3	OH	CH_3	OH	OH	OH
Ostreocin-D	H	H	H	OH	H	OH

Figure 1. PLTX and analogues, the chart summarizes the structural differences between commercial PLTX, 42-OH-PLTX and OST-D.

Progress of analytical techniques, driven by the growing interest of the scientific community around palytoxin and its analogues, allowed the identification of the complex toxins profile present in Mediterranean *Ostreopsis ovata*, with the identification of Ovatoxin-B, C, D, E

(Ciminiello et al., 2010; Rossi et al., 2010), and Palytoxin-B (Rossi et al., 2010) and, will likely be the driving force for the discovery of new molecules.

1.1.3. Producing organisms

Palytoxin was originally isolated from zoanthid of the genus *Palythoa* (Moore and Scheuer, 1971). After the discovery of the molecule, Palytoxin and analogues were isolated in a wide number of species of soft corals, such as *Palythoa toxica* (Moore and Scheuer, 1971; Ciminiello et al., 2009), *P. tuberculosa* (Kimura and Hashimoto 1973; Ishida et al., 1983) and *P.*aff. *margaritae* (Oku et al., 2004). Analysis of the coral reefs of the Caribbean Sea revealed presence of PLTX-like substances also in samples of *Palythoa caribaeorum* (Attaway and Ciereszko, 1974; Béress et al., 1983) and *P. mammillosa* (Attaway and Ciereszko, 1974). The toxin was found also in *Palythoa caribaeorum*, *P. mammillosa* from Colombian coasts, and in other zoanthid species, such as *Zoanthus solanderi and Z. sociatus*, competitors of *Palythoa* species for space in the reef (Gleibs et al., 1995). To strength the idea that other component of the coral reefs may contain PLTX-like substances, a compound closely related to reference PLTX has been isolated also in sea anemones (phylum *Coelenterata*), such as the *Radianthus macrodactylus* (Mahnir et al., 1992). Recently, zoanthids *Anthozoa* and *Hexacorallia*, normally sold in aquarium hobbyist shops in United States, were found to contain considerable amounts of palytoxin (ranging from 0.5-3.5 mg of crude toxin/g zoanthid). In more detail, parent PLTX together with its analogues 42-OH-PLTX and

deoxy-palytoxin has been recently isolated in species of *P. heliodiscus* and *P. mutuki* (Figure 2; Deeds et al., 2011).

Figure 2. Zoanthid colony, collected from a home aquarium in 2008, responsible for a severe respiratory reaction. Sample was found to contain approx. 600 mg palytoxin/g wet zoanthid. Bar represents 1 cm (doi:10.1371/journal.pone.0018235.g001 Deeds et al., 2011, modified).

In 1995, the group of Professor Yasumoto isolated and characterized PLTX-like compounds from the benthic dinoflagellate of the genus *Ostreopsis, O. siamensis* (Usami et al., 1995). From that moment, there has been a wide consensus in the scientific community in considering the unicellular microalgae as the producer of the toxin, even though the pathways of biosynthesis of the toxin are still unclear and represent a field of open and ongoing research. Beside *O. siamensis*, PLTX and analogues have been isolated from different species of *Ostreopsis*, such as *O. ovata* (Ciminiello et al., 2008; 2012a), *O. mascarenensis* (Lenoir et al., 2004). *Ostreopsis* spp. are unicellular epiphytic microalgae, classified as benthonic dinoflagellates (Schmidt, 1901; Fukuio, 1981).

Originally, they were supposed to colonize tropical and sub-tropical areas, but now they are detected more and more frequently also in temperate seas, suggesting their increasing and/or wider distribution in the benthonic environment, all over the world. In Mediterranean area, appearance and proliferations of *Ostreopsis* cf. *ovata* (Figure 3 *A*) and *O. siamensis* (Figure 3 *B*) were recorded starting from the end of the ’70s and the ’80s, respectively (Taylor, 1979; Abboud-Abi Saab M., 1989).

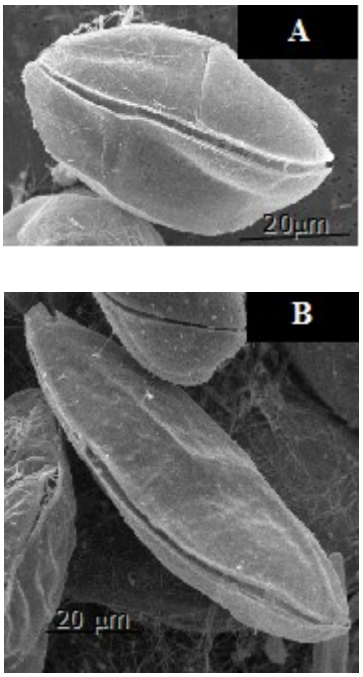

Figure 3. *Ostreopsis* cf. *ovata* (*A*) and *Ostreopsis* cf. *siamensis* (*B*) from the Tyrrhenian Sea. SEM micrographs (modified from Penna et al., 2005).

In the Mediterranean area, the specie that prevalently produces PLTX-like compound is *Ostreopsis ovata.* Even if Japanese *O. siamensis* is well-known to contain OST-D (Usami et al., 1995; Ukena et al., 2001), the same specie does not seem to produce known palytoxins in the

Mediterranean sea. To our knowledge, the only case in which Mediterranean *O. siamensis* was hypothesized to contain PLTX-like compound was in 2009, when Cagide and co-workes (Cagide et al., 2009), described functionally active compounds, that mimicked the effects of PLTX, in samples of *O. siamensis* collected along the Andalusia coast, but without chemical confirmation about structure. On the other side, the presence of PLTX-like compounds in *Ostreopsis ovata* has been proved with several techniques. Advanced liquid chromatography tandem mass spectrometry (LC/MS) has been extensively used for the detection of PLTX-like compounds in samples of *O. ovata* (Ciminiello et al., 2011). In addition, LC for the analysis of PLTX-like compounds has also been developed with precolumn derivatization and fluorescent detection by Riobò and co-workers (Riobò et al., 2008a). Recently, our research group has highlighted the advantages of the use of anti-PLTX antibodies for the immunocytochemical determination of the toxins directly in microalgae cells (Honsell et al., 2011).

Usually, the ideal habitat for the proliferation of *Ostreopsis ovata* is protected, inshore stations (Faust et al., 1996), characterized by low hydrodynamism (Vila et al., 2001). During proliferation, microalgae of *Ostreopsis* colonize all surfaces available, including macroalgae (Figure 4), rocks, bottom surfaces and also other living organisms (Faust et al., 1996; Sansoni et al. 2003; Honsell et al., 2011). This aggressive behavior may have severe consequences, and even induce mortality, for the organisms commonly populating the benthos, such as sea urchins and other echinoderms and coelenterates (Sansoni et al., 2003). In addition, also shellfish seems to suffer the presence of

Ostreopsis, showing decreased adherence to rocky substrates and higher mortality rate (Sansoni et al., 2003).

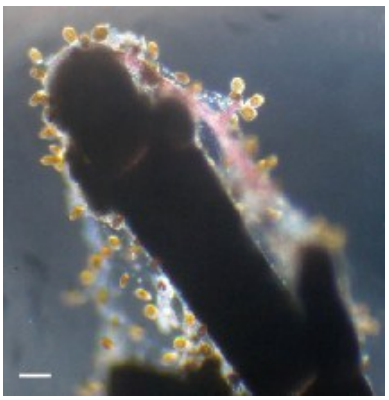

Figure 4. *Corallina officinalis* covered by cells of *O.* cf *ovata* within a mucous web, collected in the Gulf of Trieste in 2009 (modified from Honsell et al., 2011).

In Italy, the presence of *Ostreopsis* spp. was recorded for the first time in 1995, along the coasts of Lazio region (Tognetto et al., 1995). From that moment, the presence of *Ostreopsis* spp., with higher prevalence of the specie *ovata*, was recorded along all the peninsula and interested both the Tyrrhenian (Sansoni et al., 2003; Zingone et al., 2006; Barone 2007) and the Adriatic Sea (Gallitelli et al., 2005; Totti et al., 2007), up to the northern areas, such as the Gulf of Genoa (Brescianini et al., 2006; Mangialajo et al., 2008) and the Gulf of Trieste (Monti et al., 2007; Honsell et al., 2011).

Comparison of samples of *Ostreopsis ovata* collected in Tyrrhenian and Adriatic Sea revealed morphometric differences, being the Adriatic strain nearly twice bigger that the Tyrrhenian, even though they appeared genetically uniform. Moreover, comparison of the toxin

profile of the two strains, revealed in both cases the presence of putative PLTX and Ovatoxin-A (Guerrini et al., 2010).

The investigation and the comprehension of the algal growth and the factors influencing toxin production are obviously matters of crucial importance in the comprehension of the toxicity potentially associated to proliferations. To this aim, *Ostreopsis* cells can be harvested and cultured in standardized conditions giving precious information for the elucidation of the high variability of the sampling "on-field". Cells growth appears tightly regulated and, for every population it is possible to distinguish different growth phases. During the exponential phase cellular growth rate is maximal, but toxins production seems to be very limited. On the contrary, when *O. ovata* growth stops in the stationary stage toxin content in the culture usually increases, in parallel with increasing toxicity of growth medium (Guerrini et al., 2010). In spite of that, toxin content in algal cells seems to be generally higher than that measurable in growth medium (Guerrini et al., 2010; Pezzolesi et al., 2012).

Similarly to growth stages, water temperature influences cells proliferation and toxin content of *Ostreopsis ovata*, suggesting slight differences between strains of the Tyrrhenian (optimal growth 26-30 °C and proliferations usually observed in the middle of the summer; Granéli et al., 2011) and the Adriatic Seas (optimal growth 20-22 °C and maximum proliferations usually observed between end of August and October; Pezzolesi et al., 2012; Monti et al., 2007; Honsell et al., 2011). As already observed by Guerrini and co-workers (2010), there seems to be a reverse correlation between optimal conditions for toxin

production and for cells growth, being the toxin content higher at 25°C for the Adriatic Strain of *O. ovata* (Pezzolesi et al., 2012).

More recently, the question of PLTX producing organisms came again to the forth and some bacterial species were proposed in this respect. Zoanthid corals and microalgae are phylogenetically very distant and the search of common ancestors, that could explain why they both contain similar toxins, led to the hypothesis that bacteria could produce PLTXs, or at least some biosynthetic precursors. Evidence to possible bacterial origin for PLTX was given already from the discoverer of the molecule (Moore, 1982), and in 2000, Frolova and co-workers (Frolova et al., 2000) identified, in bacteria, compounds antigenically related to PLTX. In 2009 the hypothesis was further explored, and it was demonstrated that bacteria isolated from *Palythoa caribaeorum* exert PLTX-like hemolytic activity (Seemann et al., 2009). Moreover, more recently parent PLTX and its 42-hydroxyl-derivative were isolated from marine Cyanobacterium *Trichodesmium* (Kerbrat et al., 2011), giving more strength to the possibility that bacteria may be involved in the biosynthesis of PLTXs

1.1.4. Molecular target and mechanism of action

The $Na^+\backslash K^+$-ATPase is considered the main molecular target of PLTX and its analogues (Habermann 1989; Wu, 2009; Rossini and Bigiani 2011). The idea that PLTXs may interact with the $Na^+\backslash K^+$ pump arose from many experimental results, that on the whole, led to the definition of the molecular target of this family of compounds.

Evidence for the definition of the mechanisms of action of PLTX was collected even before complete structural elucidation of the molecule. The idea that the toxin may interact with cellular structures responsible of ionic homeostasis originated from the simple observation that PLTX was able to induce potent muscular contraction (Deguchi et al., 1974; Ito et al., 1976; 1977; 1979). In addition, results on mechanical properties were soon supported by the measurement of PLTX-induced depolarization in muscular tissues (Ito et al., 1976; 1977; 1979) and in peripheral (Dubois and Cohen, 1977) and central nervous system (Kudo and Shibata, 1980).

The structural elucidation of the molecule in 1981 (Uemura et al., 1981; Moore and Bartolini, 1981) on the one side provided purified working-material, and on the other, probably gave new stimuli in the definition of the mechanism of action of the toxin. The stronger evidence that lead to the identification of the $Na^+\backslash K^+$ pump as the molecular target of PLTX, came from the observation that the cardiac glycoside ouabain was able to inhibit some biological effects of the toxin. Ouabain is a potent and known inhibitor of the Na^+/K^+ ATPase (Skou, 1957) and was found to inhibit PLTX-induced contraction of human umbilical artery (Ishida et al., 1981) and, later, to exert its protective effects also on non-excitable cells, such as erythrocytes (Habermann and Chhatwal 1982). PLTX inhibition of the pump was then confirmed on purified Na^+/K^+ ATPase (Ishida et al., 1983), on mammalian pumps selectively expressed in yeast cells (Scheiner-Bobis et al., 1994; Redondo et al., 1996) and in Na^+/K^+ pumps reconstituted in planar lipid bilayers (Kim et al., 1995). It is possible that at the beginning, the idea that the $Na^+\backslash K^+$ pump was the target of palytoxin met some resistances (Wu, 2009) but

from that moment, the attention and the efforts of the scientific community focused on the interaction between the toxin and the pump molecule.

Even though PLTX and ouabain share the same molecular target, it was soon clear that there is a crucial difference between the mechanism of action of the two: ouabain blocks the pump in a conformation that inhibits ion fluxes, whereas PLTX induces the formation of a pore-channel in the pump with a conduction around 10 pS (Anner and Moosmayer, 1994; Kim et al., 1995; Artigas and Gadsby, 2002). Important insights in the comprehension of the ionic fluxes induced by the toxin came from experiments performed on ATPases expressed in yeast cells: recordings of Na^+ influx (Redondo et al. 1996) and K^+ efflux (Scheiner-Bobis et al. 1994) in this experimental condition ruled out the involvement of other cation channels in the primary action of PLTX. In physiological conditions, the pump is an active transport system that maintains the ionic balance of Na^+ and K^+ across the plasma membrane. The pump exchanges, against chemical gradient, three atoms of Na^+ and two of K^+ (Scheiner-Bobis 1996; Horisberger, 2004), whereas, in presence of PLTX, this ability is completely lost and cationic permeability is recordable with a stoichiometry near to 1:1 (Redondo et al. 1996). To obtain this effect, PLTX seems to disrupt the normal alternate gating typical of the pump, promoting the formation of a pore within the transporter (Artigas and Gadsby 2003a). After pore creation, the newly formed ion translocation pathway shares, at least in part, the same transmembrane domains used by Na^+ and K^+ during physiological binding (Guennoun and Horisberger, 2000; Horisberger et al., 2004). Even though PLTX action seems to revert the typical

features of the pump, the transporter that interacts with the toxin maintains the sensitivity to its physiological ligands, such as K^+ and ATP (Artigas and Gadsby, 2002, 2003b; 2004). On the contrary, the ATPase activity *per se* does not seem to be essential for the action of the toxin (Scheiner-Bobis and Schneider, 1997).

During the normal transport cycle, the pump adopts two major conformation: E1 in which binding sites are accessible from the cytoplasmic surface and E2, in which access is from the extracellular surface, both of them existing as phosphorylated and dephosphorylated form (Artigas and Gadsby, 2002).

The conformation in which the toxin binds to the pump is difficult to define; the peculiar effect of PLTX suggests that it may stabilize a conformation different from any other physiologically observed, so far. In spite of that, PLTX is known to exert its biological effects interacting with the cells from the extracellular side (Muramatsu et al., 1984; Kim et al., 1995). In addition, it was found that the toxin binds with highest affinity to phosphorylated pumps, exposed to K^+-free, high Na^+ external and internal solutions in presence of Mg-ATP. In these conditions, it can be expected that the most likely conformation, in the steady state could be E2P and for this reason conformation E2P is considered the more likely for PLTX binding (Figure 5; Artigas and Gadsby, 2004; Horisberger, 2004).

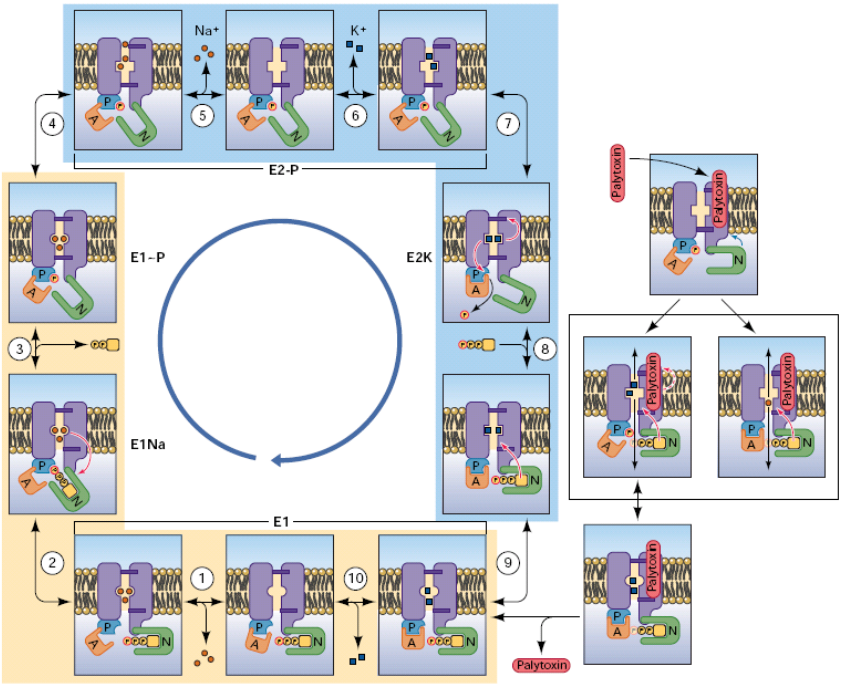

Figure 5. Left: different phases of ion transport cycle of Na^+ pump. Right: proposal of interaction between PLTX and pump, with stabilization (rectangle) of ion translocation pathway with both gates open (modified from Horisberger, 2004).

On the whole, PLTX interaction with its molecular target transforms the pump into a cationic channel-pore, that elicits Na^+ influx and K^+ efflux from the majority of mammalian cells. The consequence of this ionic fluxes varies according to the model under investigation and will be discussed in detail in the next paragraphs.

Interaction of PLTXs with molecular targets other than Na^+/K^+ ATPase, is still an on-going debate. As foreseeable, the most representative results concerning the research of alternative molecular targets involved other members of the P-ATPase family. In fact, this family of transporters is characterized by specific sequences highly

conserved between types (Horisberger, 2004). Initially, PLTX was shown to induce K^+ efflux, thus one of its typical effects, from yeast cells expressing hybrid between gastric H^+/K^+ ATPase and Na^+/K^+ ATPase (Farley et al., 2001). Later the effect of the toxin was confirmed on H^+/K^+ ATPase of rat colon. In this system, PLTX induced the formation of a pore that allowed cations to diffuse according to electrochemical gradient in a vanadate-sensitive manner (Scheiner-Bobis et al., 2002). To confirm the wide range of action of PLTXs on P-ATPases, the molecule was found to induce K^+ efflux also in chimeric enzymes expressing α-subunit of Na^+/K^+ ATPase and catalytic domain of the sarcoplasmic/endoplasmic Ca^{2+}-ATPase (SERCA; Ito et al., 2003). In addition, studies performed directly on microsomal fraction containing SERCA revealed that the toxin interacts also with this pump type. In SERCA isolated from cat atrial myocytes, it was observed that the toxins slow the Ca^{2+} uptake from the pump (Kockskämper et al., 2004). As reported for the $Na^+\backslash K^+$ pump (Artigas and Gadsby, 2004; Horisberger, 2004), also in this case the toxin seems to interact preferentially with the Ca^{2+}-ATPase in conformation E2. In spite of this similarity, PLTX blocks the Ca^{2+} pump without forming a cation channel (Coca et al., 2008). This observation, even if relatively low explored, opens interesting insights in the comprehension of the mechanisms of action of PLTXs and suggests for the toxin a mechanism related with the α-β-oligomeric structure of the pump rather than with the primary structure of the protein (Coca et al., 2008).

Although few, data suggesting effects of the toxin without involving of the pumps exist. The inhibitory action of PLTX on the transport

mechanism of ascorbic acid in cultured bovine adrenal chromaffin cells was described (Morita et al., 1996).

1.2. Exposure assessment

1.2.1. Distribution of PLTX in marine organisms and entrance into the food chain.

The accumulation of biotoxins into the food chain is a quite common and naturally occurring phenomenon (Mebs, 1998). This event may lead to the presence of considerable concentrations of toxic compounds or metabolites in organisms very different from the producing ones. Palytoxin does not make exception and was found in several species of crustaceans, fish, mollusks, gastropods and echinoderm, that can represent a threat for consumers health (Aligizaki et al., 2011). Generally, PLTX-containing marine organism were found both proliferating in the coral reef in close contact with the corals (Gleibs et al., 1995), or sharing habitat with microalgae of *Ostreopsis* (Onuma et al., 1999; Aligizaki et al., 2008).

Crustaceans living in the reef of Philippines, such as *Demania alcalai*, *Lophozozymus pictor* (Yasumoto et al., 1986) and *Demania reynaudii* (Alcala et al., 1988) were found to contain PLTX and PLTX-like compounds, quite distributed in all tissues. Similarly, small crustaceans (*Platypodiella spectabilis*) usually living under the crust of *Palythoa* colonies were found to contain PLTX, very similar to that of the "housing" colonies. Moreover, predators that eat the zoanthid corals were found to contain the toxin as well (Gleibs et al., 1995; Mebs,

1998; Gleibs and Mebs, 1999). Polychaete worms (Gleibs and Mebs, 1999), and fishes (Gleibs and Mebs, 1999; Fukui et al., 1987) were found to contain PLTXs in considerable concentrations, but apparently without suffering dangerous consequences (Gleibs and Mebs, 1999).

To mimic the naturally-occurring toxin uptake by filtering mollusks, experiments were performed feeding shellfish with *Ostreopsis siamensis* containing PLTX. Shellfish were observed actively feeding microalgae for over 84 hours and toxin content and toxicity were assessed at the end of the observation period. Analysis of mussels, oysters and scallops (hepatopancreas/ muscle and roe) revealed traces of toxins prevalently in oysters. Moreover, detectable PLTX-like compounds in scallops hepatopancreas were also found (Rhodes et al., 2002). In addition, to support the idea that shellfish living in close contact with *Ostreopsis* spp may accumulate PLTXs, natural samples of shellfish, collected during microalgae proliferation in the Aegean sea, were found to be contaminated with PLTX-like compounds (Aligizaki et al., 2008).

In spite of the ability of these toxins to enter the food chain, PLTXs may also affect life and development of aquatic organisms (Vasconcelos et al., 2010). From the available data, in the Mediterranean area, presence of PLTXs-producing organisms seems to have more severe impact for marine ecosystem, in comparison to tropical environment. As, in some aspect, already described in section (Producing organisms), massive proliferation of *Ostreopsis ovata* has been associated with mortality of a broad range of organisms populating the benthos (Aligizaki et al., 2011; Sansoni et al., 2003).

This sensitivity was confirmed by recent experiments that demonstrated how the exposure of crustaceans (*Artemia salina*, *Tigriopus fulvus*, and *Amphibalanus amphitrite*) and fish juveniles (*D. labrax*) to laboratory cultured and natural samples of *Ostreopsis ovata* increases morbidity and mortality of this marine vertebrates and invertebrates (Faimali et al., 2011). Moreover, it was demonstrated that the PLTXs, not only accumulate in shellfish, but may also have toxic effects on them. In particular, it was proved that the toxin decreases, in concentration and time dependent manner, the metabolic rate of mussels mantle and of hepatopancreatic cells. This toxic effect was not observed for other toxins, normally accumulating in shellfish, such as okadaic acid (Louzao et al., 2010). To strength the idea that PLTX may have negative effects on mollusks, it was also demonstrated that the toxin induces response of the immune systems of *Mytilus galloprovincialis*, stimulating the phagocytic activity of immunocytes mussels (Malagoli et al., 2008).

1.2.2. Epidemiological data

Epidemiological data about the effects for human heath of PLTXs are described both in tropical and temperate areas. Primary route of exposure, which can be identified in description of PLTX-intoxication, are four: ingestion, inhalational, dermal and ocular. Ingestion is obviously related to the entrance of the toxin into the food chain, since PLTX-producing microalgae and soft corals are not edible species. To support the idea that PLTX may enter the food chain, there is its widespread presence in several organisms, such as several species of

fish, crustaceans and echinoderms. Inhalational exposure, even if not confirmed, has been related to the presence of PLTX-like compounds in *Ostreopsis* cells during massive proliferation and to the exposure to the steam of boiling water on *Palythoa* corals. Dermal exposure can be related both to the direct contact with PLTX-containing corals, especially by aquaria hobbyist, to the contact with *Ostreopsis* cells in seawater or in laboratory. Ocular exposure is very rare, but has been described in literature as well (Moshirfar et al., 2010).

1.2.2.1. Oral exposure

The analysis of literature data reveals the presence of discrepancies in methodology used for the identification and classification of cases of intoxication related to the presence of PLTX in seafood. In particular, chemical analysis of food leftover or of human specimens were rarely carried out; in many cases the causative agent of the intoxication was postulated to be PLTX on the basis of symptoms or type of seafood involved. On this basis, cases of human poisoning ascribed to PLTX and PLTX-like compounds were classified in a recent review, published during the development of this thesis (Tubaro et al., 2011a).
Cases of intoxication with direct identification of PLTX in the leftovers are summarized in table I. In these cases, the presence of PLTXs was identified directly in leftovers, with chemical or immunological methods. From the analysis of literature data, it was possible to identify the main symptoms associated to the ingestion of PLTXs-contaminated seafood; intoxication seems usually characterized by initial involvement of the gastrointestinal apparatus with nausea, vomiting and

diarrhea. After these symptoms, that can be virtually associated to every food intoxication, more specific ones usually set on.

Location year	Poisoning Source	Cases (n°)	Outcome	Symptoms and clinical data	Reference
Philippines 1984	*Demania Reynaudii*	1	1 death	Metallic taste, dizziness, tiredness, numbness of extremities, restlessness, g.i disturbances. bradicardia, respiratory probl., cyanosis, renal failure	Alcala et al., 1988
Japan 1986	*Scarus Ovifrons*	2	1 death	Myalgia, dyspnoea, convulsions. Myoglobinuria, high serum levels of CPK, AST, LDH	Noguchi et al., 1987
Madagascar 1994	*Herklotsichtys quadrimaculatus*	1**	1 death	Metallic taste of the flesh, malaise, vomiting, diarrhoea tingling of the extremities, delirium	Onuma et al., 1999
Japan 2000	*Epinephelus bruneus, E. fuscogattus*	11	Recovery	Myalgia, black urine, shoulders pain. Serum CPK elevation.	Taniyama et al., 2002

Table I. Oral exposure. Cases of intoxication with direct identification of the toxin. (AST = alanine aminotransferase; CPK = creatine phosphokinase; LDH = lactate dehydrogenase; Tubaro et al., 2011a, modified).

In 1988, Alcala and co-workers described alternating periods of normal heart rate and severe bradycardia (30 beats/min), shallow breathing, followed by cyanosis around mouth and hands and renal failure. Probably, the most distinguishing feature of PLTX intoxication is the

involvement of the skeletal muscle as one of the main target organs. Patients often complain severe myalgia, associated to increased serum level of Creatin Phospho Kinase (CPK; Noguchi et al., 1987; Taniyama et al., 2002).

Other cases of intoxication were grouped together because they were ascribed to PLTX on the basis of analysis of samples collected or purchased after or before the poisoning episode, rather than directly on leftovers. In these cases, seafood was known to potentially contain PLTX, but the analysis was not carried out on the samples that caused the intoxication. Even if, the correlation with PLTX was not proved, the observed symptoms supported the idea that PLTX-like compounds may be involved in the intoxication. In particular, predominant symptoms impaired the muscular apparatus, with myalgia, even severe and muscle spasms (Fusetani et al., 1985; Kodama et al., 1989; Okano et al., 1998; Mahmud et al., 2000; Yoshimine et al., 2001). When hematoclinical analysis was performed, results generally supported the idea that the muscular apparatus was one of the most sensitive target organs for this family of toxins. In fact, elevated serum level of CPK was accompanied in nearly all cases with myoglobinuria, as a likely consequence of rabdomyolysis (Fusetani et al., 1985; Ichida et al., 1988; Kodama et al., 1989; Tabata et al., 1989; Okano et al., 1998; Mahmud et al., 2000; Yoshimine et al., 2001). Among the species involved in the cases of intoxication, there were crustaceans of the species *Demania* spp (Alcala and Halstead, 1970) and *Lophozozimus pictor* (Gonzales and Alcala, 1977; Tan and Lee, 1988), well known to contain PLTX or PLTX-like compounds (Yasumoto et al., 1986; Lau et al. 1995). Fishes mainly involved in the other cases belonged to the

specie *Tetraodon* (Mahmud et al., 2000), which was known to contain PLTX-like substances, on the basis of its hemolytic activity inhibited by ouabain and anti-PLTX antibodies (Taniyama et al., 2001). Moreover, in several other cases *Scarus (Ypsiscarus) ovifrons* (Fusetani et al., 1985; Ichida et al., 1988; Tabata et al., 1989; Okano et al., 1998; Yoshimine et al., 2001) and *Decapterus Macrosoma* (Kodama et al., 1989) were involved. However, for both species, analysis was performed on samples different from those involved directly in the intoxication.

In addition, palytoxin and/or its analogues have been considered responsible of a high number of human food-borne poisonings, without a confirmatory analysis aimed to toxin identification. In this group were classified all the cases where PLTX was involved only on the basis of clinical observations, signs and symptoms (Llewellyn, 2001; Shinzato et al., 2008; Arakawa et al., 2010), but the toxin has never been found in the specie.

1.2.2.2. Inhalational exposure

Inhalational exposure to PLTX-like compounds has been hypothesized in two different case scenarios.

The first scenario describes symptoms of people that came into contact with marine aerosol during massive proliferation of *Ostreopsis ovata.* Even if a direct correlation between the symptoms and the microalgae, or PLTXs, has never been found, other algal species are known to cause intoxications after inhalational exposure (Fleming et al., 2007). Disturbances of the respiratory tract, characterized by severe

rhinorrhoea and cough, have been described for the first time along the Apulia coast near Bari during an unusual proliferation of microalgae of *Ostreopsis* (Gallitelli et al., 2005). The phenomenon manifested with higher intensity in summer 2005 along the Liguria coasts, when hundreds of people suffered the so-called "Algal Syndrome" (Durando et al., 2007). In this case, people developed symptoms that involved respiratory tract, such as sore throat, dyspnoea, rhinorrhoea and cough. Moreover, systemic symptoms like fever, nausea and vomiting, in some cases associated with mild leucocytosis and neutrophilia, were also observed (Table II). Respiratory symptoms and systemic symptoms such as fever and/or headache were observed many times during *Ostreopsis* proliferation in all the Mediterranean area: Italian, (Di Turi et al., 2003; Sansoni et al., 2003; Gallitelli et al., 2005), Spanish (Kermarec et al., 2008 ; Barroso García et al., 2008) and French coasts (Kermarec et al., 2008 ; Tichadou et al., 2010) were all involved.

The second scenario of inhalational exposure to PLTX, is less common and foreseeable. The use of boiling water to remove invasive *Palythoa* corals from aquaria is a common habit among hobbyists. The use of this procedure on PLTX-containing zoanthids has exposed people to toxic aerosol with consequences like shortness of breath, chest pain and bronchospasm, as described by Deeds and Schwarz (2010). A similar case occurred also in New York (Majlesi et al., 2008) but the identity of the coral has never been confirmed. In Table II, are listed cases of intoxication with direct identification of PLTX-like compounds in the causing organisms. In particular, samples of *O. ovata* collected along the Liguria coasts during the "Algal Syndrome" revealed the presence of putative PLTX and Ovatoxin-A (Ciminiello et al., 2008), and

similarly, also in corals examined in USA, a PLTX-like compound was detected. In all other cases, even if the species of microalgae or soft-corals were identified, no toxin quantification was reported.

Location, year	Poisoning source	Cases (n°)	Outcome	Symptoms and clinical data	Reference
Italy (Tyrrhenian Sea), 2005	*O. ovata*	209	Recovery (209/209) within 3 days	Fever, sore throat, cough, dyspnoea, headache, nausea, rhinorrhea, lacrimation, vomiting, dermatitis. leukocytosis, neutrophilia	Durando et al., 2007
Italy (Tyrrhenian Sea), 2006	*O. ovata*	19	Recovery (19/19) within 3 days	Cough, sore throat, dyspnoea, fever, rhinorrhea, nausea, headache, lacrimation, vomiting	Durando et al., 2007
USA (Virginia), 2008	*Palythoa* sp.	1	Recovery (1/1) within 1 month	Foul odor. Shortness of breath and chest pain from bronchospasm	Deeds and Schwartz, 2010

Table II. Inhalational exposure. Cases of intoxication with direct identification of the toxin (Tubaro et al., 2011a, modified).

1.2.2.3. Dermal exposure

As previously described for inhalational exposure, dermal exposure may occur after direct contact with the *Palythoa* corals or after contact with seawater containing *Ostreopsis* spp. The first typically occurs in home aquaria after contact with the soft corals the latter during working or recreational activities associated with the sea. Cases of dermatitis associated with the exposure to *Ostreopsis* spp. were usually documented together with inhalational exposure. Even if really widespread and probably underestimated for incidence, this symptom

seems to be less severe in comparison with the respiratory ones and it is often underestimated. Dermal contacts were described for aquaria hobbyists (Hoffmann et al., 2008), but also for researchers that collected the corals of *Palythoa toxica* (Moore and Scheuer 1971; Moore et al., 1982). The case described by Hoffmann and co-workers (2008) was probably more severe than others because the corals produced small cuts in the fingers of the patient, providing an access for the toxin to the systemic circulation. In fact, myalgia, electrocardiographic alterations and elevated serum levels of CPK and LDH were observed (Table III).

Location, year	Poisoning source	Cases (n°)	Outcome	Symptoms and clinical data	Reference
Hawaii, USA, 1962	*P. toxica*	1	Recovery (1/1) within 1 week	Malaise, dizziness, nausea, headache, and discomfort to the hands and feet	Moore and Scheuer 1971; Moore et al., 1982
Germany, 2008	*Parazo-anthus* sp.	1	Recovery (1/1) within 48h	Myalgia, dizziness, weakness of the extremities. Swelling and erythema of cut fingers with numbness of the arm. Abnormal ECG. Slightly elevated CPK, LDH, and CRP	Hoffman et al., 2008

Table III. Dermal exposure. Cases of intoxication with direct identification of the toxin (Tubaro et al., 2011a, modified).

Symptoms similar to those described in Germany were recorded also in Georgia (Deeds and Schwarz, 2010) and California (Nordt et al., 2011), with chest pain, lightheadedness, weakness and numbness of the arm,

sinus tachycardia, elevated CPK in the first and perioral paresthesia, dysguesia, edema, erythema and pruritus of both hands, in the latter.
Also these cases were ascribed to PLTX containing corals, but there are some uncertainties for specie identification and no quantification of the toxin was carried out.

1.2.2.4. Ocular exposure

In comparison to the other exposure/absorption sites, ocular mucosa is the less studied but, for sure one of the most sensitive ones. Ocular involvement has been described in several cases of inhalation exposure to *Ostreopsis* spp. Conjunctivitis (Di Turi et al., 2003; Durando et al., 2007) and eye irritation (Kermarec et al., 2008; Barroso García et al., 2008; Tichadou et al., 2010) have been recorded many times, but it was not clear if they could be attributed to a direct action of the *Ostreopsis* containing aerosol or to a secondary effect of the severe rhinorrhea. In 2010, Moshirfar and co-workers described keratoconjunctivitis occurred in two patients while handling zoanthid corals in home aquaria (Moshirfar et al., 2010). Authors attributed the ocular damage to PLTX, but did not provide any chemical analysis of the coral or, at least, their precise taxonomical identification. The first patient experienced a metallic bitter taste while handling the coral, that is one of the most typical characteristic associated to PLTX-containing seafood (Alcala et al., 1988; Onuma et al., 1999). The day after, the patient developed eye pain, eyelid swelling, photophobia, and purulent discharge from both eyes. Recovery was slow (around 12 weeks) and not complete, possibly also for the presence of contact lenses that

increased exposure time to the toxic agent. The second case was very similar, for both exposure scenario (home aquaria cleaning) and effects, but resolved completely in two weeks treatment (Moshirfar et al., 2010). Taken together, these data are far from provide a complete characterization of the effects of PLTX at ocular level, but, in spite of that, provide precious suggestion for the evaluation of the possible exposure scenarios and on the sensitivity of this tissue.

1.3. Toxicity assessment

1.3.1. *In vitro* studies

For a better comprehension of the mechanism of toxicity of PLTX on biological systems the effects of the molecule have been investigated on several *in vitro* models. Considering that the Na^+/K^+ pump is expressed in all mammalian cells, toxicity has been observed in all cells tested, but with some peculiar differences in the mechanisms of action, related to cell type.

1.3.1.1. Effects on excitable cells and tissues

Immediately after the discovery of PLTX, its effects have been investigated on smooth muscular tissue and cells culture. Even though, in early studies, molecular weight of the toxin was estimated to be 3,300 (Ito et al., 1979), data obtained before complete structural elucidation and purification of PLTX are in good agreement with those obtained after 1981. At macroscopic level, the toxin induces a sustained

contraction of muscular tissue described in a wide variety of samples, such as vascular, intestinal, tracheal and papillary smooth muscles (Ito et al., 1976; 1977; 1979; Ozaki et al., 1983; Ishida et al., 1985). PLTX-induced contraction is recordable from concentrations in the picomolar range (Robinson and Franz, 1991; Robinson et al., 1992). Development of tension usually sets within seconds and is hard to be relaxed, even after toxin removal (Ito et al., 1977). Contraction appears to be dependent on external Ca^{2+} but insensitive to commonly used relaxants, such as atropine, tripenelamine or tetrodotoxin, phentolamine, phenoxybenzamine (Ito et al., 1976; Ozaki et al., 1983). PLTX is also known to disrupt electrical properties of smooth muscle, causing persistent depolarization of cellular membrane (Ito et al., 1977; 1979; Sheridan et al., 2005). In agreement with the proposed mechanism of action, the toxin induces K^+ efflux from ileal smooth muscle (Hori et al., 1988). Moreover, contraction and intracellular Ca^{2+} increase ($[Ca^{2+}]_i$) were found to be dependent on extracellular Na^+ (Ozaki et al., 1983; Ishii et al., 1997). According to this data, it was suggested that Na^+ influx could trigger the activation of voltage-dependent Ca^{2+} channels, Na^+/Ca^{2+} exchanger and Ca^{2+} release from intracellular stores, leading to an $[Ca^{2+}]_i$ as a secondary event (Ishii et al., 1997). The direct involvement of the toxin on muscular contraction was supported from data obtained in vascular muscle pre-incubated with reserpine. Reserpine induces pre-synaptic release of norepinephrine and effects of PLTX in this condition suggest a mechanism of action independent from the release of endogenous neurotransmitters (Karaki et al., 1988). Beside impairment of electrical and mechanical properties, PLTX is also highly cytotoxic. Toxicity was observed at

nanomolar concentrations and was accompanied by huge morphologic changes such as vacuolation, rounding and development of granulation on cellular surface (Sheridan et al., 2005).

The characterization of PLTX-induced ionic unbalance and toxicity has been quite deeply characterized in smooth muscles, on the contrary there are only few data that deal with skeletal muscle. Similarly to smooth muscle, also in skeletal tissue the toxin triggers an irreversible and Na^+-sensitive membrane depolarization (Deguchi et al., 1976; Ecault and Sauviat, 1991). This event appears insensitive to blockers of voltage-dpendent Na^+ channels, such as tetrodotoxin (TTX) and amiloride (Ecault and Sauviat, 1991).

Similarly, in cardiac cells, PLTX induces depolarization of cellular membrane sustained by Na^+ conductance (Sauviat et al., 1987; Muramatsu et al., 1988; Artigas and Gadsby, 2002). Na^+ entrance in these cells seems to be the result of the interaction of the toxin with the Na^+/K^+ pump, but also with the result of the contribution of the Na^+/Ca^{2+} antiporter (Frelin et al., 1991; Frelin and Van Renterghem, 1995). Beside Na^+ current, PLTX was also reported to induce an outward K^+ current, occurring also in Na^+-free solutions (Kinoshita et al., 1991). In line with previous results, it was demonstrated that the Na^+ current elicited by the toxin needed external Ca^{2+} for activation (Van Renterghem and Freling, 1993). In addition, it was also observed that PLTX promotes intracellular acidification, possibly as one of the extreme consequences of the primary ionic unbalance (Frelin et al., 1990). Morover, it was also demonstrated on cultured cat myocytes, that the toxin disrupts excitation-contraction coupling at atrial level

(Kockskämper et al., 2004). Even if electrophysiological experiments have been performed extensively on cardiac cells, no data about the cytotoxicity of PLTXs in this model are currently available.

Commonly to other excitable cells, also in neurons PLTX is known to induce membrane depolarization (Muramatsu et al., 1984; Kudo and Shibata, 1980; Louzao et al., 2006) insensitive or scarcely sensitive to TTX, and disappearing after removal of external Na^+ (Muramatsu et al., 1984). In primary cultures of neurons of the suprachiasmatic nucleus, the PLTX induces transient increase of spontaneous firing, followed by a total elimination of spontaneous spiking activity (Wang and Huang, 2006). As secondary action of PLTX on the Na^+/K^+ pump and membrane depolarization, the toxin triggers an $[Ca^{2+}]_i$ increase sensitive to nifedipine (blocker of voltage-dependent Ca^{2+} channels) and saxitoxin (blocker of voltage-dependent Na^+ channels), when present together in the bathing solution, before toxin addition. The uncontrolled increase of $[Ca^{2+}]_i$ is usually precursor of high cytotoxic events and, in fact, PLTX induces release of exocytotic synaptic vesicles in cerebellar granule neurons (Vale et al., 2006). Moreover, in the same cellular model, it was also shown that PLTX decreases intracellular pH, possibly through the involvement of the plasma membrane Ca^{2+}-ATP-ase (Vale-Gonzáles et al., 2007). The effect of the toxin has been investigated also in neuroblastoma cells. In order to deeper investigate the mechanism of cytotoxic action of palytoxin, typical apoptotic markers were evaluated, such as mitochondrial membrane potential, activation of caspases, DNA damage. The only parameter that resulted to be influenced by PLTX was mitochondrial membrane potential, suggesting minor importance for apoptotic

pathways in PLTX-induced cell death (Valverde et al., 2008). Similar conclusions were drawn also by Sagara and co-workers (2011), that suggested a non-oxidative necrotic damage to PC12 cells incubated with PLTX. As already described for primary cultures, also in neuroblastoma cells, PLTX and analogues trigger $[Ca^{2+}]_i$ increase (Louzao et al., 2007). Moreover, this family of toxins also causes disorganization of filamentous actin (Louzao et al., 2007), and also of globular actin (Ares et al., 2009).

1.3.1.2. Effects on non-excitable cells

Since Na^+/K^+ ATPase, is distributed in all mammalian cells (Horisberger, 2004), even if the primary action of the toxin is disruption of ionic equilibrium, also non excitable cells are heavily affected from these family of compounds.

Among effects on non-excitable cells, particular scientific relevance has been given to the effects of PLTXs on erythrocytes. The ability of the toxin to induce delayed hemolysis is one of its most peculiar and distinguishing features, and has been extensively used for the detection of the toxin in several matrices, such as fish (Onuma et al., 1999; Gleibs and Mebs, 1999; Wachi et al., 2000) and shellfish (Aligizaki et al., 2008; 2011). The assay was developed from Dr. Bignami (1993), and later used and further developed also from other research groups (Riobò et al., 2008b; 2011).

In culture, the toxicity of PLTX and PLTX-like compound has been demonstrated in a wide variety of cellular models. One of those are cultured intestinal cells (Valverde et al., 2008), whose sensitivity is

among the highest ever recorded, with an EC_{50}, after only four hours of incubation, in the picomolar range (Pelin et al., 2012). Skin keratinocytes were also found to be a very sensitive target for PLTX. On this model PLTX is highly cytotoxic and induces the production of reactive oxygen species (ROS) (Pelin et al., 2011). Among the effects of PLTX on skin, particular attention should be given to the discovery that the toxin is also a skin tumor promoter. Generally skin tumor promoters involve the activation of the protein kinase C, exactly like the 12-*O*-tetradecanoylphorbol-13-acetate (TPA). PLTX is defined as a non-TPA tumor promoter, because it is a tumor promoter without activating the protein kinase C (Fujiki et al., 1986; Wattenberg, 2007). Also in this case, Na^+ influx seems to play a crucial role in the mechanism of action of PLTX. In fact, experimental evidences suggest that the activation of stress activated protein kinase JNK require the monovalent cation (Kuroki et al., 1996).

1.3.2. *In vivo* studies

For more complete comprehension of the toxicological risk associated with the entrance of PLTX into the food web some *in vivo* studies were also performed. Unfortunately, many of the studies were carried out before complete structural elucidation of the molecule and, in some cases, a different molecular weight was reported (Wiles et al., 1974).
A considerable amount of studies was performed on dogs, that are considered among the most sensitive species to this family of toxins. Intravenous administration of PLTX, isolated from different species of *Palythoa*, causes severe impairment of function of the cardiovascular

apparatus. In more detail, the administration of extract of *P. mamillosa* (Kaul et al., 1974; Munday 2008), *P. caribaeorum* (Kaul 1981; Munday 2008) and *P. tuberculosa* (Ito et al., 1982) caused abnormalities of blood pressure and ECG profile, that finally lead to death for cardio-circulatory arrest. Similar alterations of the blood pressure and disturbances of the electrocardiographic profile were observed also in cats treated with PLTX isolated from *P. tuberculosa* with estimated molecular weight of 3300 Da (Deguchi et al., 1974).

Parenteral administration (i.v.) of partially purified PLTX (m.w. 3300 Da) isolated from *P. vestitus* to rats caused sedation, dyspnea and convulsion prior to death, with an LD_{50}= 0.089 μg/kg and no effects were seen with the administration *per os* of the same toxin up to the dose of 40 μg/kg (Wiles et al., 1974).

According to the available data, the most sensitive animal after intravenous administration of PLTX-like compounds seems to be the rabbit with an LD_{50} of 0.025 μg/kg (Wiles et al., 1974). This result presents some uncertainties, once again due to the limited purification of the toxin, but nevertheless, it allows to classify PLTX as one of the most dangerous natural toxin ever isolated.

Administration of the toxin via intra-tracheal route was also reported. Literature offers few example in this respect. Intra-tracheal administration of toxins from *P. vestitus* in rats, elicited symptoms and toxicity similar to those observed after i.v. administration, with an DL_{50} of 0.63 μg/kg (Wiles et al., 1974). Similarly, Ito and Yasumoto, observed death of mice within 2 hours from the administration of commercial PLTX, starting from the dose of 2 μg/kg. Thus, mortality

was recorded at a dose 100 times lower than that recorded after gavage administration, and symptoms were paralysis, alveolar bleeding and gastro-intestinal erosion (Ito and Yasumoto, 2009).

Mouse is probably the most used experimental model for the investigation of *in vivo* toxicity. Among literature studies, only few of them were performed with commercial PLTX and the other were performed with toxins purified with different protocols from several sources, without any information about purity. The majority of the data describe the effects of the toxin after intra-peritoneal (i.p.) administration. The i.p. administration of different doses of pure PLTX caused mortality in the nanomolar range and the Lethal Dose for the 50% of the treated animals (LD_{50}) was found to be around 0,31µg/kg (Riobò et al., 2008b) and 0,72µg/kg (Rhodes et al., 2002). Main symptoms were abnormal gait (Riobò et al., 2008b; Rhodes et al., 2002), convulsions and breathing difficulties (Riobò et al., 2008b). Similar symptoms were described also for toxin isolated from *Demania alcalaii* (Ito et al., 1996), from extracts of *Ostreopsis mascarenensis* (Lenoir et al., 2004), *Palythoa toxica* (Munday 2008), *Scarus ovifrons* (Tanyiama et al., 2003) and *Lophozozimus pictor* (Chia et al., 1993).

Studies after oral administration in mice are more informative for the investigation of the potential threat related to the entrance of PLTX into the food chain, but data in this respect are more limited in number. Initially, LD_{50} was calculated with the "up and down" method to be 510 µg/kg (Munday, 2008). Later, to obtain more information about the target organs of these compounds, a study was performed in our laboratory following the "classical method" for the acute toxicity testing (Sosa et al., 2009). Toxin was administered *per os*, and

calculated LD_{50}, according to the Finney method (Finney, 1971), was 767 µg/kg. Symptoms observed were in good agreement with those described after i.p. administration, such as paralysis, convulsions and severe breathing difficulties (Sosa et al., 2009). Similar toxicity (LD_{50}, 650 µg/kg) was observed also in mice treated with 42-OH-PLTX (Tubaro et al., 2011b). In this context, more detailed experiments to investigate the mechanism of action of PLTXs have been performed revealing the muscular apparatus as one of the target organs of the molecule also in mouse (Figure 6).

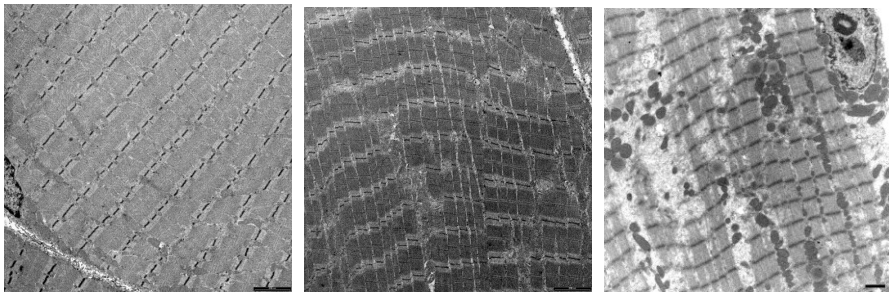

A. Control B.42-OH-PLTX C. PLTX

Figure 6. Electron micrographs of skeletal muscle (*A*) control mouse; (*B*) 42-OH-PLTX treated mouse dose 424µg/kg; (*C*) PLTX treated mouse dose 1200 µg/kg; scale mark: 1µm.

2. AIM

OF THE PROJECT

On the whole, the present project was developed to contribute to the definition of risk characterization of PLTX and analogues as seafood contaminants.

From the epidemiological data describing the effects of the ingestion of PLTX-contaminated seafood, it results clear that one of the peculiar and distinguishing characteristic of the intoxication is the damage/impairment of the skeletal muscle. In spite of this evidence, the mechanism of toxicity of this family of compounds on skeletal muscle has never been studied in detail. For this reason, to complete risk characterization and to implement the information about the mechanism of action of PLTX and analogues, one of the target of the present project was the elucidation of the mechanism of toxic action of PLTXs on primary cultures of mouse skeletal muscle cells.

From the exposure assessment emerges that these toxins, initially, detected only in tropical and subtropical areas, are more and more frequently found in seafood collected and commercialized in temperate seas. This geographic shift, poses new concerns from scientific and regulatory point of view. In fact, together with the growing interest of the scientific community for this family of compounds, there is also an alarming gap regarding their regulation. In Europe, some efforts have been made to try to fulfill legislative empty spaces with the publication, in 2009, of a scientific opinion by European Food Safety Authority (EFSA, 2009). The experts gave a general evaluation of the molecule suggesting, from the available data, an Acute Reference Dose (ARfD) for mixed PLTXs and Ostreocins of 0.2 μg/kg b.w. These data were calculated starting from an acute toxicity study and in particular from a LOAEL (Lowest Observed Adverse Effect Level) published by Ito and

Yasumoto (2009) of 200 μg/kg of toxin given orally to mice. In spite of that, the absence in literature of scientific studies that describe the effects of repeated oral intake of PLTXs, represents a sever limitation in the development of the risk assessment. Indeed, it is possible that toxins accumulate in different species of seafood in the same geographical area. For this reason, consumers, according to personal habit, may come into contact with toxin more than once and, in this case, only testing the effects of repeated administration could help in the comprehension of the real hazard associated to the exposure. Moreover, toxicity studies are necessarily the basis for the calculation of regulatory limits for the presence of biotoxins in seafood and, as a consequence, gives also the range of sensitivity that detection methods should have for monitoring purposes. In light of this, the second goal of the present project was to investigate sub-acute toxicity of PLTX.

3. MATERIALS

METHODS

3.1. Materials

3.1.1. Toxins

Palytoxin (declared purity of more than 90%) was purchased from Wako Chemicals GmbH (Neuss, Germany).

42-OH-PLTX was a non-commercial sample and has been kindly provided by Dr. Mark Poli of the US AMRID; the toxin was provided in frame of a bilateral agreement between University of Trieste and the American USAMRID. Briefly, the sample 42-hydroxy-palytoxin was obtained from *Palythoa toxica* collected in Hawaii, according to the procedure described by Moore and Scheuer (1971) and modified by Bignami et al. (1992). The toxin was extracted from *P. toxica* with 70 % aqueous ethanol. The extract thus obtained was concentrated *in vacuo* and then extracted with dichloromethane. The toxic fraction was purified from the aqueous layer by column chromatography on Amberlite XAD-2, followed by chromatography on DEAE-Sephadex A-25 and CM-Sephadex C-25. The toxic fraction was finally desalted on Bond Elut C18 eluted with 80 % aqueous ethanol. The analysis of the toxins have been carried out by the research group of Prof. Ciminiello and Prof. Fattorusso at the University Federico II of Neaple and details are reported in Ciminiello et al., 2009 (purity more than 90%).

Ostreocin-D has been kindly gifted from Prof. Takeshi Yasumoto (Japan Food Research Laboratories, Tama Laboratory, Tokyo, Japan).

For *in vivo* toxicity studies, PLTX was dissolved in phosphate buffered saline (PBS), pH 7.0. To avoid chemical instability, solutions were prepared every morning immediately before administration to the animals.

For *in vitro* studies toxins were stored in glass vials, in aqueous/ethanol solution (1:1) at -20°C. The day of the experiment working dilutions were freshly prepared according to experimental protocol.

3.1.2. Animals

Female CD-1 mice (18–20 g body weight, 4 weeks old) were purchased from Harlan Italy (S. Pietro al Natisone, Italy). Animals were acclimatized in our facilities for 2 weeks before treatment. Animal room controls were set to maintain controlled temperature (21 ± 1°C) and humidity (60-70 %). The room was illuminated with a fixed artificial light cycle (7.00 a.m.–7.00 p.m.). Animals were caged, in groups of 6, using dust free poplar chips for bedding and fed with the standard diet for rodents (Harlan Italy, S. Pietro al Natisone, Italy). Diet composition, as indicated by Harlan Italy, was: proteins (18.5 %), fats (5.5 %), fibers (4.5 %), hashes (6.0 %), non-nitrogen compounds (53.5 %), water (12.0 %). Dietary supplements present in fed are listed in table IV. Water and fed were provided *ad libitum* during all phases of the study.

Experiments were carried out at the University of Trieste in conformity with Italian D.L. n. 116 of 27 January 1992 and associated guidelines in the European Communities Council Directive of 24 November 1986 (86/609 ECC), concerning animal welfare and appendix A of the European Convention ETS 123.

Ingredient	Quantity	Ingredient	Quantity
Vitamin A	15,000 UI	Pantothenic acid	21.0 mg
Vitamin D_3	1,500 UI	Colin	300.0 mg
Vitamin B_1	9.8 mg	Folic acid	3.0 mg
Vitamin B_2	12.0 mg	Iron	50.0 mg
Vitamin B_6	11.5 mg	Manganese	44.0 mg
Vitamin B_{12}	0.08 mg	Zinc	30.0 mg
Vitamin E	81.0 mg	Copper	7.0 mg
Vitamin H	0.23 mg	Cobalt	0.5 mg
Vitamin K_3	50.0 mg	Iodide	6.1 mg
Vitamin PP	27.0 mg	Chromium	0.5 mg

Table IV. Supplementary ingredients of animals fed.

3.1.3. Reagents

Bovine fetal calf serum (FCS) was from PAA Laboratories (Mascia Brunelli; Milan, Italy). The ion channels blockers cyclopiazonic acid, gadolinium, lanthanum and cadmium were purchased from Sigma (Milan, Italy). Verapamil, KB-R7943, SKF-96365 and tetrodotoxin (TTX) were from Tocris Bioscience (Bristol, UK).

Mouse monoclonal anti-desmin antibody D33 was from Dako (Glostrup, Denmark) and Rhodamine-conjugated goat anti-mouse IgG was from Jackson ImmunoResearch Laboratories (Suffolk, UK).

[^{3}H]-ouabain (specific activity 30 Ci/mmol) was from Perkin Elmer Italia (Monza, Italy).

If not otherwise specified, other chemicals were from Sigma (Milano, Italy).

Technical details of instruments used in the present thesis are reported in specific methods sections.

3.2. Methods

3.2.1. *In vitro* studies

3.2.1.1. Primary culture of skeletal muscle cells

Cultures were established from mouse satellite cells (Irintchev et al., 1997). Briefly, myoblasts were isolated from the hind leg muscles of 7-day-old male Balb/c mice killed by cervical dislocation as approved by the local Animal Care Committee and in agreement with the European legislation. Muscle tissue was minced and then treated with collagenase and trypsin. Expansion and enrichment of desmin-positive cells was achieved by repeated plating and cultivation in Dulbecco's modified minimal essential medium (DMEM) with D-valine containing 20% FCS. Myoblasts were maintained as exponentially growing cells in the presence of medium consisting of HAM'S F-10 containing 20% FCS, L-glutamine (2 mM), penicillin (100 units/ml), and streptomycin (100 mg/ml). To induce cell differentiation and fusion of myoblasts into myotubes, the medium was replaced with DMEM supplemented with 2% horse serum and L-glutamine, penicillin, and streptomycin as above. Undifferentiated and differentiated cells were maintained at 37°C in CO_2 (5%)-enriched air (Lorenzon et al., 2002; Luin and Ruzzier, 2007).

Experiments were performed on differentiated on myotubes between the 5^{th} and the 8^{th} day after plating. In these experimental conditions, spontaneous contractile activity was detectable as cell twitches clearly visible using a bright field microscope (20X objective).

3.2.1.2. Sulforhodamine B assay

Experiments were performed according to Dell'Ovo et al. (2008). Cells seeded in 96-wells microplates and treated with PLTX or 42-OH-PLTX according to the experimental protocol. At the end of cell treatments medium was removed. Cells were rinsed twice with PBS (100 µl), and fixed with 50 µl of 50% trichloroacetic acid (1 hour, 4°C). After fixation, cells were rinsed twice with twice-distilled water (100 µl), and an equal volume of sulforhodamine B (SRB, 0.4% in 1% acetic acid) was added. After 30 min, cells were rinsed three times with acetic acid (1%) and solubilised with 200 µl Tris (10 mM). Sample absorbance was read on an Automated Microplate Reader EL 311s (Bio-Tek Instruments; Winooski, VT) with a single wavelength of 570 nm. If not otherwise specified, experimental results are expressed as mean of at least four independent experiments performed in triplicate ± SE.

3.2.1.3. May-Grunwald Giemsa stain

At the end of treatment, cells were immediately fixed in methanol for 1 minute to stop progression of the cellular damage. Staining was started incubating cells for 5 minutes with the May-Grunwald solution. Colour excess was removed rinsing twice the dish with PBS. Second stain was performed with Giemsa solution diluted in PBS (2 times 7 minutes). At the end of incubation cells were rinsed twice with distilled water and dried prior to observation.

3.2.1.4. Atomic Force Microscopy

Single cells were analyzed using a Solver-Pro M (NT-MDT, Moscow, Russia) atomic force microscope. Living cells were scanned in a contact mode. The AFM cantilever was equipped with a PNP-DB silicon nitride tip (Nanoworld, Neuchâtel, Switzerland). Scan time was 10 minutes for 100x100 μm^2, with a

resolution of 256x256 points and pixel size 0,4x0,4 μm^2. The AFM was equipped with liquid scanning set-up and measurements were performed at room temperature. Cells were maintained in NES solution (for details see section Videoimaging) for the whole experiment. With a Solver-Pro controller it is possible to have multiple types of measurements during a single scan. For the purposes of this study, the variation of displacement along the z-axis has been recorded during the outward and return scan. Moreover the variation of lateral force (LF) was also acquired.

3.2.1.5. Videoimaging

Videoimaging experiments were carried out according to Lorenzon et al. (2002). Cells were plated on glass coverslips coated with Matrigel. Loading of the Ca^{2+} indicator fura-2 pentacetoxymethylester (fura-2 AM) was performed by incubating cells (30 min, 37°C) in a normal external solution (NES) supplemented with 1 mg/ml of bovine serum albumin and 5 mM fura-2 AM. After loading, cells were rinsed and maintained in NES for an additional 15 min at 37 °C to allow de-esterification of the dye. Experiments were performed in NES complete or with modified ionic composition, according to experimental purposes (Table V).

SOLUTION	Na^+ (mM)	K^+ (mM)	Ca^{2+} (mM)	Mg^{2+} (mM)	Cl^- (mM)	Hepes (mM)	Glucose (mM)	pH
NES	140	2.8	2	2	150.8	10	10	7.35
NES Ca^{2+} free	140	2.8	-	4	150.8	10	10	7.35
NES Na^+ free	-	2.8	2	2	150.8	10	10	7.35
NES Cl^- free	140	2.8	2	2	-	10	10	7.35

Table V. Ionic composition of normal external solutions (NES).

Ca^{2+} salts were substituted with Mg^{2+}, NaCl was replaced with N-methyl-D-glucamine chloride in Na^{+}-free solution. In Cl^{-}-free solution, all chloride salts were replaced with gluconate (K^{+}) and sulphate salts (Na^{+}, Mg^{2+} and Ca^{2+}) according to Jared et al. (2009), with slight modifications. The concentration and the composition of the cationic components were kept constant.

PLTXs and blockers (verapamil; KB-R7943; SKF-96365; lanthanum and cadmium; TTX), except those preincubated (ouabain, cyclopiazonic acid and gadolinium), were gently applied to the bathing solution by loading appropriate volumes of concentrated solution into a 5-ml syringe connected to the micro-incubator chamber. For all drugs, preliminary control experiments were performed to select a protocol (working concentrations and time exposures) that did not cause *per se* cell toxicity. The digital fluorescence-imaging microscopy system consisted of an inverted microscope (Zeiss Axiovert 135; Oberkochen, Germany) equipped with an intensified CCD camera (Hamamatsu Photonics; Hamamatsu, Japan). A temperature-controlled micro-incubator chamber (Medical Systems Corporation; Davie, Fl) maintained the temperature at 37 °C during the experiments. Loaded cells were alternatively excited at 340 and 380 nm by a modified dual wavelength microfluorimeter (Jasco CAM-230; Tokyo, Japan). The ratio of corresponding images at 340 and 380 nm and the temporal plots of the fluorescence signal were calculated offline. Being image acquisition performed at two frames/second, our time resolution was one ratio image/second. In the temporal plots (i.e. fluorescence ratio *vs* time), the fluorescence ratio at rest was assumed to be 1. Variation of the $[Ca^{2+}]_i$ was expressed as increase in fluorescent signal relative to the fluorescence ratio at rest. Each set of experiments was carried out on at least three different cell preparations. Each experimental point was expressed as mean ± SE, with *n* being the number of cells tested.

3.2.1.6. Immunocytochemistry

Myotubes were fixed in paraformaldehyde (3.7% in PBS; 15 min), permeabilized with 100% methanol and then incubated with a mouse monoclonal anti-desmin antibody (60 min; 1/50 dilution). For visualization, cells were then incubated at room temperature with Rhodamine-conjugated goat anti-mouse IgG (60 min; 1/200 dilution). For nuclear staining, bis-Benzimide H-33258 (5 min; 1/1000 dilution) was used. Slides were observed with a standard fluorescence microscope (40X objective). Observations were performed on two different cell preparations.

3.2.1.7. Binding experiments

Binding experiments were performed on differentiated myotubes seeded in 24-wells microplates. To determine the characteristic of ouabain binding of in our cellular model, preliminary experiments were performed: time-course and concentration dependence were verified before performing experiments with toxins. Once optimized incubation time and concentration of tritiated ligand, experiments were performed to measure the ability of PLTXs to displace [^{3}H]-ouabain from its binding site. To reach equilibrium between bound and unbound [^{3}H]-ouabain cells were pre-incubated with 100 µM of the ligand for 90 min. Displacement reaction started with the addition of increasing concentrations of PLTXs. Both toxins and [^{3}H]-ouabain were diluted in NES (composition in Table V, section 3.2.1.5. Videoimaging). At the end of incubation (90 minutes at 37°C), the reaction was blocked by fast aspiration of the surnatant. Cells were rinsed twice with ice cold buffer in order to remove unbound [^{3}H]-ouabain. At this point, cells were lysed with 250 µL NaOH (1 M) supplemented with 1% Sodium Dodecyl Sulphate. The lysate (200 µL) was then transferred in a reading plate and SuperMix scintillation cocktail was added (250 µL per well). The plate was read in a MicroBeta Trilux counter (Wallac, Turku, Finland). In

parallel, to ensure that cellular viability was not decreased during the treatment, event that *per se* would trigger cellular detachment and decrease [^{3}H]-ouabain binding, cytotoxicity assessment was also performed. Twenty-four wells microplates, identical to that used for binding experiments, were incubated with toxins and cold ouabain to exactly as in binding experiments. At the end of incubation cellular mass was measured with SRB assay, following the protocol described in section 3.2.1.2.

3.2.1.8. Statistical analysis

Data are given as means ± SE. The Student's *t* test was used to examine statistical significance at $p < 0.05$ level.

3.2.2. *In vivo* studies

3.2.2.1. Experimental design

Groups of six female mice were treated at each dose level of PLTX (30, 90, 180 μg/kg) or vehicle (PBS). The toxin was administered daily by gavage at 10 ml/kg, adjusted on the basis of mouse weight. Control animals received the vehicle alone (PBS) at the same volume. After dosing, the mice were observed at regular intervals. Symptoms and mortality were recorded every 30 minutes within the first 3 hours post administration and again at longer times. Body weight and cage food consumption were recorded daily in the morning, before treatment. After 7 days of treatment, animals were weighed and anesthetized with ketamine hydrochloride and sacrificed (350 mg/kg; Inoketam100; Virbac; Milan, Italy). The main organs (see paragraph 2.6) were removed weighed and fixed in neutral buffered 10 % formalin. Animals that died during the observation period were immediately weighed and

necropsied; as previously described, the main organs and tissues were collected, weighed and fixed for the histological evaluations.

3.2.2.2. Recovery

In order to evaluate progression or recovery of the changes induced by the administration of PLTX some mice of each dose group were kept for a 14-day withdrawal period. As previously described, lethality symptoms, food consumption and body weight were recorded daily. After 14 days, mice were subjected to necropsy; the main organs and tissues were collected weighted and fixed for histological evaluations (see paragraph 3.2.2.3.).

3.2.2.3. Light microscopy

Heart, liver, lungs, kidneys, spleen, stomach, duodenum, jejunum, colon, rectum, pancreas, thymus, cerebrum, cerebellum, spinal cord, uterus, ovaries and skeletal muscle (soleus) were embedded in paraffin and sectioned (5 μm). Sections were deparaffinized, rehydrated and stained with haematoxylin-eosin, following standard techniques for histological analyses by light microscopy. Histopathological examination by light microscopy was carried out in a blinded study. Pictures were obtained with a Nikon eclipse *i* 50 microscope equipped with a DS-Vi1 digital camera and NIS-Elements Microscope Imaging Software (all from Nikon Instruments Europe) and presented at the magnitude indicated in the legends.

4. RESULTS

4.1. Results *in vitro*

4.1.1. Toxicity of PLTXs on differentiated skeletal muscle cells

In order to characterize the toxicity induced by PLTX and 42-OH-PLTX, the two molecules were tested on primary cultures of differentiated skeletal muscle cells (Figure 7 and 8).

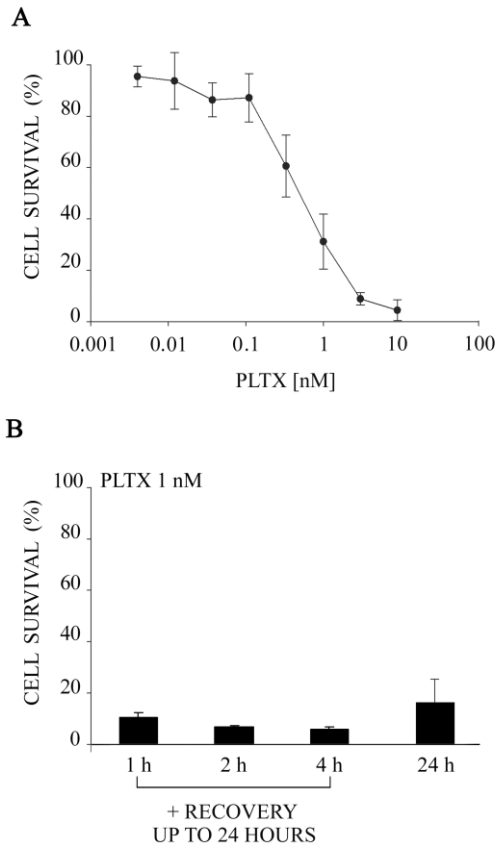

Figure 7. Toxicity of PLTX on mouse skeletal muscle cells assessed by sulforhodamine B assay. (*A*) Cell survival after 24 hours of exposure to increasing concentrations of PLTX. (*B*) Cell survival after 1, 2, or 4 hours of exposure to PLTX (1 nM) and recovery up to 24 hours in toxin-free medium compared to 24 hours of continuous exposure.

The toxic effect of PLTX and 42-OH-PLTX was measured using the sulforhodamine-B after 24 hours of incubation (Figure 7*A* and 8*A*).

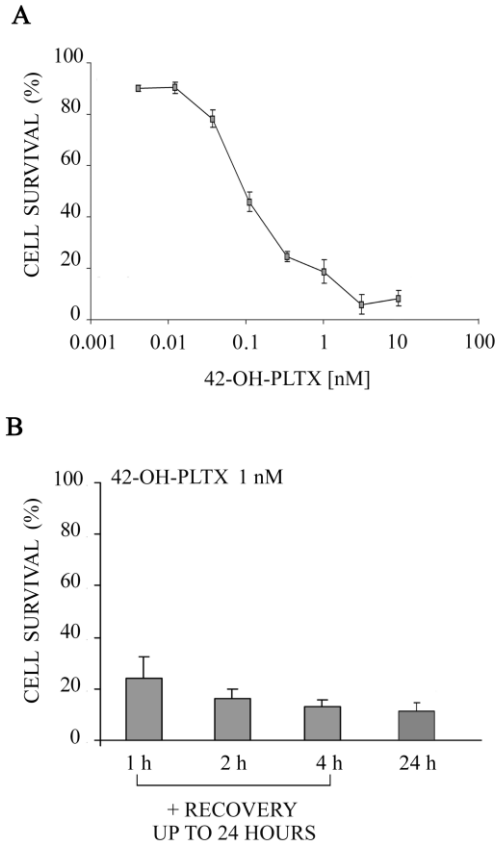

Figure 8. Toxicity of 42-OH-PLTX on mouse skeletal muscle cells assessed by sulforhodamine B assay. (*A*) Cell survival after 24 hours of exposure to increasing concentrations of PLTX. (*B*) Cell survival after 1, 2, or 4 hours of exposure to PLTX (1 nM) and recovery up to 24 hours in toxin-free medium compared to 24 hours of continuous exposure.

Both toxins induced cellular damage already at subnanomolar concentrations. Starting from the concentration of 0.012 nM the spontaneous contractile activity of the cultured myotubes, visible in bright field microscopy as cell twitching, was completely abolished.

However, at this concentration, the cellular damage was hardly appreciable at morphological level.

PLTX and 42-OH-PLTX caused a concentration-dependent decrease of cell viability, detectable from the concentration of 0.037 nM. At this concentration, the mean reduction of viable cells was around 20% (Figure 7*A* and 8*A*). A 100 % toxicity was observed after incubation with PLTXs at the concentration of 3 nM or higher.

From the analysis of the data the mean Effective Concentration on the 50 % of the cellular population (EC_{50}) was estimated as:

$$EC_{50} \text{ (PLTX)} = 0.54 \text{ nM} \pm 0.07$$

$$EC_{50} \text{ (42-OH-PLTX)} = 0.36 \text{ nM} \pm 0.06$$

In order to establish if the cellular damage induced by PLTXs was directly related to the presence of the toxin into the cellular medium or, if a short time exposure could be sufficient to trigger the toxic effect, a second set of experiments was planned. In more detail, toxins were added to the culture medium for a short time (1, 2 or 4 hours) and then removed rinsing culture wells. Complete, toxin-free, medium was then restored and cellular viability was measured after 24 hours of recovery. The withdrawal of the toxin from the culture medium did not influence the development of cytotoxicity in the following 24 hours (Figure 7*B* and 8*B*). Thus, the brief exposures of skeletal muscle cells to PLTX and 42-OH-PLTX induced a decrease in cell viability similar to that recorded after 24 hours of continuous exposure.

4.1.2. Effects of PLTXs on the cell morphology

During toxicity studies, it was evident that differentiated skeletal muscle cells underwent prominent morphologic changes. After the addition of the toxins to the culture medium, cellular rounding and vacuolation were observed within few hours (Figure 9).

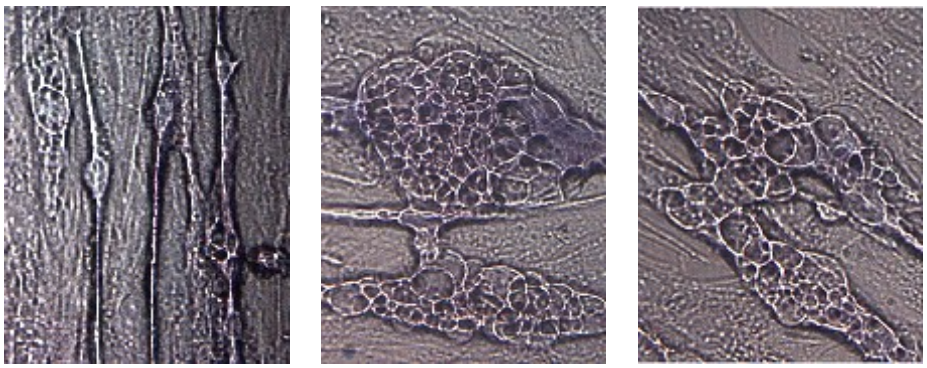

A. Control B. PLTX C. 42-OH-PLTX

Figure 9. Light micrographs of skeletal muscle cells. Control condition (*A*) or after 2 hours incubation with 1 nM PLTXs (*B*, *C*). May-Grunwald Giemsa Stain. 40x.

The morphology of the treated cells, obtained with the immunolabeling for the intermediate filament desmin, confirmed the harmful effect of the toxins. After treatment with PLTXs (24 hours, 0.1 nM), disorganisation of the desmin architecture, associated with a loss of the normal fibre shape, was observed in comparison to controls (Figure 10).

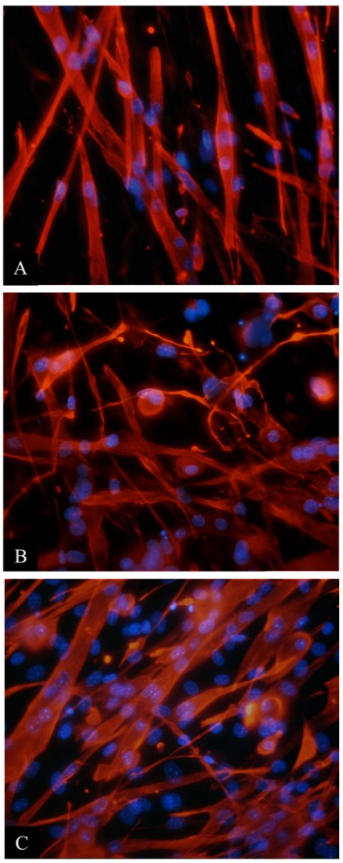

Figure 10. Effect of PLTXs on cytoarchitecture of mouse skeletal muscle cells. Representative images of control culture (*A*) and after incubation for 24 hours with 0.1 nM PLTX (*B*) and 42-OH-PLTX (*C*). Cells were stained for desmin (red) and nuclei (blue). See Materials and Methods for further details. Magnification 20X in (*A*), (*B*) and (*C*).

To quantify the progression of the morphological alteration of the cells incubated with PLTX, a series of experiments with atomic force microscope was performed. The variation of displacement along the z-axis was recorded during the outward and return scan. Cells were scanned before toxin addition, as control (Figure 11*A*), and after toxin

application to the external bathing solution (Figure 11*B*-*F*) up to 50 minutes post-exposure. Experiments revealed a mean increase of cellular volume of 9.0 ± 3.4 % (n = 5 cells) associated to cell swelling.

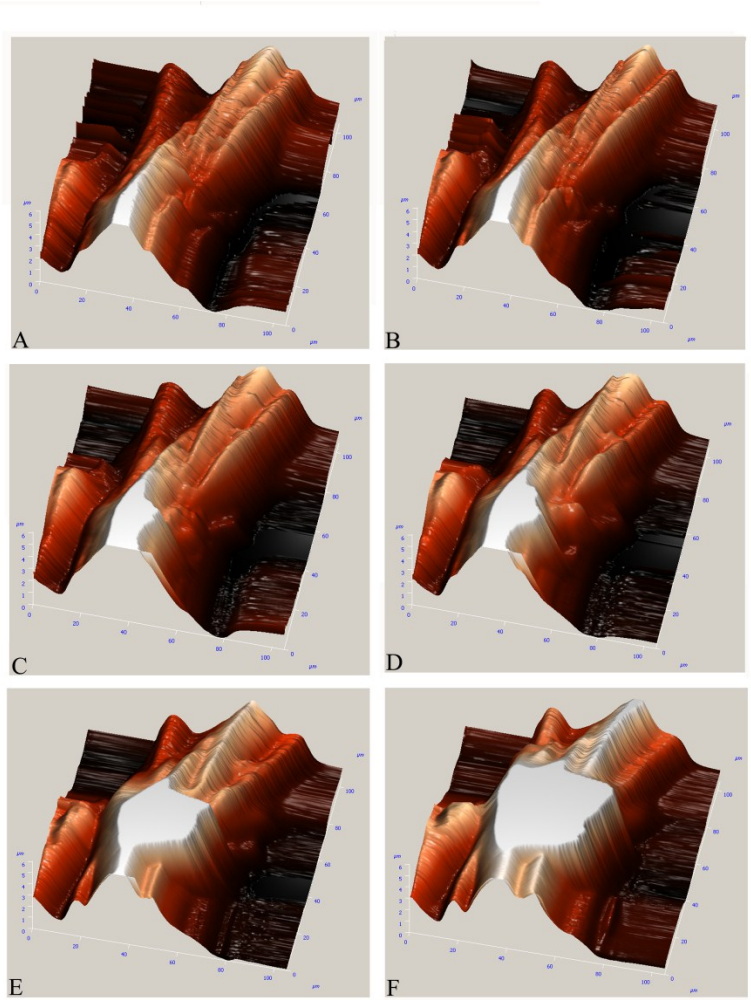

Figure 11. Atomic force microscopy of skeletal muscle cells. Representative 3 dimension image of a skeletal muscle cell in control conditions (*A*) and after the addition of 6 nM PLTX (*B*- *F*). Axes: x 0-100 µm, y 0-100 µm, z 0-6 µm.

In addition, a decrease adherence of the cells was noticed. Loss of cell adhesion determined cellular shift during the acquisition as revealed by

the comparison between outward (Figure 12*A*) and return scan (Figure 12*B*).

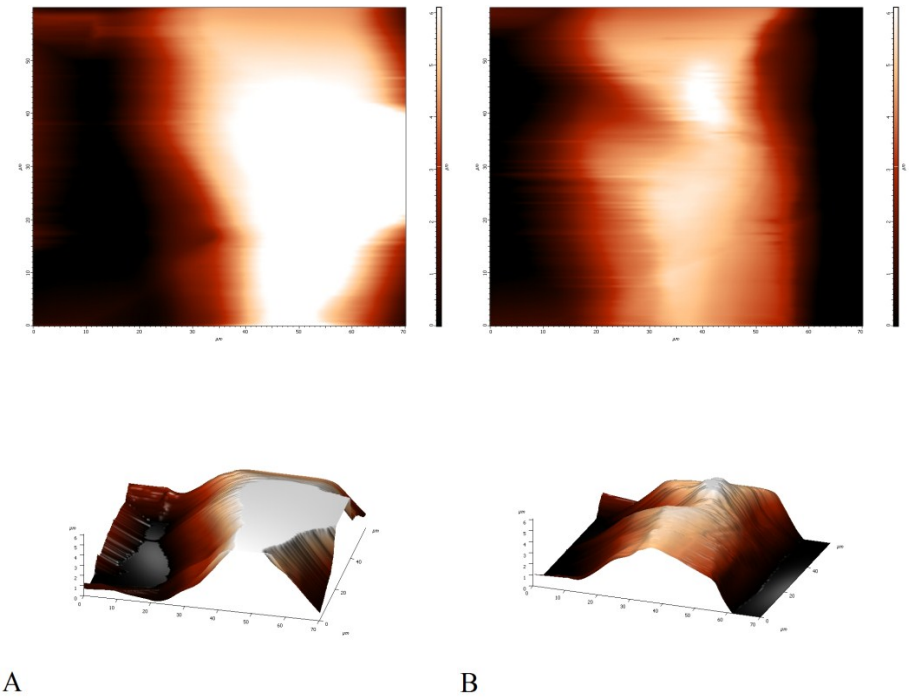

A B

Figure 12. Atomic force microscopy of skeletal muscle cells. Representative cellular shift during acquisition after 50 min of incubation with 6 nM (axes: *x* 0-70 µm, *y* 0-60 µm, *z* 0-6 µm). The same cell is shown in 2 D (upper panel) and in 3 D (lower pannel) *A*. Acquisition during outward scan. *B*. Acquisition during return scan.

4.1.3. Effect of PLTXs on cell response to Acetylcholine

In order to evaluate the functional activity of skeletal muscle cells after exposure to PLTXs, the responsiveness of myotubes to the neurotransmitter acetylcholine (ACh) was tested. In physiological condition, the neurotransmitter ACh binds to the ionotropic receptors

expressed in skeletal muscle cells; the binding of ACh causes a conformational change of the receptor that allows a Na^+ influx into the cell. The Na^+-mediated depolarization triggers the opening of the voltage-sensitive Ca^{2+} channels and, consequently, an increase of the $[Ca^{2+}]_i$. In line with this, cellular response to ACh was assessed measuring the $[Ca^{2+}]_i$ by the videoimaging technique (Figure 13).

All the experiments were performed after 24 hours of incubation with the toxins at concentration of 0.1 nM. This concentration was chosen because, even if the cellular damage was already appreciable, the viability was maintained in approximately 80 % of the cells (Figure 7*A* and 8*A*). Cells incubated with the two toxins maintained the same sensitivity to ACh observed in controls (100 %). In spite of that, the amplitude of the $[Ca^{2+}]_i$ transients elicited by the neurotransmitter was considerably reduced in cells treated with PLTXs, being 6 times lower (Figure 13*A*). In control dishes, the mean value of the $[Ca^{2+}]_i$ increase after the addition of ACh (20 μM) was 130.2 ± 11.8 % (n = 37 cells); the mean $[Ca^{2+}]_i$ increase in the cells incubated with PLTX (0.1 nM) was approximately 21.8 ± 5.8 % (*n* = 20 cells). The ACh response in the cells incubated with 42-OH-PLTX was significantly higher than that of the cells treated with the parent PLTX. In particular, the amplitude of the transient was almost 3 times higher than that obtained with PLTX treated cells (65.6 ± 13.2 %; *n* = 38 cells; Figure 13*B*).

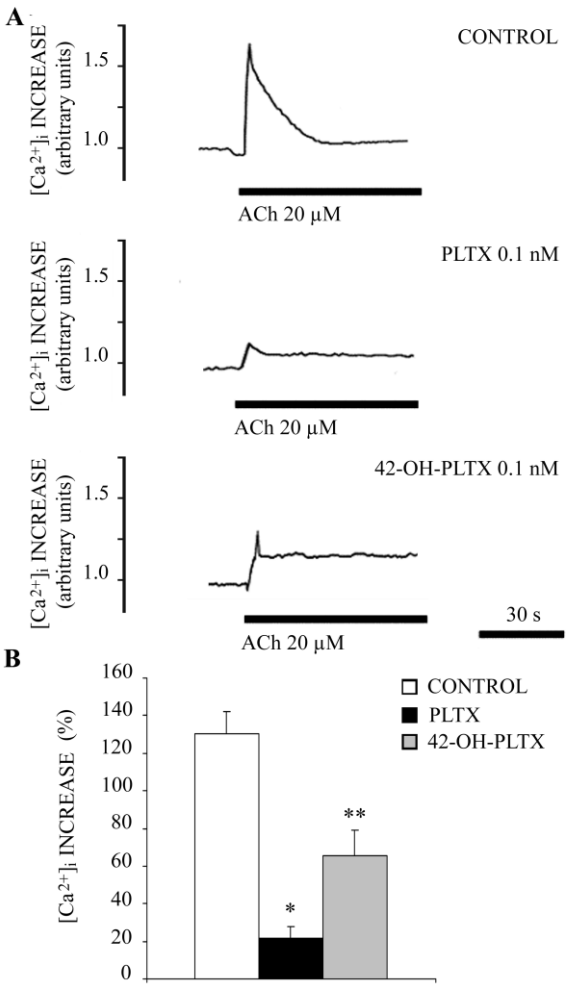

Figure13. Functional response of skeletal muscle cells after incubation with PLTXs. (*A*) Representative temporal plots of the Ca^{2+} response induced by ACh (20 µM) in control conditions and after 24 hours incubation with 0.1 nM PLTX (n = 20 cells) or 42-OH-PLTX (n = 38 cells). (*B*) Mean increase of $[Ca^{2+}]_i$ after the stimulation with ACh (20 µM) in cells incubated for 24 hours with 0.1 nM PLTX (n = 20 cells) or 42-OH-PLTX (n = 38 cells) in comparison to controls (n = 37 cells; * and ** $p < 0.05$ at the Student's t-test as compared to controls).

4.1.4. $[Ca^{2+}]_i$ increase induced by PLTXs

PLTX and 42-OH-PLTX caused a significant biphasic increase in $[Ca^{2+}]_i$ (Figure 14 and 15). Changes in $[Ca^{2+}]_i$ levels began with a transitory increase (transient phase). The transient usually peaked within 20 s and was followed by a slower increase that reached a plateau within 300 s and remained unchanged even 30 minutes after the toxin application (long-lasting phase). Even if the kinetic of PLTX-induced $[Ca^{2+}]_i$ increase was quite reproducible, with the two phases clearly distinguishable, the amplitude of the increase resulted to be more variable. Rise in $[Ca^{2+}]_i$ reached during transient and long-lasting phases can range from values around 50 % to nearly double, with an increase of 100 %.

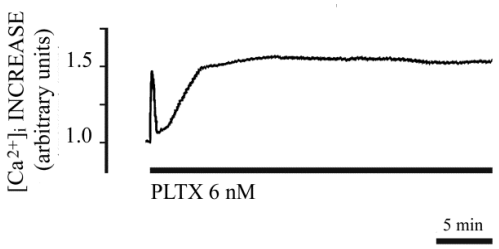

Figure14. Effect of PLTX on the $[Ca^{2+}]_i$ of mouse skeletal muscle cells. Representative temporal plot of the biphasic $[Ca^{2+}]_i$ increase induced by PLTX (6 nM).

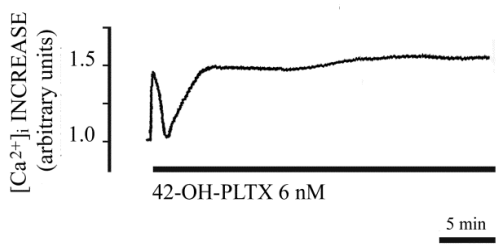

Figure15. Effect of 42-OH-PLTX on the $[Ca^{2+}]_i$ of mouse skeletal muscle cells. Representative temporal plot of the biphasic $[Ca^{2+}]_i$ increase induced by 42-OH-PLTX (6 nM).

Dose-response experiments revealed a good correlation between the concentration of toxins used in the experiments and the number of responsive cells, in a concentration range between 0.67 and 6 nM. (Figure 16).

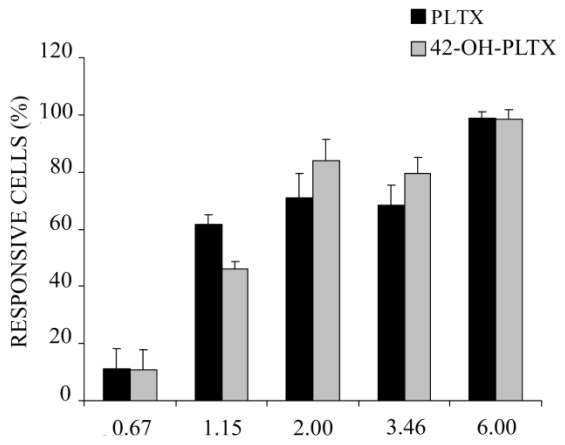

Figure 16. Cell responsivity to PLTXs. The percentage of responsive cells in terms of increase of the $[Ca^{2+}]_i$ after the addition of PLTXs to the extracellular medium followed a dose-response relationship (each experimental point is mean of at least n = 20 cells observed).

At the concentration of 0.67 nM, the number of responsive cells was around 10 % and reached the maximum at the concentration of 6 nM.

4.1.5. Contribution of extracellular Na^+ and Ca^{2+} in the mechanism of action of PLTXs

In order to investigate the influence of extracellular sodium ($[Na^+]_e$) in PLTXs-induced $[Ca^{2+}]_i$ increase, experiments were performed in absence of the extracellular cation. The absence of Na^+ in the extracellular solution (for further detail see Materials and Methods), completely abolished the $[Ca^{2+}]_i$ increases triggered by the two toxins (Figure 17 and 18).

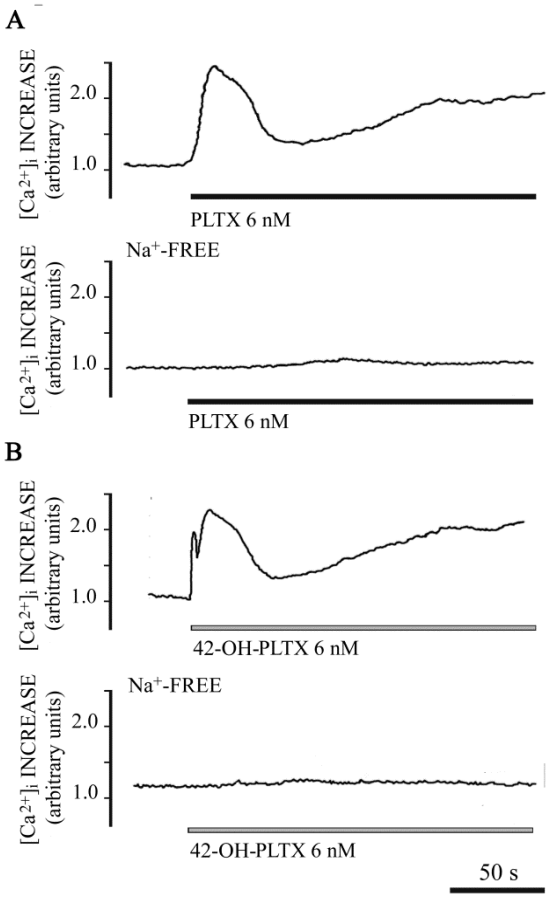

Figure 17. Effect of Na^+-free on PLTX and 42-OH-PLTX induced $[Ca^{2+}]_i$ transients. Representative temporal plots of the $[Ca^{2+}]_i$ variations induced by 6 nM PLTX (*A*) and 42-OH-PLTX (*B*), in the presence or in the absence of $[Na^+]_e$.

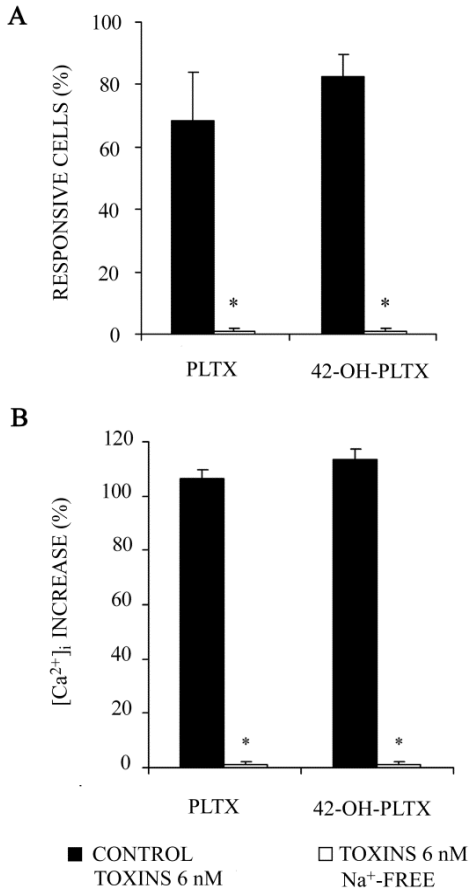

Figure 18. Effect of Na^+-free on cell response to PLTX and 42-OH-PLTX. . Percentage of responsive cell (*A*) and $[Ca^{2+}]_i$ increase (*B*) after addition of 6 nM PLTXs in control conditions (black) or in the absence of $[Na^+]_e$ (white) (* $p < 0.05$ in comparison to 6 nM PLTXs as control; $n = 15$ cells).

Since in Na^+-free solution PLTXs-induced $[Ca^{2+}]_i$ increase was completely abolished, the influence of the role of voltage-dependent Na^+ channels was investigated. To this aim, the widely used blocker TTX was employed. TTX 1 μM completely abolished the cellular response to PLTX (Figure 19*A* and 20; $n = 19$ cells). On the contrary, 42-OH-PLTX was still able to trigger a transient $[Ca^{2+}]_i$ increase

(Figure 19*B* and 20; n = 19 cells), but lower than that elicited by the toxin alone.

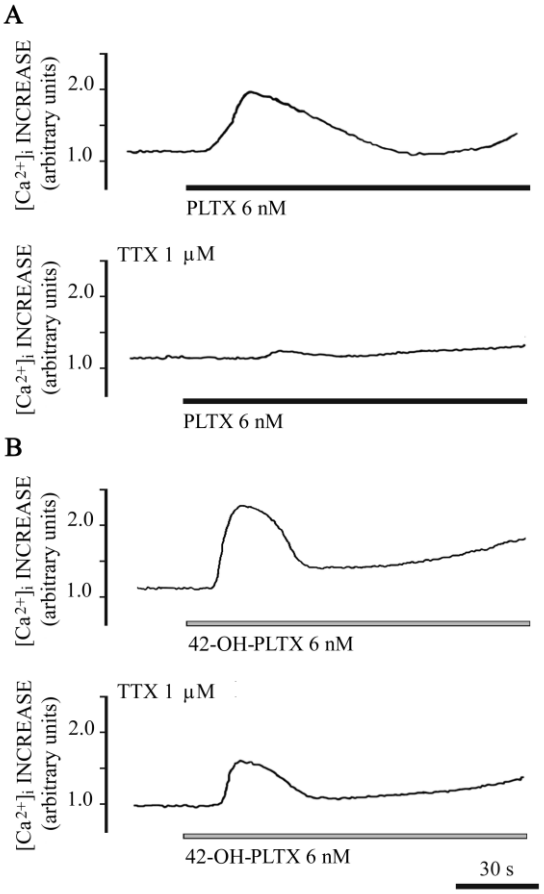

Figure 19. Effect of TTX on PLTX and 42-OH-PLTX induced $[Ca^{2+}]_i$ transients.. Representative temporal plots of the biphasic $[Ca^{2+}]_i$ increase induced by 6 nM PLTX (*A*) and 42-OH-PLTX (*B*) in the absence or in the presence of 1 μM TTX.

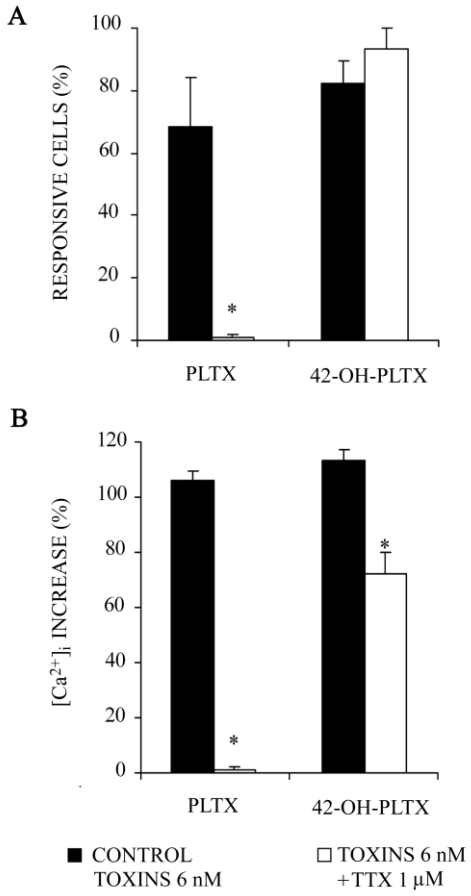

Figure 20. Effect of TTX on cell response to PLTX and 42-OH-PLTX. Percentage of responsive cell (*A*) and $[Ca^{2+}]_i$ increase (*B*) after addition of 6 nM PLTXs alone (black) or in the presence of 1 μM TTX (white) (* $p < 0.05$ in comparison to 6 nM PLTXs as control; $n = 19$ cells).

A set of videoimaging experiments were also performed in the absence of extracellular Ca^{2+} ($[Ca^{2+}]_e$; Figure 21 and 22).

As previously described for experiments performed without $[Na^+]_e$, also in the absence of $[Ca^{2+}]_e$ the cellular answers triggered by PLTX and 42-OH-PLTX were completely abolished (Figure 21 and 22).

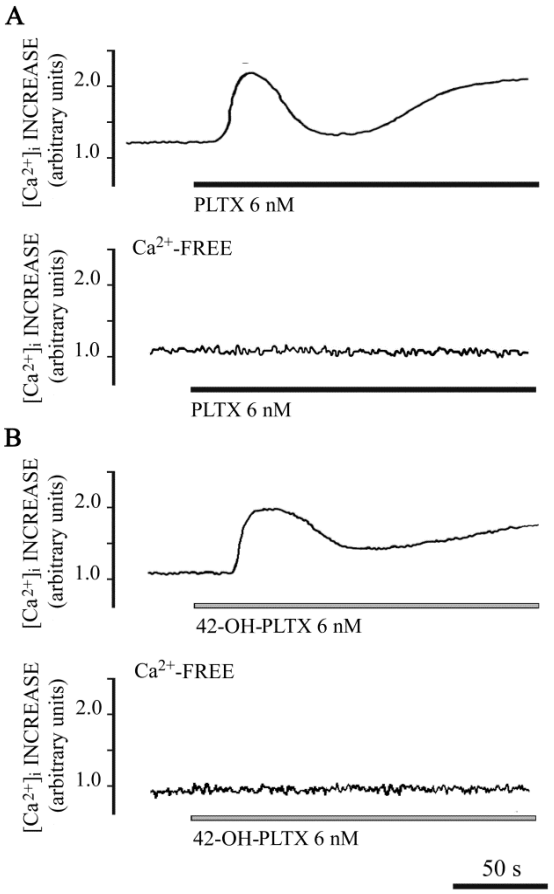

Figure 21. Effect of Ca^{2+}-free on PLTX and 42-OH-PLTX induced $[Ca^{2+}]_i$ transients. Representative temporal plots of the $[Ca^{2+}]_i$ increase induced by 6 nM PLTX (*A*) and 42-OH-PLTX (*B*), in the presence or in the absence of $[Ca^{2+}]_e$.

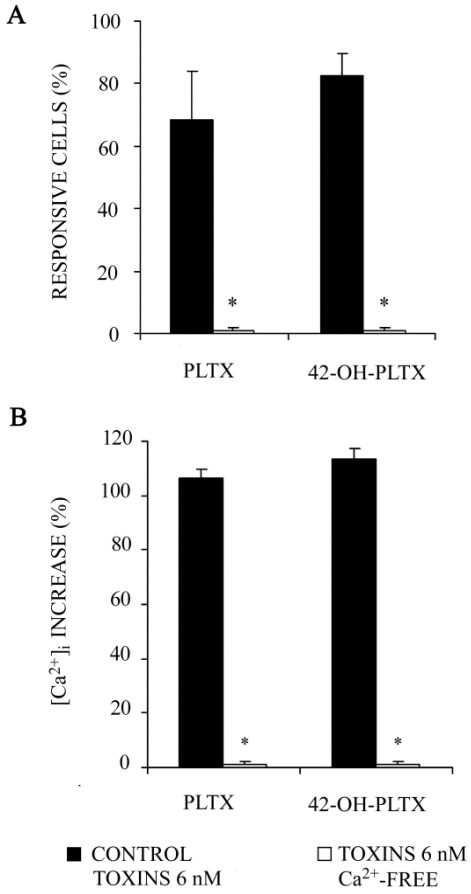

Figure 22. Effect of Ca^{2+}-free on cell response to PLTX and 42-OH-PLTX. Percentage of responsive cell (*A*) and $[Ca^{2+}]_i$ increase (*B*) after addition of 6 nM PLTXs in the presence (black) or in the absence of $[Ca^{2+}]_e$ (white). (* $p < 0.05$ in comparison to 6 nM PLTXs as control; $n = 15$ cells).

A number of experiments was planned to analyse the cytotoxicity induced by PLTXs in the absence of $[Na^+]_e$ or $[Ca^{2+}]_e$. SRB assay revealed that the absence of Na^+ or Ca^{2+} in the extracellular milieu prevent the development of the toxic insult independently from the exposure times to PLTXs (Figure 23 and 24).

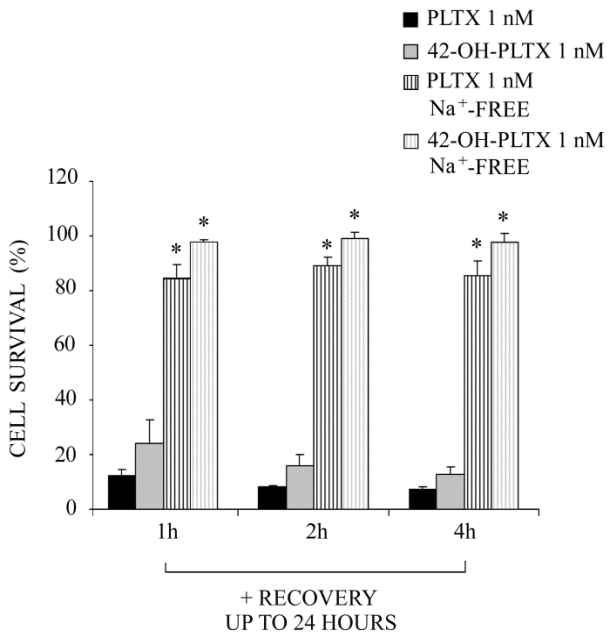

Figure 23. Toxicity of PLTX on mouse skeletal muscle cells assessed by sulforhodamine B assay. Cell survival after 1, 2, or 4 hours of exposure to PLTXs (1 nM) and recovery up to 24 hours in toxin-free medium. (* $p < 0.05$ in comparison to control; $n = 3$).

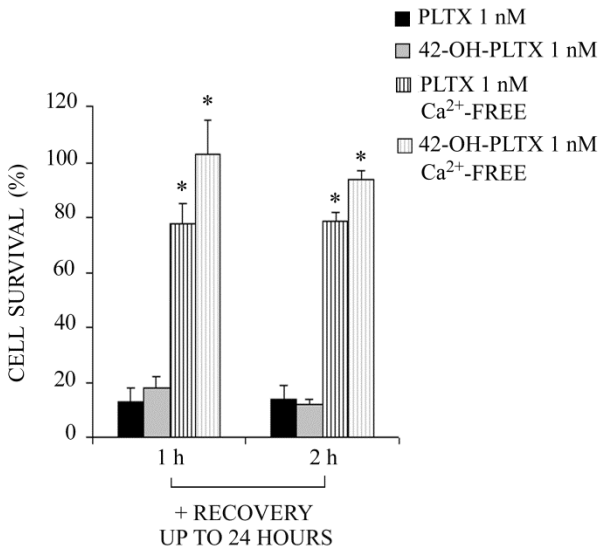

Figure 24. Toxicity of PLTX on mouse skeletal muscle cells assessed by sulforhodamine B assay. Cell survival after 1 or 2 hours of exposure to PLTXs (1 nM) and recovery up to 24 hours in toxin-free medium. (* $p < 0.05$ in comparison to control; $n = 3$).

4.1.6. Influence of Ca^{2+} on PLTX binding

Binding experiments have been performed to verify the interaction of PLTXs with the Na^+/K^+ pump in the absence of $[Ca^{2+}]_e$. Since radioactive PLTXs are not commercially available, an indirect approach was applied; [^{3}H]-ouabain, was used as radiolabelled ligand and experiments were performed to measure the ability of PLTX and 42-OH-PLTX to displace it.

First of all, the reversibility of the binding between [^{3}H]-ouabain and intact skeletal muscle myotubes was verified and the concentration-dependence relationship was established (Figure 25).

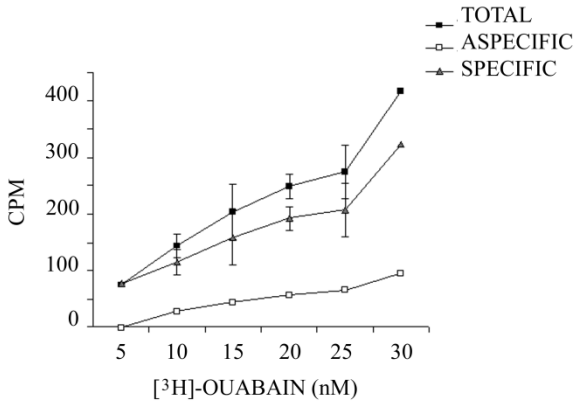

Figure 25. [^{3}H]-ouabain binding on skeletal muscle cells. CPM detected on skeletal muscle cells after 90 minutes of incubation with increasing concentrations of [^{3}H]-ouabain. Data are the mean of 4 independent experiments performed in triplicate ± S.E.

The concentration of 15 nM [^{3}H]-ouabain was chosen for the displacement binding assays.

The total binding of [^{3}H]-ouabain (Figure 26, grey triangles) was slightly reduced in presence of Ca^{2+}, however the difference was not significant.

In the presence of extracellular Ca^{2+} (control), PLTX started to displace [^{3}H]-ouabain from the concentration of 3 nM. Increasing the concentration of PLTX (10 nM), a significant reduction of the binding of [^{3}H]-ouabain was observed (mean reduction of about 60 %). On the contrary, no significant displacement of [^{3}H]-ouabain occurred when the same experiment was conducted, adding PLTX in the absence of $[Ca^{2+}]_e$.

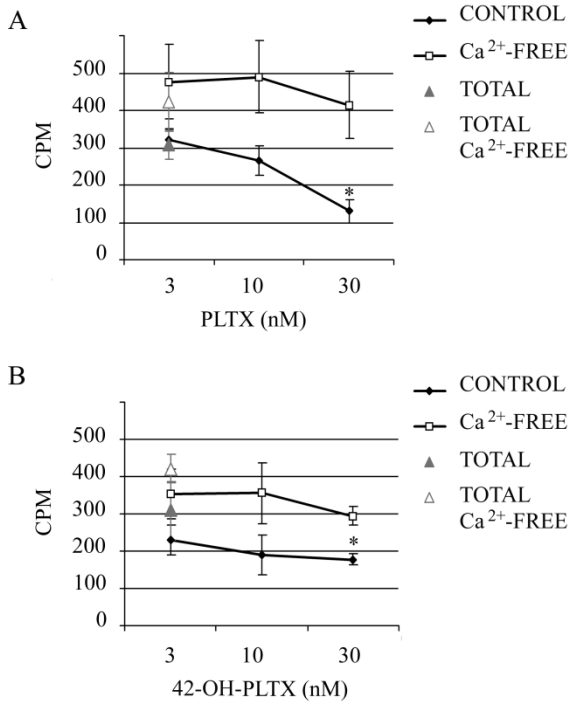

Figure 26. PLTX binding on skeletal muscle cells. CPM detected on skeletal muscle cells after 90 minutes of incubation with increasing concentrations of PLTX (*A*) or 42-OH-PLTX (*B*), in presence of 15 nM [^{3}H]-ouabain. Data are the mean of 3 (*A*) and 2 (*B*) independent experiments performed in triplicate ± S.E. (* p <0.05 at the Student's t-test as compared to control).

Similarly, the addition of 42-OH-PLTX (1, 3, 10 nM) to the skeletal myotubes in presence of [^{3}H]-ouabain caused a concentration-dependent displacement of the tritiated molecule. As previously observed for PLTX, in Ca^{2+}-free external solution, the ability of 10 nM 42-OH-PLTX to displace [^{3}H]-ouabain was reduced in comparison to controls.

4.1.7. Contribution of Ca^{2+} stores to the $[Ca^{2+}]_i$ increase and cytotoxicity induced by PLTX

In order to verify the role of intracellular Ca^{2+} stores in the $[Ca^{2+}]_i$ increase triggered by PLTX, videoimaging experiments were performed in the presence of 1 μM cyclopiazonic acid (Cyc; Figure 27), a well-known blocker of the sarcoplasmic Ca^{2+}-ATPase pump (Plenge-Tellechea et al., 1997). By blocking the pump, cyclopiazonic acid causes emptying of the intracellular Ca^{2+} reservoir and abolishes any possible contribution of Ca^{2+} release from intracellular stores. Pre-incubation with cyclopiazonic acid significantly decreased the amplitude of the transient phase of the $[Ca^{2+}]_i$ increase triggered by PLTX (control 6nM PLTX: 49.7 ± 4.7 % of $[Ca^{2+}]_i$ increase *versus* 6 nM PLTX in Cyc: 7.6 ± 3.7 %), but did not decreased the amplitude of the long-lasting phase (n = 12 cells; Figure 27).

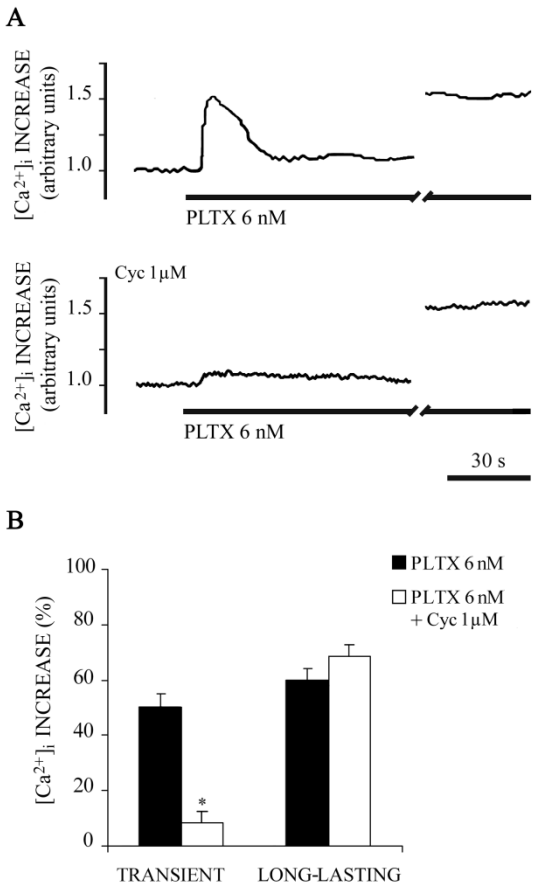

Figure 27. Contribution of intracellular Ca^{2+} stores to the $[Ca^{2+}]_i$ increase elicited by PLTX. (*A*) Representative temporal plots of $[Ca^{2+}]_i$ response after addition of 6 nM PLTX in control conditions and in the presence of 1 µM Cyc. Trace interruption stands for 30 minutes. (*B*) Effect of depletion of the intracellular Ca^{2+}stores on amplitude of transient and long-lasting phases of the $[Ca^{2+}]_i$ increase (* $p < 0.05$ in comparison to 6 nM PLTX; $n = 12$ cells).

4.1.8. Contribution of Ca^{2+} influx to the $[Ca^{2+}]_i$ increase and cytotoxicity triggered by PLTX

Videoimaging experiments were performed in cells bathed in an external solution without Ca^{2+} but preserving the ionic strength of it. To do this, Ca^{2+} was substituted with equimolar concentration of Mg^{2+} (Figure 28).

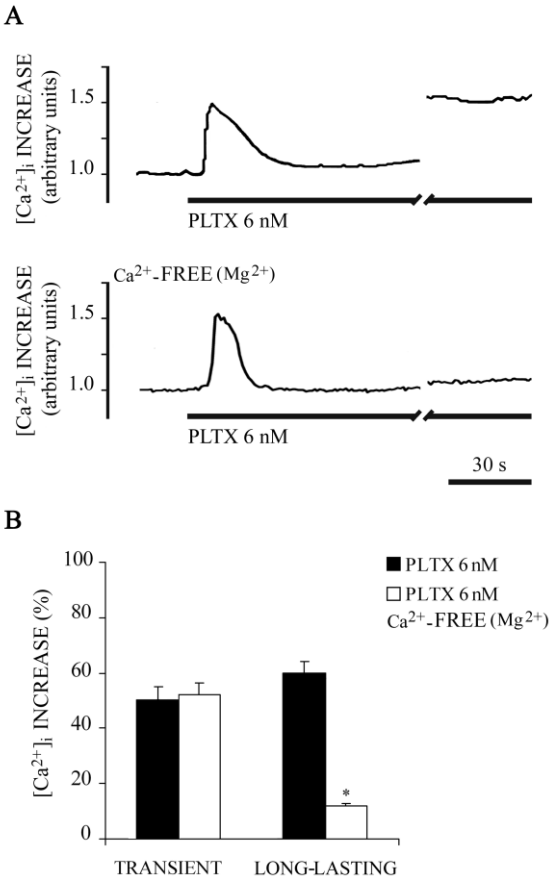

Figure 28. Contribution of extracellular Ca^{2+} influx to the $[Ca^{2+}]_i$ increase induced by PLTX. (*A*) Representative temporal plots of $[Ca^{2+}]_i$ measured in mouse skeletal muscle cells after addition of PLTX (6 nM) in control and Ca^{2+}-free conditions (Ca^{2+} replaced with Mg^{2+}). Trace interruption stands for 30 minutes. (*B*) Effect of the absence of extracellular Ca^{2+} on the amplitude of transient and the long-lasting phases of the $[Ca^{2+}]_i$ increase (* $p < 0.05$ in comparison to 6 nM PLTX; $n = 28$ cells).

In this experimental condition, the transient phase of the $[Ca^{2+}]_i$ increase was not altered (52.3 ± 4.3% higher than basal $[Ca^{2+}]_i$; n = 28 cells), but the absence of extracellular Ca^{2+} almost abolished the long-lasting phase, whose amplitude was reduced to 11.9 ± 1.0 % (n = 28 cells; Figure 28).

SRB experiments were performed incubating cells with toxin in presence of 1 µM Cyc or in Ca^{2+}-free solution, following the same protocol described for videoimaging experiments (Figure 29). The presence of Cyc did not affect the PLTX-induced cytotoxic effect. Interestingly, when Ca^{2+} in the extracellular solution was replaced with Mg^{2+}, toxicity was completely prevented. This results strongly suggested a correlation between the long-lasting phase of the $[Ca^{2+}]_i$ transient induced by PLTX and its toxicity.

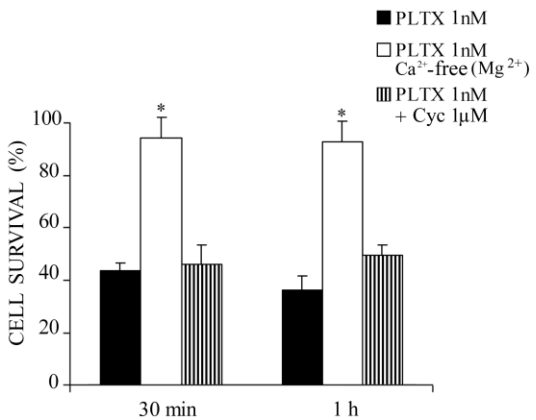

Figure 29. Contribution of extracellular and intracellular Ca^{2+} to PLTX toxicity. Cell survival measured after 30 minutes and 1 hour of incubation with PLTX (1 nM) in Ca^{2+}-free solution or in presence of 1 µM Cyc, compared to control (* $p < 0.05$ in comparison to 1 nM PLTX).

4.1.9. Extracellular Ca^{2+} influx through voltage-dependent channels and Na^{+}/Ca^{2+} exchanger

In our experimental model (more than 5 days of differentiation), the prevalent class of voltage-dependent Ca^{2+} channels expressed by myotubes is the L-type (Luin et al., 2007). For this reason, we planned to study the response of PLTX in the presence of the specific blocker verapamil (20 μM) (Flockerzi et al., 1986). Verapamil decreased by nearly 60 % the amplitude of the transient phase of the Ca^{2+} response elicited by 6 nM PLTX in comparison to controls. However, it did not affect the long-lasting phase (*n* = 34 cells; compare Figure 30*A* and *B*; Figure 30*F*). The non selective blockers of the voltage-dependent Ca^{2+} channels cadmium (500 μM) and lanthanum (100 μM) had similar effects, inhibiting the transient (*n* = 12 cells) but not the long-lasting phase (*n* = 12 cells; compare Figure 30*A* and *C*; Figure 30*F*). These results ruled out the possibility that voltage-operated Ca^{2+} channels other than L-type were involved in the long-lasting phase of the $[Ca^{2+}]_i$ increase.

To test the role of the Na^{+}/Ca^{2+} exchanger, cells were exposed to 6 nM PLTX in the presence of 5 μM KB-R7943, which prevents the reverse mode of the exchanger (Naro et al., 2003).

As observed with verapamil, KB-R7943 inhibited the transient phase by ~ 30 %, (*n* = 42 cells) and did not alter the sustained phase of PLTX-induced Ca^{2+} response (Figure 30*A* and *D*; Figure 30*F*). The long-lasting phase of the $[Ca^{2+}]_i$ increase remained unchanged even when 6 nM PLTX was added to the cells in presence of both blockers (*n* = 46 cells; Figure 30*A* and *E*; Figure 30*F*).

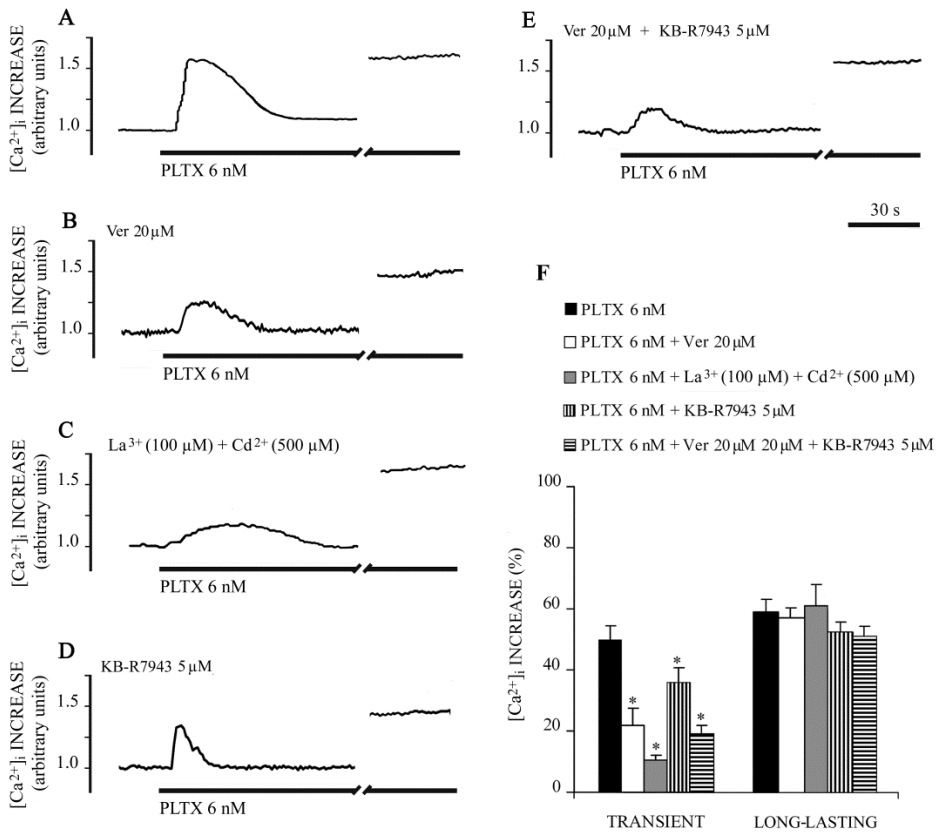

Figure 30. Contribution of L-type channels and Na^+/Ca^{2+} exchanger (reverse mode) to the $[Ca^{2+}]_i$ increase induced by PLTX. Representative temporal plots of $[Ca^{2+}]_i$ after addition of PLTX (6 nM) in control conditions (*A*), in the presence of 20 µM verapamil (*B*; $n = 34$ cells), 100 µM La^{3+} and 500 µM Cd^{2+} (*C*; $n = 12$), 5 µM KB-R7943 (*D*; $n = 42$ cells), or Ver and KB-R7943(*E*; $n = 46$ cells). Trace interruption stands for 30 minutes. (* $p < 0.05$ in comparison to 6 nM PLTX).

The effect of verapamil and KB-R7943 on $[Ca^{2+}]_i$ increase induced by 42-OH-PLTX, was even more limited than for the parent compound (Figure 31).

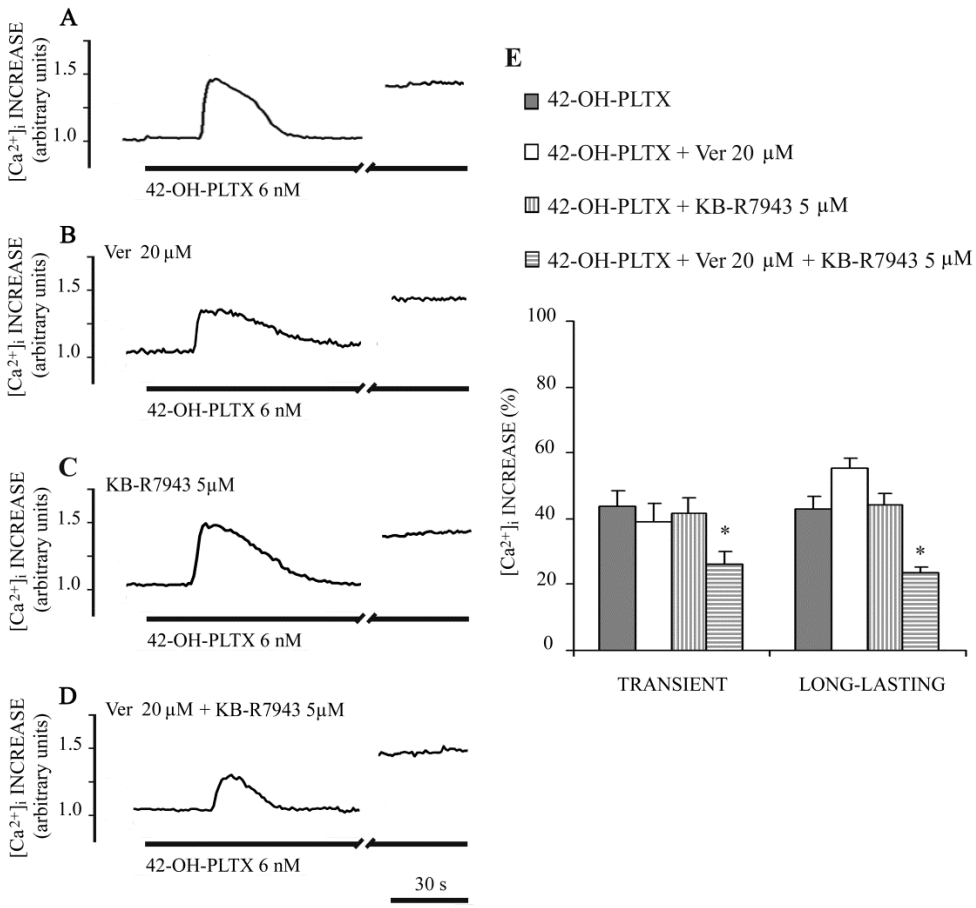

Figure 31. Contribution of L-type channels and Na^+/Ca^{2+} exchanger (reverse mode) to the $[Ca^{2+}]_i$ increase induced by 42-OH-PLTX. Representative temporal plots of $[Ca^{2+}]_i$ after addition of 42-OH-PLTX (6 nM) in control conditions (*A*), in the presence of 20 µM verapamil (*B*; n = 34 cells), 5 µM KB-R7943 (*C*; n = 42 cells), or Ver and KB-R7943 (*D*; n = 46 cells). Trace interruption stands for 30 minutes (* $p < 0.05$ in comparison to 6 nM 42-OH-PLTX).

Verapamil altered neither the amplitude of the transient phase (39.1 ± 5.3 %; n = 42 cells) nor the delayed and long-lasting increase of the $[Ca^{2+}]_i$ (55.5 ± 3.0 %, n = 42 cells; Figure 31*A-B* and *E*). Similar effects were also observed after incubation with KB-R7943 (Figure 31*A-C* and *E*).

The only experimental conditions able to reduce $[Ca^{2+}]_i$ increase triggered by 42-OH-PLTX was the concomitant addition of the two blockers. In this case, the transient phase of the $[Ca^{2+}]_i$ increase was reduced to 26.2 ± 3.7 % (*n* = 38 cells) and the long-lasting phase to 23.6 ± 1.7 % (*n* = 38 cells). We have also checked possible beneficial effect of verapamil and KB-R7943 in reducing and/or slowing down the progression of the cytotoxicity of PLTXs The presence of the blockers did not prevent or inhibit the development of the cytotoxic effect induced by PLTX and 42-OH-PLTX (Figure 32).

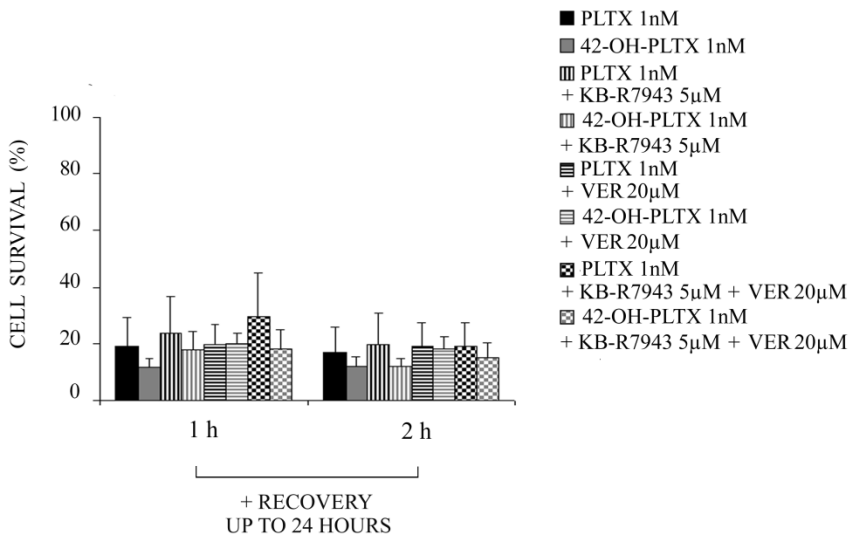

Figure 32. Contribution of L-type channels and Na^+/Ca^{2+} exchanger (reverse mode) to the toxicity of PLTX on mouse skeletal muscle cells. Cell survival after 1 or 2 hours of exposure to 1 nM PLTX (black) and 42-OH-PLTX (grey) and recovery up to 24 hours. Experiments were performed with toxins alone (full bars), in presence of KB-R7943 (horizontal bars), verapamil (vertical bars) or both (squared bars) (* $p < 0.05$ in comparison to control; $n = 3$).

4.1.10. Extracellular Ca^{2+} influx through voltage-independent Ca^{2+} channels and its contribution to the cytotoxicity

The contribution of store-operated and stretch-activated channels to the Ca^{2+} influx triggered by 6 nM PLTX was investigated using SKF-96365 or gadolinium (Gd^{3+}), widely used as blockers of both voltage-independent channel types (Molgo et al., 1991; Hamill and McBride, 1996; Ducret et al., 2006; Formigli et al., 2007; Ducret et al., 2010). Videoimaging experiments showed that, in cell preincubated with 20 μM SKF-96365 (30 min at 37 °C), the first transient of the Ca^{2+} response elicited by PLTX was significantly decreased (by ~ 75 %; 16.1 ± 5.2 % of $[Ca^{2+}]_i$ increase) compared to controls. The long-lasting phase was reduced, but the effect of SKF-96365 was not statistically significant (n = 18; Figure 33).

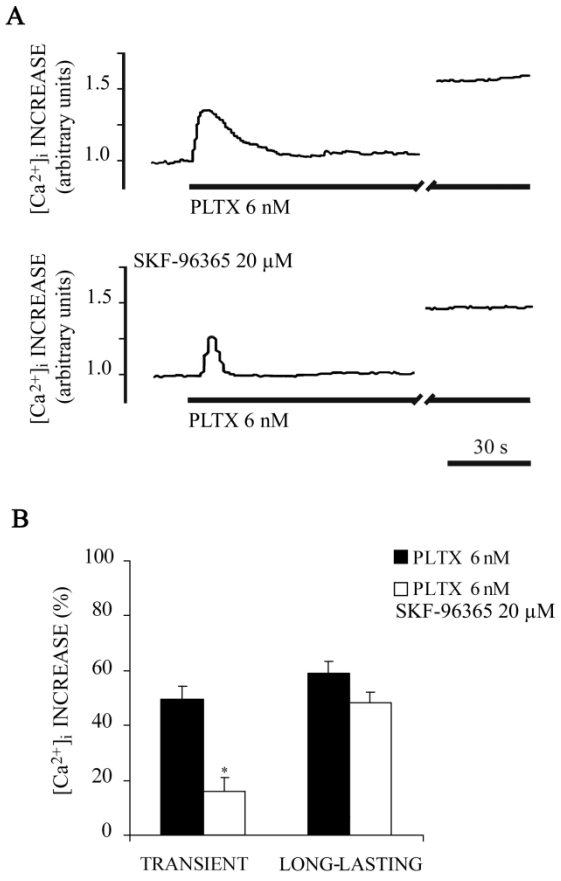

Figure 33. Contribution of store-operated Ca^{2+}-channels to the $[Ca^{2+}]_i$ increase induced by PLTX. (*A*) Representative temporal plots of $[Ca^{2+}]_i$ after addition of PLTX (6 nM) in control conditions or presence of SKF-96365 20 µM. Trace interruption stands for 30 minutes. (*B*) Effect of SKF-96365 on the two phases of the PLTX-induced $[Ca^{2+}]_i$ increase (* $p < 0.05$ in comparison to 6 nM PLTX; $n = 18$ cells).

Gd^{3+} did not significantly affect the amplitude of the transient phase of the PLTX-induced response ($n = 45$ cells). However, Gd^{3+} markedly decreases the long-lasting phase of the $[Ca^{2+}]_i$ increase ($n = 45$ cells; Figure 34).

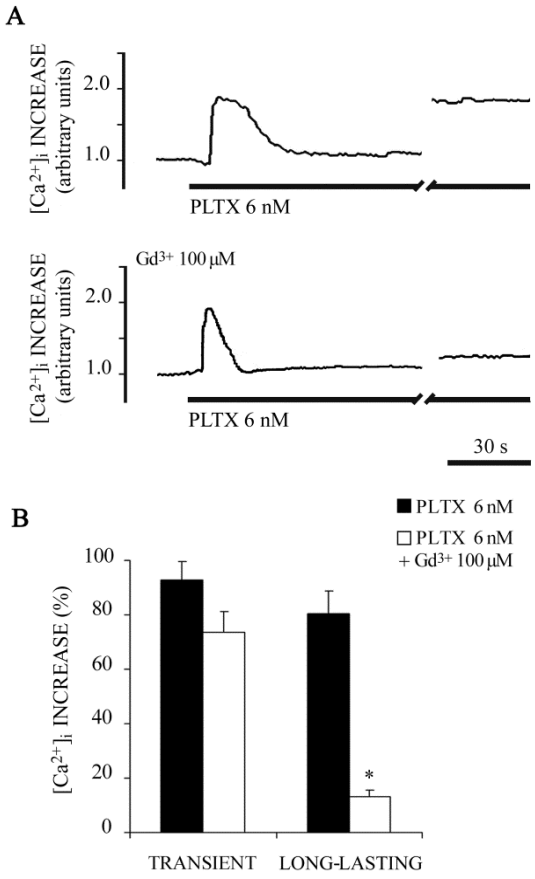

Figure 34. Contribution of stretch-activated Ca^{2+}-channels to the $[Ca^{2+}]_i$ increase induced by PLTX. (*A*) Representative temporal plot of $[Ca^{2+}]_i$ after addition of PLTX (6 nM) in control conditions or presence of 100 µM Gd^{3+}. Trace interruption stands for 30 minutes. (*B*) Effect of Gd^{3+} on the two phases of the PLTX-induced $[Ca^{2+}]_i$ increase (* $p < 0.05$ in comparison to 6 nM PLTX; $n = 45$ cells).

The washout of Gd^{3+}resulted in a restoration of the long-lasting Ca^{2+} signal induced by PLTX ($n = 17$ cells; Figure 35).

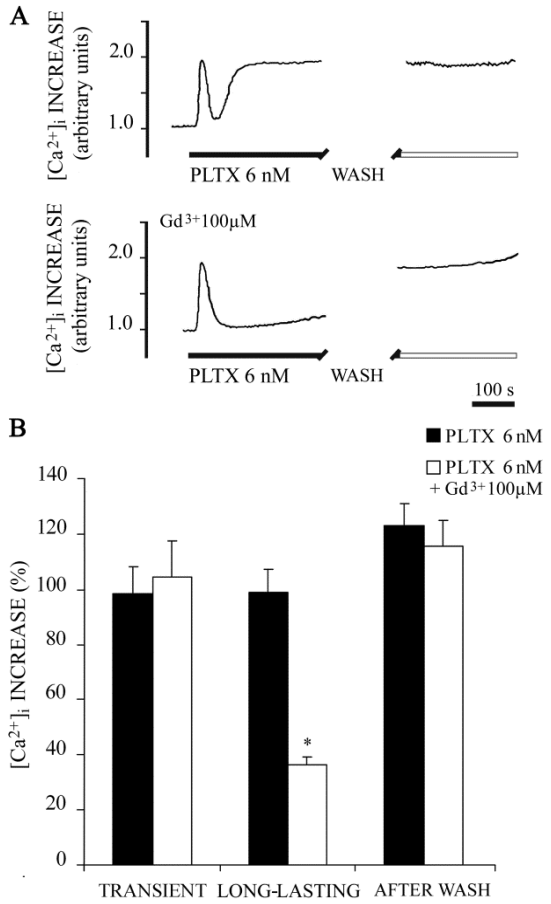

Figure 35. Contribution of stretch-activated Ca^{2+}-channels to the $[Ca^{2+}]_i$ increase induced by PLTX. (*A*) Representative temporal plot of $[Ca^{2+}]_i$ after addition of PLTX (6 nM) in control conditions or presence of 100 µM Gd^{3+}. Trace interruption represents wash necessary for toxin removal. (*B*) Effect of washout procedure on PLTX-induced $[Ca^{2+}]_i$ increase in control conditions (black bars) and in presence of Gd^{3+} (white bars) (* $p < 0.05$ in comparison to 6 nM PLTX; $n = 17$ cells).

To confirm the connection between the long-lasting phase of $[Ca^{2+}]_i$ increase triggered by PLTX and toxicity, sulforhodamine B assay was performed in the presence of Gd^{3+}. Under these conditions, the

cytotoxicity of PLTX was significantly reduced with a 30% increase in cell survival after 1 h exposure to 1 nM PLTX (Figure 36).

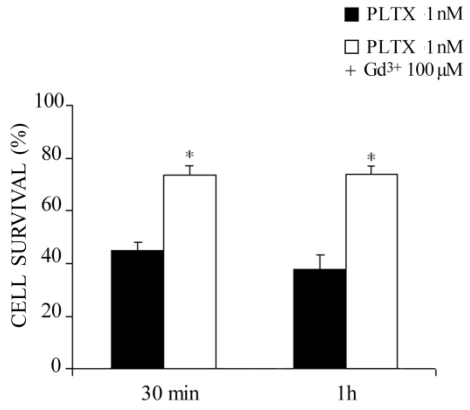

Figure 36. Contribution of stretch-activated Ca^{2+}-channels to the toxicity induced by PLTX. Cell survival measured after 30 minutes and 1 hour of incubation with PLTX (1 nM) in presence of 100 µM Gd^{3+} compared to controls (* $p < 0.05$ in comparison to 1 nM PLTX; $n = 4$ independent experiments performed in triplicate).

Cytotoxicity test were also performed incubating the cells in the presence of 20 µM SKF-96365. No effect was observed (Figure 37).

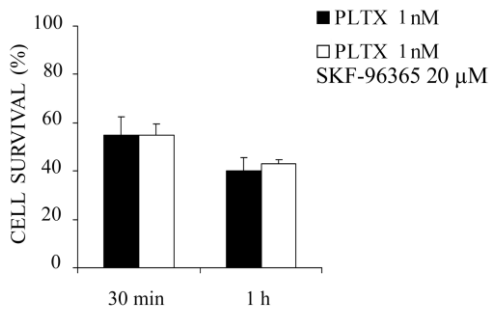

Figure 37. Effect of the broad spectrum Ca^{2+}-channels blocker SKF-96365 to the toxicity induced by PLTX. Cell survival measured after 30 minutes and 1 hour of incubation with PLTX (1 nM) in the presence of 20 µM SKF-96365 compared to controls (* $p < 0.05$ in comparison to 1 nM PLTX, $n = 3$ independent experiments performed in triplicate).

Since the activation of stretch-activated Ca^{2+} channels and the consequent $[Ca^{2+}]_i$ increase seems to play a crucial role in the mechanism of action of PLTX, further experiments were performed to deepen their correlation with the development of the myotoxic insult. The activation of stretch-activated Ca^{2+} channels is known to trigger ROS production in skeletal muscle cells and PLTX by itself triggers the production of reactive oxygen species in several cell models (Sala et al., 2009; Pelin et al., 2011). For these reasons it was decided to verify if a radical scavenger could prevent, or at least reduce, PLTX-induced damage on skeletal muscle cells. With this aim, the well-known antioxidant Trolox was tested. The presence of 100 µM Trolox significantly reduced PLTX-induced toxicity on myotubes during the first 30 min of exposure to the toxic insult; the protective effect of trolox decreases within 1 h and was completely lost after 2 h (Figure 38).

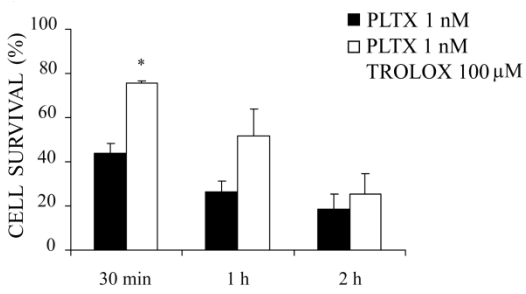

Figure 38. Contribution of ROS to PLTX toxicity. Cell survival measured after 30 minutes, 1 and 2 hours of incubation with PLTX (1 nM) in presence of 100 µM Trolox compared to controls (* $p < 0.05$ in comparison to 1 nM PLTX; n =3 independent experiments performed in triplicate).

4.1.11. Contribution of Cl^- to the PLTX-induced toxicity

Since channels and exchangers for Cl^- have been related to the development of PLTX-induced toxicity (Pérez-Gómez et al., 2010), some experiments were carried out to investigate this aspect. We observed that the cytotoxic effect of PLTX was dependent on the presence of $[Cl^-]_e$: the absence of the anion in the extracellular solution protected skeletal muscle cells from PLTX-induced damage. In more detail, we observed that the absence of $[Cl^-]_e$ prevented the acute damage induced by PLTX (Figure 39).

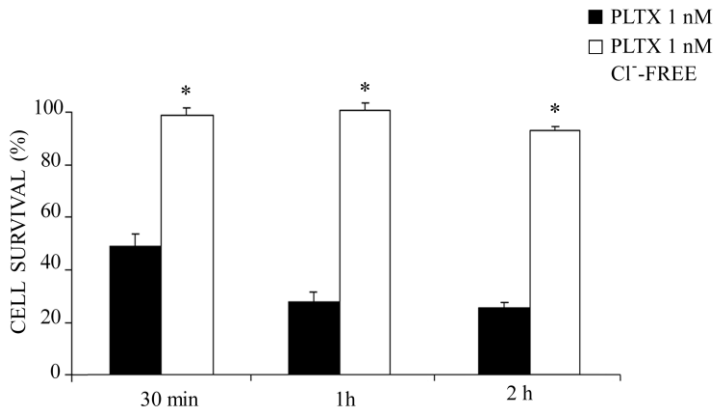

Figure 39. Effect of Cl^--free solution on PLTX-induced acute toxicity. Cell survival measured after 30 min, 1 h and 2 h of incubation with PLTX (1 nM) in the presence or in the absence of $[Cl^-]_e$ compared to control (* $p < 0.05$ in comparison to 1 nM PLTX; $n = 3$ independent experiments performed in triplicate).

The absence of $[Cl^-]_e$ prevented the toxic effects that usually develop within 24 h *post* PLTX application, but only when the incubation with the toxin lasted no more than 1 h (Figure 40).

In parallel, the effect of 1 mM DIDS (4,4'diisothio-cyanatostilbene-2,2'-disulfonic acid) an inhibitor of Cl^- channels, was also studied. Although the blocker is among those characterised by wider spectra, it was not as efficient as Cl^--free conditions in blocking toxicity. However, the cell survival in presence of DIDS was significantly higher than in the presence of the toxin alone (Figure 40).

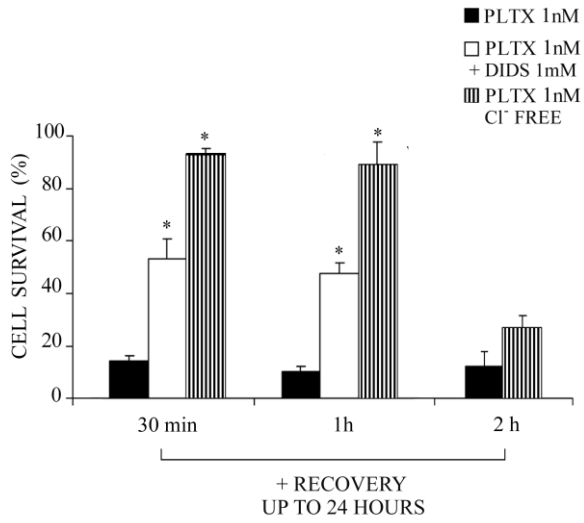

Figure 40. Effect of Cl^--free solution on PLTX-induced delayed toxicity. Cell survival measured after 30 min, 1 h and 2 h of incubation with PLTX (1 nM) in the presence or in the absence of extracellular Cl^- and 1 mM DIDS followed by recovery up to 24 hours, compared to control (* $p < 0.05$ in comparison to 1 nM PLTX; $n = 3$ independent experiments performed in triplicate).

Videoimaging experiments were then performed to evaluate the effect of Cl^--free conditions on PLTX- induced $[Ca^{2+}]_i$ transients (Figure 41).

In Cl^--free conditions, the toxin was still able to cause an increase of the $[Ca^{2+}]_i$, however the amplitude of the transient phase (42.6 ± 6.0 % of $[Ca^{2+}]_i$ increase, $n = 10$ cells) and of the long lasting phase (69.6 ± 5.0 %) appeared reduced (Figure 41).

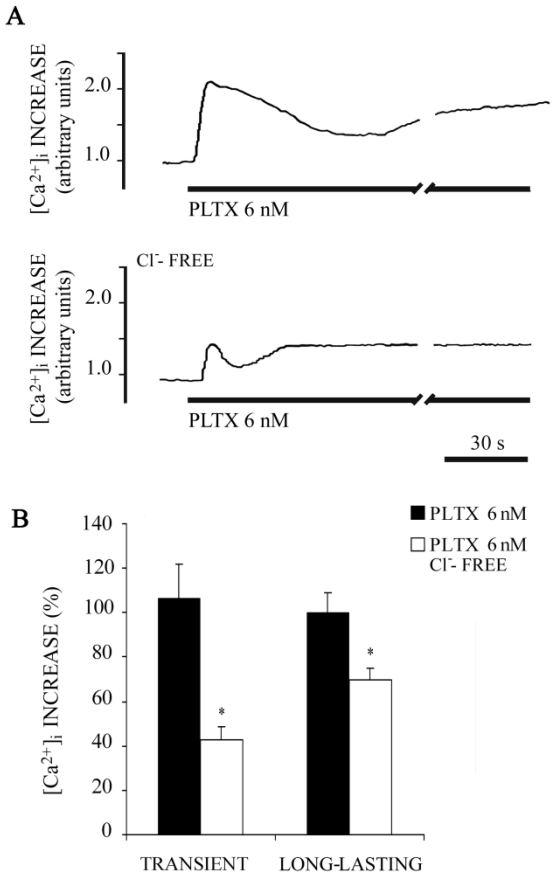

Figure 41. Effect of Cl^--free conditions on the $[Ca^{2+}]_i$ increase induced by PLTX. (*A*) Representative temporal plots of $[Ca^{2+}]_i$ measured in mouse skeletal muscle cells after addition of PLTX (6 nM) in control and Cl^--free conditions. Trace interruption stands for 30 minutes. (*B*) Effect of the absence of extracellular Cl^- on the amplitude of thetransient and the long-lasting phases of the $[Ca^{2+}]_i$ increase (* $p < 0.05$ in comparison to 6 nM PLTX; $n = 10$ cells).

To further analyse the role of Cl^- ions, the activation of Ca^{2+}-activated Cl^- channels was also investigated. To this aim a derivative of niflumic acid was used (Figure 42).

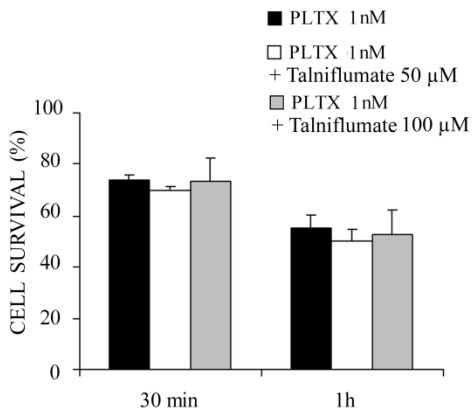

Figure 42. Contribution of Ca^{2+}-dependent Cl^- channels to PLTX-induced toxicity. Cell survival measured after 30 min and 1 h of incubation with PLTX (1 nM; black bars) in presence or absence of Talniflumate 50 and 100 µM (white and grey bars, respectively) (* $p < 0.05$ in comparison to 1 nM PLTX; $n = 3$ independent experiments performed in triplicate).

Results excluded any significant role of Ca^{2+}-dependent Cl^- channels in the cytotoxicity induced by PLTX.

4.1.12. Structure activity relationship: PLTX-analogue OST-D

To further investigate the correlation between structural variation of PLTXs and biological responses of skeletal muscle cells in relation to toxicity, additional experiments were performed with OST-D. Videoimaging experiments revealed that OST-D triggers an $[Ca^{2+}]_i$ increase different from that triggered by commercial PLTX (Figure 43).

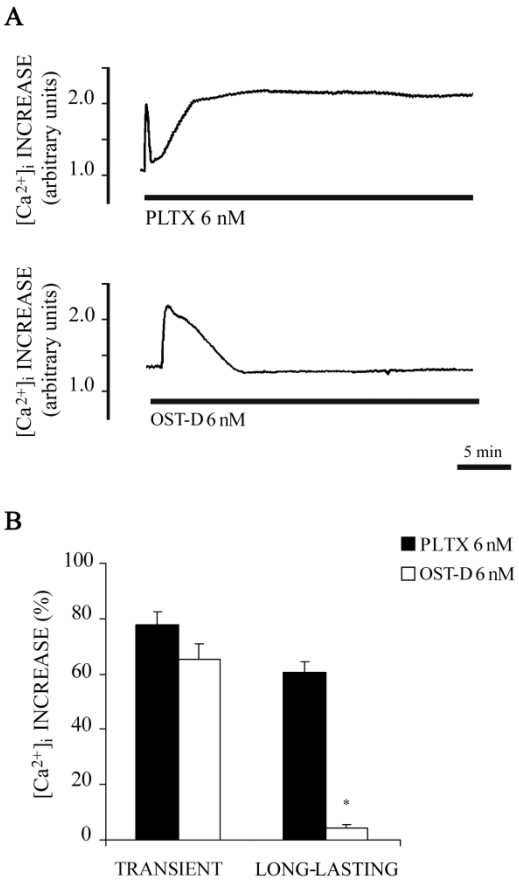

Figure 43. Effect of PLTX and OST-D on the $[Ca^{2+}]_i$ of mouse skeletal muscle cells. (*A*) Representative temporal plots of $[Ca^{2+}]_i$ after addition of PLTX (6 nM) or OST-D (6 nM). (*B*) Quantification of toxins-induced $[Ca^{2+}]_i$ increase: PLTX (black bars) and OST-D (white bars) (* $p < 0.05$ in comparison to 6 nM PLTX; $n = 40$ cells).

In more detail, the transient phase of $[Ca^{2+}]_i$ increase was comparable in cells stimulated with the two toxins (6 nM PLTX, 77.3 ± 4.8 % *versus* OST-D, 65.0 ± 5.4 % of $[Ca^{2+}]_i$ increase). On the contrary, in cells stimulated with the analogue, the second long lasting phase of the $[Ca^{2+}]_i$ increase was completely abolished.

Cytotoxicity was measured after 24 hours of incubation with OST-.D (concentration range from 0.004 to 9 nM), following the same experimental protocol used to assess cytotoxicity of PLTX and 42-OH-PLTX (Figures 7*A* and 8*A*). The EC_{50} for OST-D was 2.5 ± 0.05 nM, thus five times higher than the parent compound. Thus, OST-D resulted less cytotoxic than parent compound.

4.2. *In vivo* studies

To characterize the effects of oral intake of PLTX, as possible seafood contaminant, a sub-acute toxicity study was performed in mice. Groups of 6 mice were daily administered with the toxin (30, 90, 180 µg/kg/die) for 7 days, and observed up to 24 h (3 mice) or 14 days (3 mice) after the last treatment.

4.2.1. Lethality

Daily repeated oral administration of PLTX for 7 days (30, 90, 180 µg/kg/day) caused mortality at all the doses tested. Up to 24 hours after the last treatment, lethality was observed in a dose-dependent manner (Figure 44*A*).

In fact, 2/6 mice treated with 30 µg PLTX/kg, 2/6 mice treated with 90 µg/kg and 5/6 mice with 180 µg/kg died during the observation period.

Analysis of lethality *versus* time (Figure 44*B*), revealed that mortality started after the 3rd day of treatment.

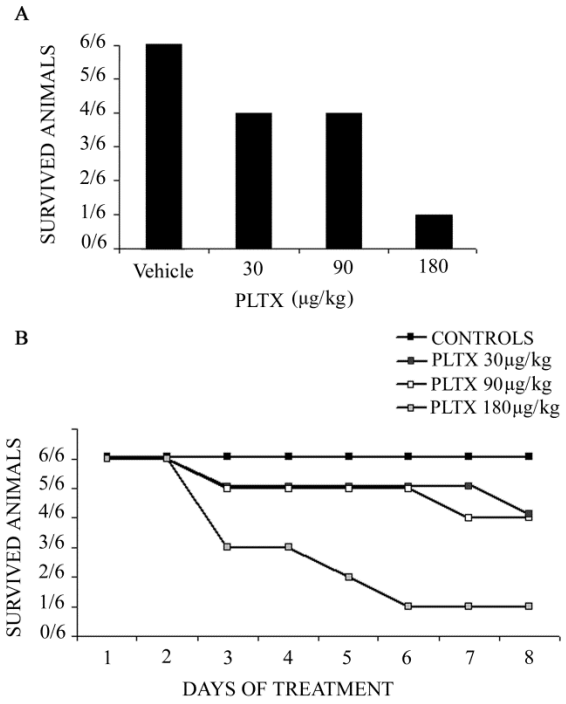

Figure 44. Lethality recorded during the first 8 days of treatment. Dose-dependent lethality (*A*). Time-dependent lethality (*B*).

4.2.2. Symptoms

Animals that died during the treatment presented several signs and symptoms involving both the gastrointestinal apparatus and other systemic targets, possibly the central nervous system.

One of the most peculiar signs observed during the p.o. administration of PLTX was swelling of the abdominal cavity. In particular, this sign was recorded from the 3rd day of toxin administration (30 µg/kg) in 4/6 animals and also in 3/6 animals treated with 90 µg/kg. At the dose of 180 µg/kg, abdominal swelling was recorded just in 1/6 mice that died during the observation period.

In general, immediately before death, loss of coordination and hypo-reactivity were observed. General sedation, persistent also after mild stimulation, was associated to loss of the righting reflex and, in the worst cases, to paralysis of the hind limbs.

Breathing difficulties and gasping were also observed in some cases prior to death, indicating severe impairment of respiratory function.

Even if the mortality was lower in mice treated with 30 and 90 μg/kg with respect to the highest administered dose, signs of general malaise during the period of toxin administration were also recorded. In particular, presence of chromodacryorrhoea (visible as a red secretion around the eyes) was visible in 2/6 and 1/6 animals treated with PLTX at 30 and 90 μg/kg, respectively.

4.2.3. Body weight

During the whole study, body weight of the animals was monitored daily. All the animals underwent prominent decrease of body weight prior to death (Figure 45).

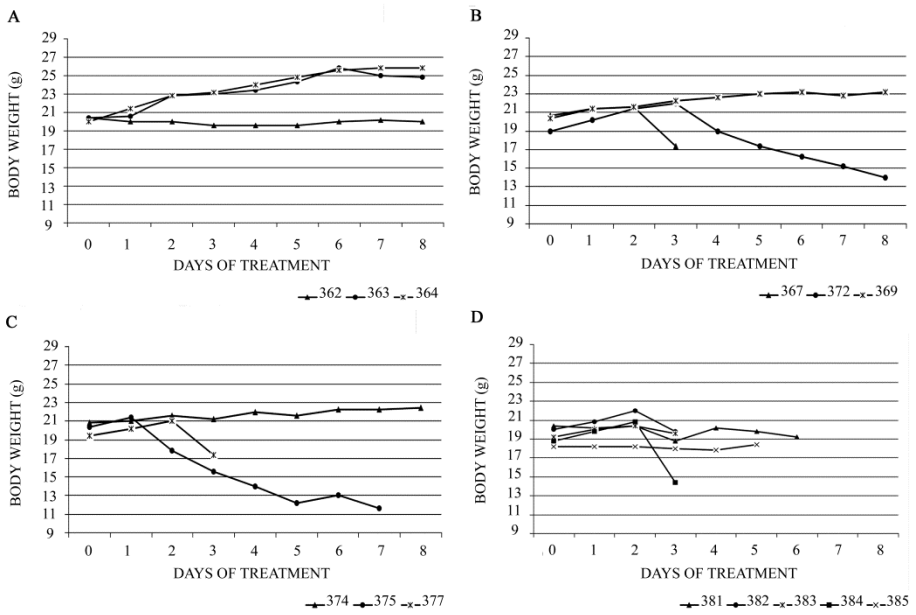

Figure 45. Body weight recorded during toxin administration in the four groups of treatment. Trace interruption corresponds to animal death. *A*. Control. *B*. 30 µg/kg. *C*. 90 µg/kg. *D*. 180 µg/kg.

4.2.4. Necroscopic examination

Necroscopic examination was performed on all animals of the study. Animals that presented swelling at the abdomen were found to have massive liquid accumulation in the intestinal tract. Stomach and both small and large intestine were characterized by decreased content of digested feed and organs wall were tensed from swelling (Figure 46*B* and *C*) in comparison to control (Figure 46*A*).

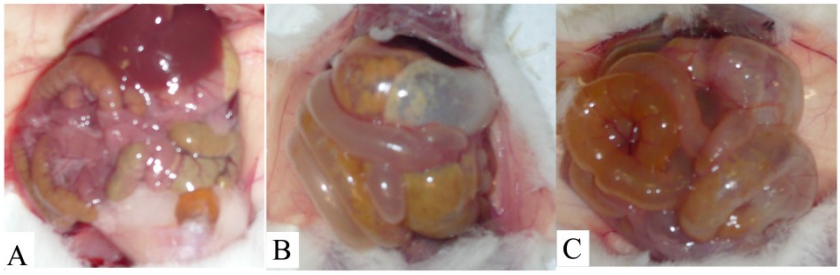

Figure 46. Appearance of the abdominal cavity of mice during necroscopic examination. *A*. Control. *B*. 30 µg/kg. *C*. 90 µg/kg..

Moreover, in 1/6 of the mice treated with the dose of 180 µg/kg, areas of discoloration, compatible with necrosis were observed in the liver (Figure 47).

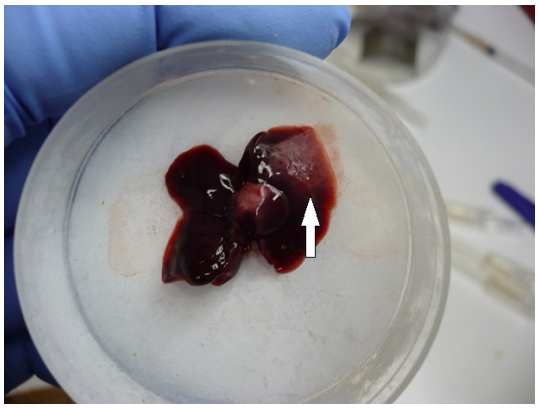

Figure 47. Appearance of the liver during necroscopic examination. Arrow indicates discoloration compatible with necrosis (dose: 180 µg/kg).

4.2.5. Recovery

At the end of toxin administration, 3 animals from each group of treatment were kept alive for a recovery study of 14 days; for the group

treated with 180 µg PLTX/kg, the recovery study was performed on the only survived animal.

During recovery period we observed mortality in 1/3 and 2/3 animals that had been treated with 30 and 90 µg/kg, respectively. As previously described, during the recovery a marked decrease in body weight was recorded in mice that died within the end of the recovery period (Figure 48).

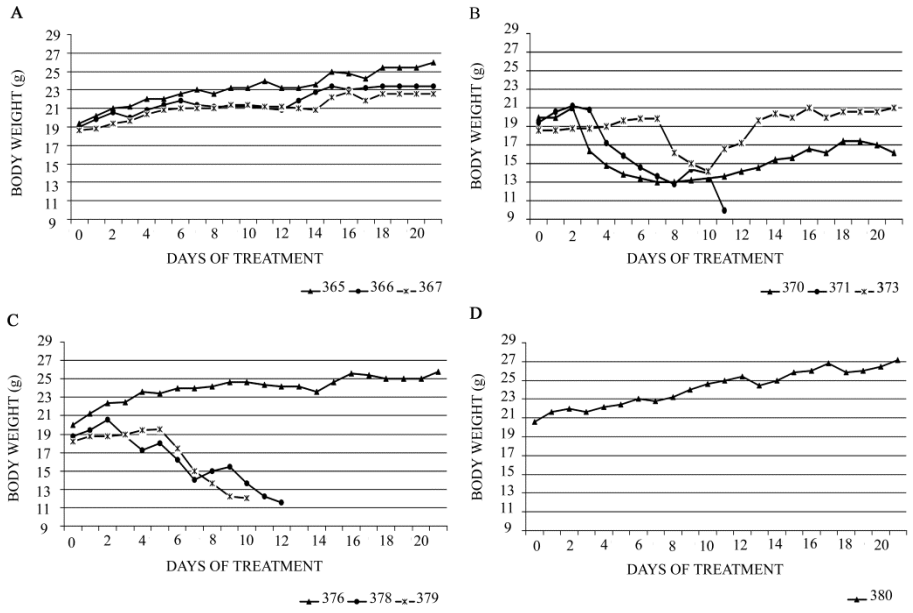

Figure 48. Body weight recorded during the whole study in four groups of treatment. Trace interruption corresponds to animal death. *A*. Control. *B*. 30 µg/kg. *C*. 90 µg/kg. *D*. 180 µg/kg..

4.2.6. Histological analysis

Although no specific cause of death was found in dead mice, multi-organ alterations were observed microscopically in mice that died

during the treatment and recovery period, throughout the dosed groups, which are most likely linked to treatment.

In the lungs, alveolar edema slight to severe in degree, in some cases associated to acute inflammation (Figure 50) and necrosis (Figure 51), was observed in 2/6 animals treated at the dose of 30 µg/kg, 2/6 treated at 90 µg/kg and 2/6 treated at 180 µg/kg. No alterations were recorded in control animals (Figure 49).

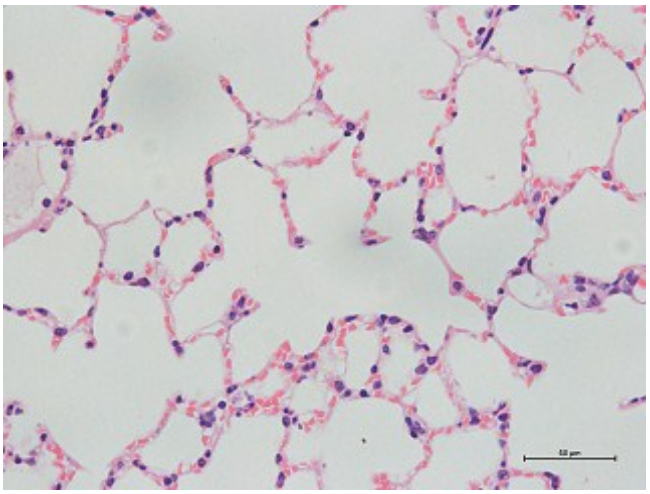

Figure 49. Lungs. Representative histological section of the lung from a control mouse. Scale bar stands for 50 µm.

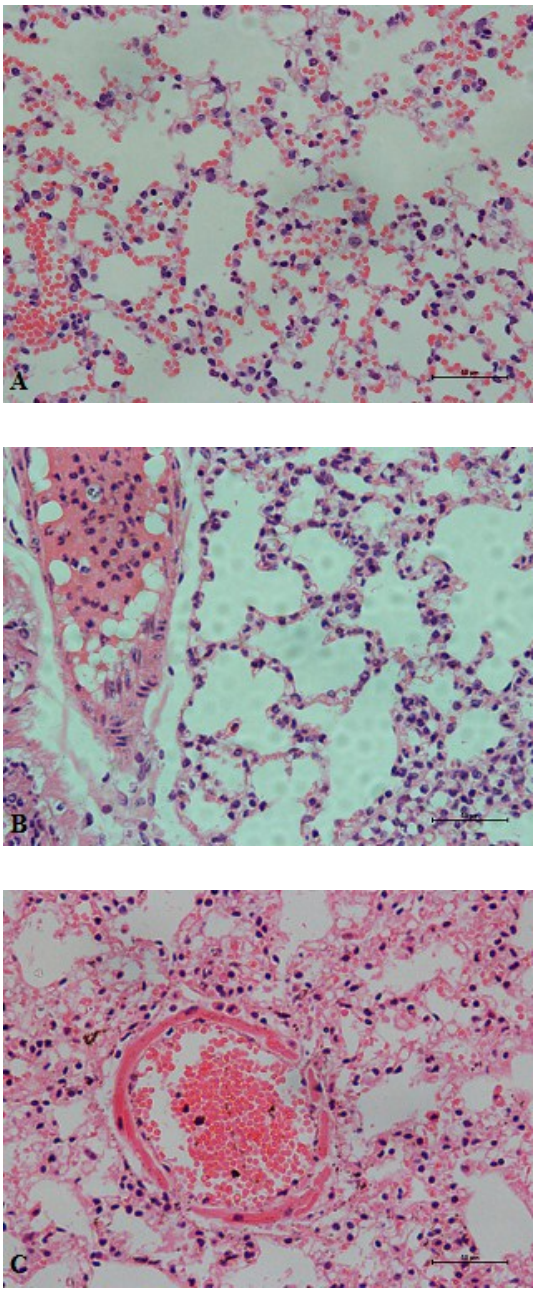

Figure 50. Lungs. Representative histological sections of acute inflammation in PLTX treated animals. *A*. 30 µg/kg; *B*. 90 µg/kg; *C*. 30 µg/kg. Scale bars stand for 50 µm.

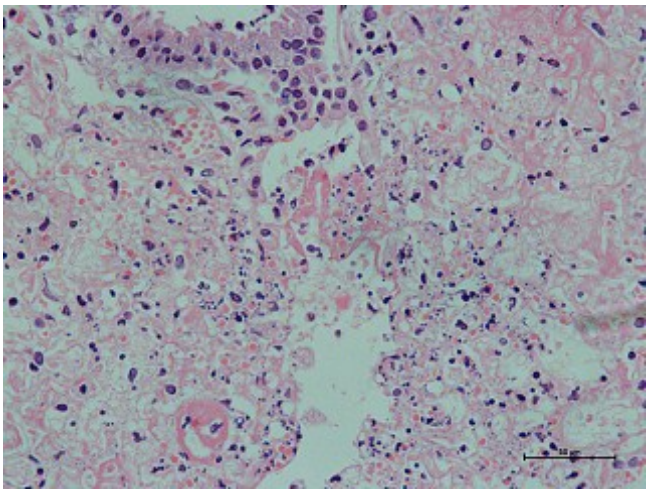

Figure 51. Lungs. Representative histological section of necrotic area (dose 30 µg/kg) . Scale bar stands for 50 µm.

At the hepatic level, it was observed a depletion of the glycogen content in the hepatocytes, visible as more a consistent structure of the hepatic cells (Figure 52 and 53).

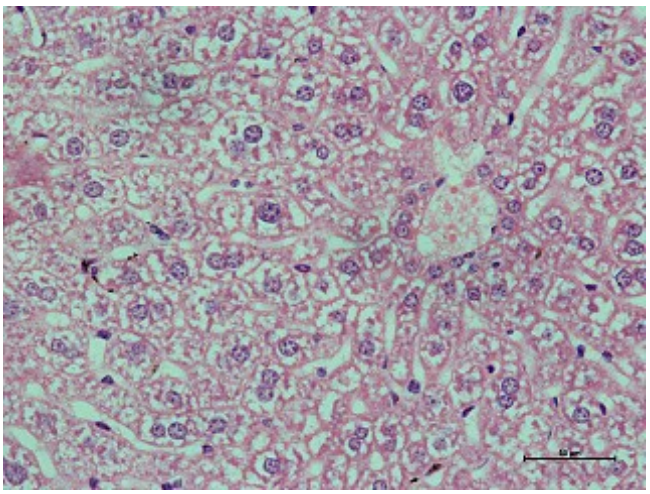

Figure 52. Liver. Representative histological section of the liver from a control mouse. Scale bar stands for 50 µm.

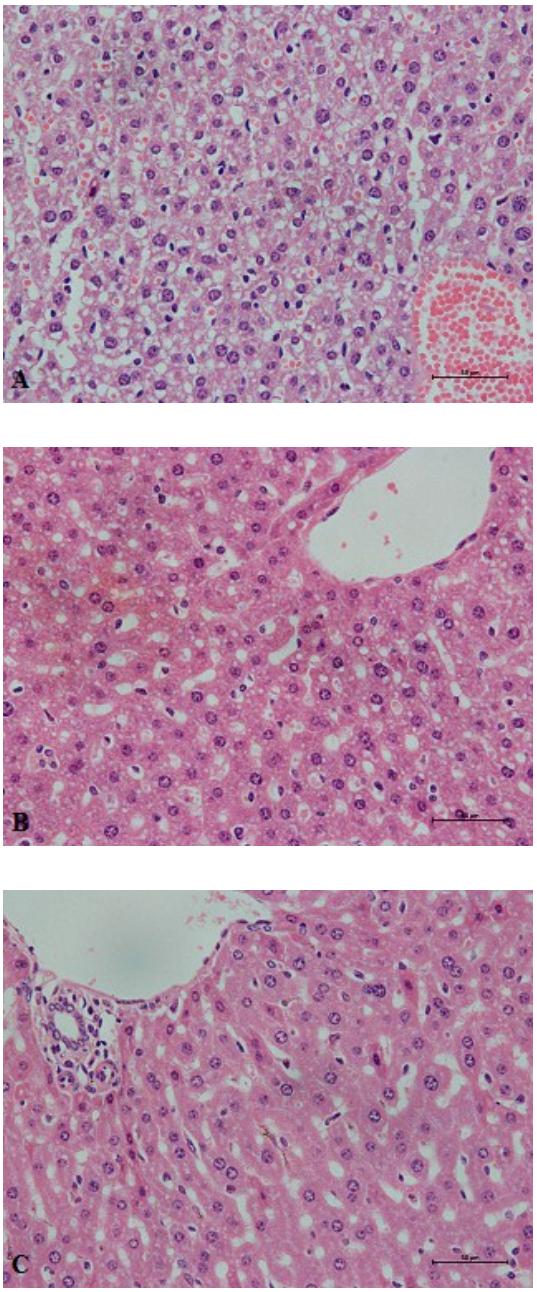

Figure 53. Liver. Representative histological sections of glycogen depletion in PLTX treated animals. *A*. 30 µg/kg; *B*. 90 µg/kg; *C*. 30 µg/kg. Scale bars stand for 50 µm.

Various degrees of glycogen depletion were noted among the doses groups without relationship (Figure 53). In the liver of 1/6 animals treated with 180 µg/kg of PLTX, focal foci of hepatic necrosis were observed (Figure 54).

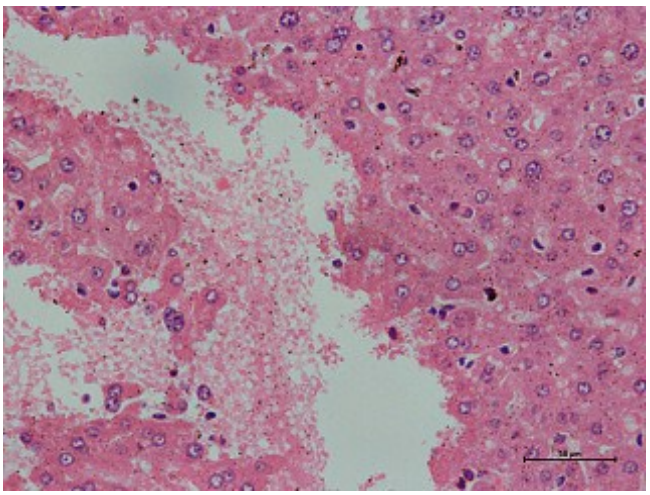

Figure 54. Liver. Representative histological section of necrotic area (dose 180 µg/kg). Scale bar stands for 50 µm.

In one animal treated with 30 µg PLTX/kg it was also possible to identify the presence of mild gastric ulcers, even if they were limited to the non-glandular stomach.

At cardiac level some fibers presented hyper-eosinophylia with incidence of 2/6 in mice treated at 30 µg/kg, 1/6 treated at 90 µg/kg and 5/5 at 180 µg/kg (Figure 55 and 56).

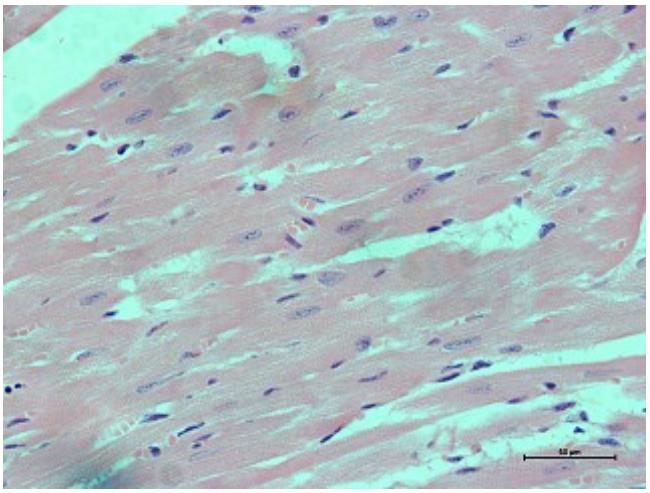

Figure 55. Cardiac muscle. Representative histological section of the heart from a control mouse. Scale bar stands for 50 µm.

Moreover, in some areas of the cardiac muscle from animals treated with the dose of 180 µg/kg, concomitant degenerative process, notable as cytoplasm vacuolization was also noted (Figure 56*C*, full arrows). Slight edema of the cardiac muscle, observed as separation of the muscle fibres was also recorded in the same animals treated with the highest dose of toxin (Figure 56*B* and *C*, empty arrows).

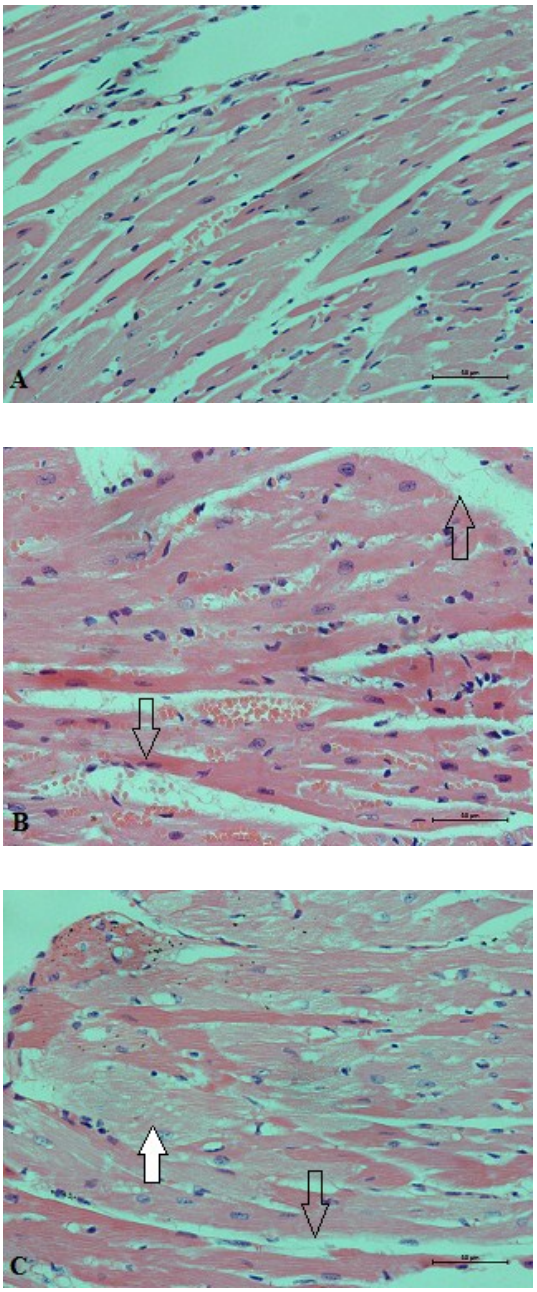

Figure 56. Cardiac muscle. Representative histological sections of muscular damage in PLTX treated animals. *A*. 30 µg/kg; *B*. 90 µg/kg; *C*. 30 µg/kg. Scale bars stand for 50 µm.

Increased cellularity between fibers was noted in skeletal muscle from 2/3 and 4/4 mice that died during the study, after the treatment with the toxin at 30 µg/kg and 90 µg/kg, respectively (Figure 57 and 58).

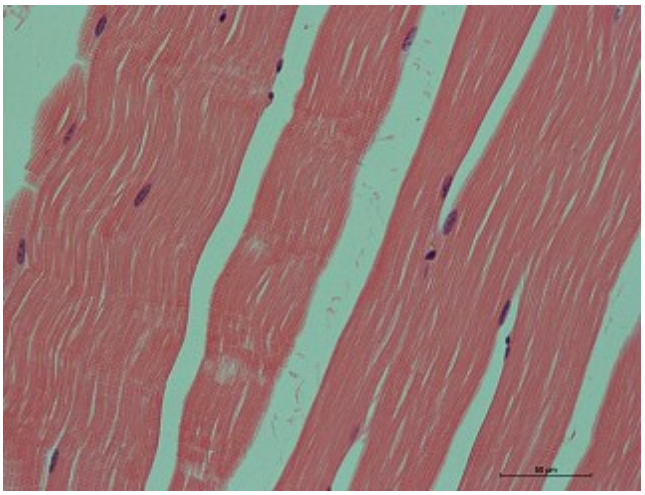

Figure 57. Skeletal muscle. Representative histological section from the skeletal muscle of a control mouse. Scale bar stands for 50 µm.

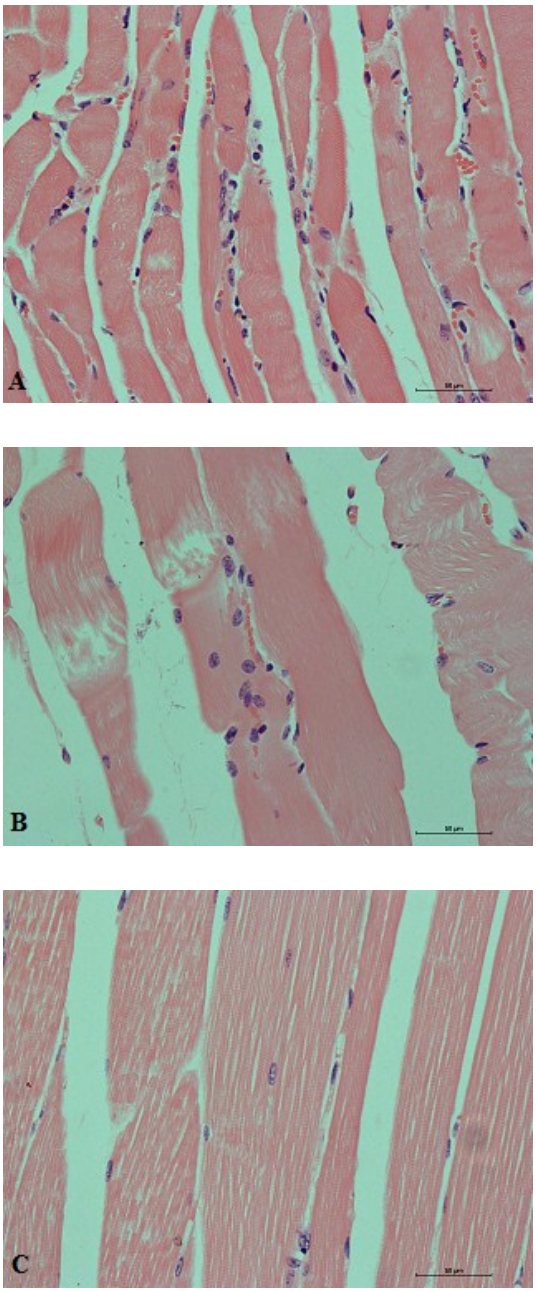

Figure 58. Skeletal muscle. Representative histological sections of muscular alterations in PLTX treated animals. *A*. 30 µg/kg; *B*. 90 µg/kg; *C*. 30 µg/kg. Scale bars stand for 50 µm.

Histological analysis of the kidneys of treated animals revealed presence of erythrocytes in several areas of the tubuli and of Bowman's capsules in comparison to control (Figure 59 and 60). Incidence of this observation was 3/6 in animals that were treated with 30 µg PLTX/kg, 4/6 in animals treated at 90 µg/kg and 1/6 at the dose of 180 µg/kg. At the highest dose some degree of tubular dilatation and congestion was also observed (Figure 60*C*).

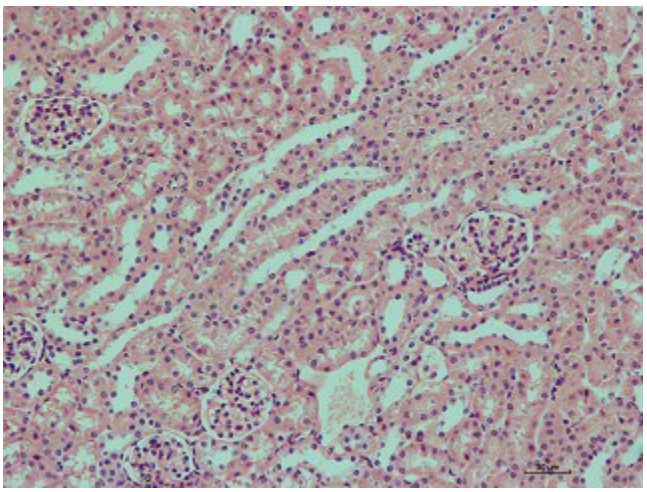

Figure 59. Kidney. Representative histological section of a kidney from a control mouse. Scale bar stands for 50 µm.

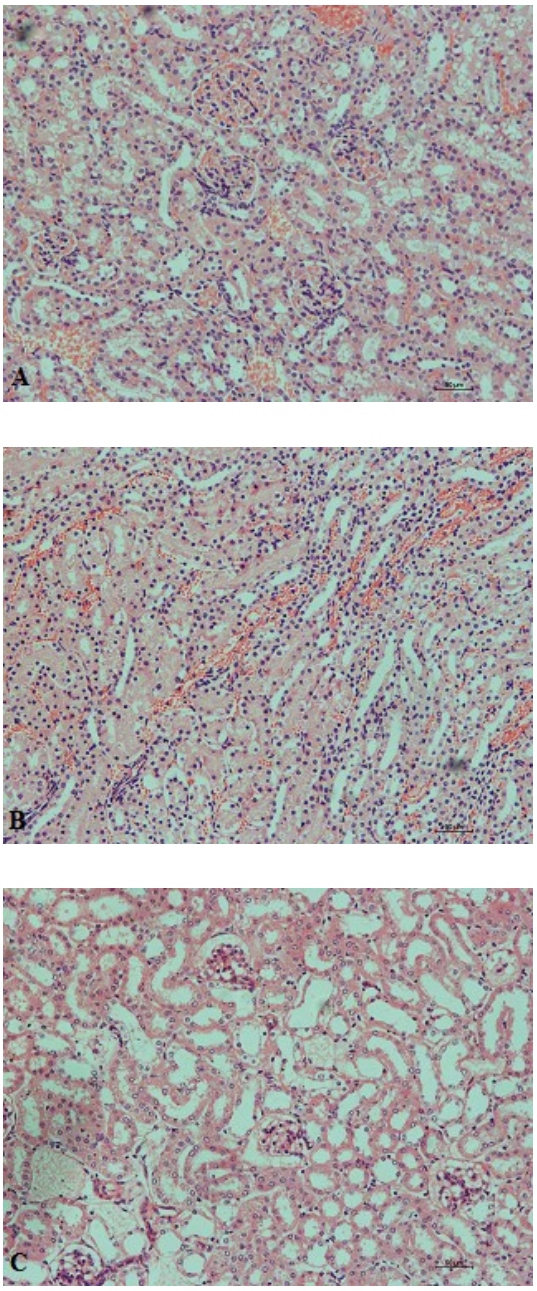

Figure 60. Kidney. Representative histological sections of renal alterations in PLTX treated animals. *A*. 30 µg/kg; *B*. 90 µg/kg; *C*. 30 µg/kg. Scale bars stand for 50 µm.

In comparison to controls, in the spleen of the animals treated with two lower doses (30 and 90 µg/kg), a moderate depletion of the lymphoid elements of the lymphatic follicles was observed (Figure 61 and 62). The finding was not consistent and not dose-dependent since it was not observed at the highest dose.

Animals that were sacrificed at the scheduled time-points did not present any of the above mentioned histological alterations in organs observed related to the administration of the toxin.

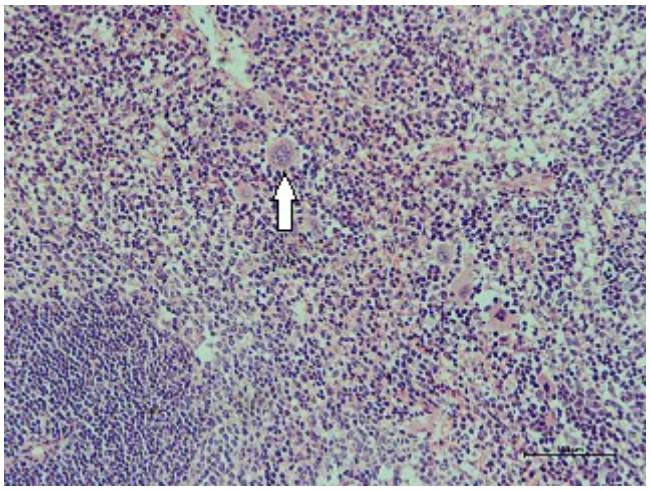

Figure 61. Spleen. Representative histological section of the spleen from a control mouse (arrow: lymphoid elements). Scale bar stands for 100 µm.

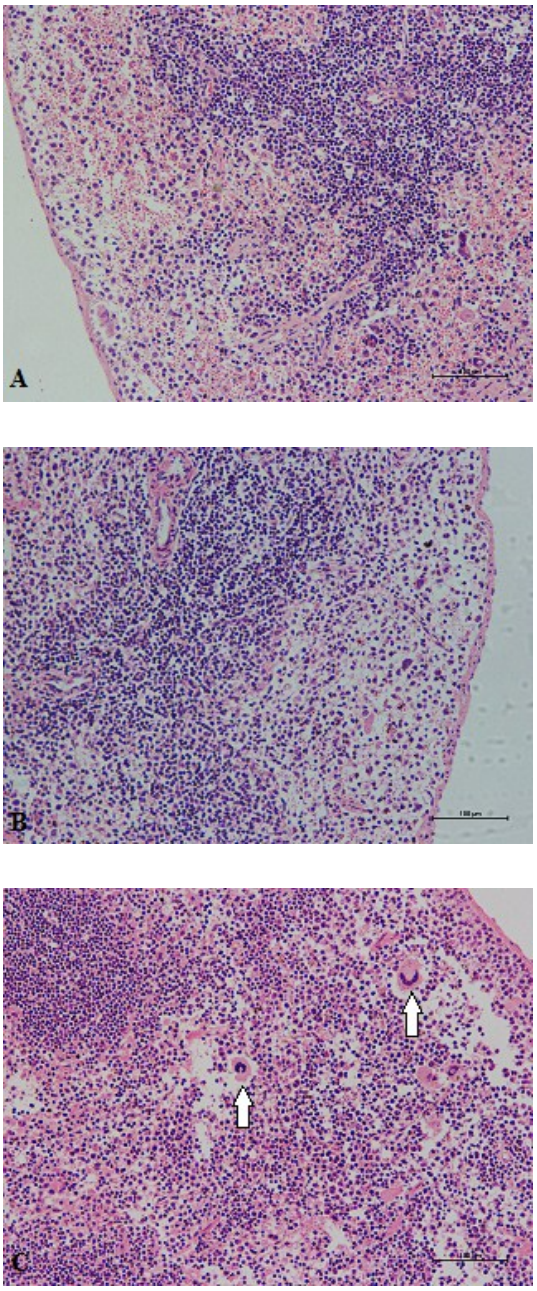

Figure 62. Spleen. Representative histological sections of spleen alterations in PLTX treated animals. *A*. 30 µg/kg; *B*. 90 µg/kg; *C*. 30 µg/kg (arrow: lymphoid elements). Scale bars stand for 50 µm.

5. DISCUSSION

5.1. *In vitro* studies

One of the goals of the PhD project was to investigate the effect of PLTXs on primary culture on mouse skeletal muscle cells, a predictive *in vitro* model for the study of the mode of action of PLTXs on skeletal muscle tissue, one of their primary toxicological targets. To this aim, at first the experiments were performed in parallel with PLTX and 42-OH-PLTX to provide, not only toxicological data on the muscular toxicity of these compounds, but also to highlight the potential differences between the parent (commercial) compound and its analogue (unfortunately available only in very limited quantities). Once assessed the similar behaviour of the two toxins in terms of ability to trigger $[Ca^{2+}]_i$ increase, cytotoxic effects, binding properties, the further experiments for a detailed elucidation of the mechanism of action were limited to the parent compound. However, once identified the crucial steps for the development of the cytotoxicity, to give a more complete overview of the effects of this family of toxins on skeletal muscle, selected experiments with OST-D were also performed.

The first finding of the present work is that PLTXs reduce the viability of differentiated skeletal muscle cells with an EC_{50} of 0.54 and 0.36 nM after 24 h of continuous incubation with PLTX and 42-OH-PLTX, respectively (SRB assay). These values are in agreement with recent reports for the potency of this family of compounds on excitable cells (Pérez-Gómez et al., 2010). In addition, PLTXs significantly reduced cell survival, indicating that limited exposures to these toxins are sufficient to trigger irreversible toxic effects on skeletal muscles. Also the observation that PLTXs induce persistent toxic effects on skeletal muscle cells even

after exposures as short as 1-4 hours finds support in literature. Indeed, experiments performed on HaCaT (Pelin et al., 2011) and Caco-2 cells (Pelin et al., 2012) cells revealed that incubation with PLTX induces a cellular damage that develops even after the removal of the toxic stimulus from the culture medium. Moreover, from the functional point of view, it was also observed that the toxin triggers an irreversible contraction of frog heart muscle (Sauviat, 1989) and in smooth muscle (Ito et al., 1977).

We have also observed that exposure of differentiated skeletal muscle cells to both PLTX and 42-OH-PLTX, in the nanomolar range, induced morphological changes, as rounding and formation of vacuoles within cells. Similar observation were reported also by Sheridan and co-workers in smooth muscles (Sheridan et al., 2005), suggesting that, independently from muscle type, the toxins induce a defined degeneration pathway in this type of tissue. AFM microscopy confirmed the effects of PLTX at morphological level showing a clear progression of the skeletal muscle cell damage with prominent membrane swelling. It is worth noticing that, even if recent experiments have reported no effects of PLTX on the morphology and mechanical properties of breast cancer MCF-7 cells, these experiments have been performed at a concentration 20 times lower than that used in the present study (Prandi et al., 2011). Using AFM microscopy, we have also observed loss of cell adhesion recordable as cellular shifts associated to the movement of the cantilever. Ionic unbalance caused by PLTX is likely to play a prominent role in the skeletal muscle cell detachment, as reported in other non-muscular cellular models such as neuroblastoma cells (Louzao et al., 2007; Valverde et al., 2008).

In our experimental conditions, primary skeletal mouse myotubes express ACh receptors (Bandi et al., 2005). As at the neuromuscular junction level *in vivo,* binding of ACh to the receptors causes membrane depolarization and activation of excitation-contraction cascade. The latter begins with the activation of L-type voltage-dependent Ca^{2+} channels coupled with ryanodine receptors and $[Ca^{2+}]_i$ increase and ends with mechanical contraction of the muscle cell. In light of this, responsivity to the neurotransmitter acetylcholine (ACh) has been chosen as index of the functionality of skeletal muscle cells exposed to PLTXs, and Ca^{2+} imaging has been used to assess it. The decreased sensitivity to the physiological neurotransmitter ACh observed in myotubes after exposure to PLTXs could be the result of several effects of the toxins. For example, PLTX was already known to impair the excitation-contraction coupling of cultured atrial myocytes (Kockskämper et al., 2004). However, independently from the specific mechanism, our observation suggests that the toxin can impair crucial functional properties of excitable cells long before inducing cellular death.

The effect of PLTX and 42-OH-PLTX by staining for desmin, an intermediate filament of cytoskeleton, has been presented here for the first time. Even if PLTX and its analogue OST-D are known to induce disorganization of actin cytoskeleton in several excitable and non-excitable cell models (Louzao et al., 2011), the effects of the toxins on the intermediate filaments of skeletal muscle have never been reported so far. Intermediated filaments represent not only major structural and scaffold proteins of skeletal muscle cells, but they also regulates the position of the cellular organelles and vesicles (Capetanaki et al., 2007). Thus impairment at this level may result into a severe functional damage

for the cell. Even if more stable than other cytoskeletal elements, desmin filaments are sensitive to $[Ca^{2+}]_i$ variations being degraded from Ca^{2+}-dependent proteases (Traub and Nelson, 1981). Considering the $[Ca^{2+}]_{i.}$ increase induced by PLTXs in our cell model, it is very likely that the morphological alteration could be the result of desmin disorganization.

Videoimaging experiments carried out at high time resolution (1 ratio image/s), for up to 30 min after toxin exposure, revealed that both PLTX and 42-OH-PLTX triggered a peculiar biphasic $[Ca^{2+}]_i$ increase in the skeletal muscle cells. A first short-lasting increase of the $[Ca^{2+}]_i$ ("transient phase") was followed by a second persistent $[Ca^{2+}]_i$ increase, which remained stable up to 30 min after toxin exposure ("long-lasting phase"). PLTX has been reported to induce an increase of the $[Ca^{2+}]_i$ increase even before the structural elucidation of the molecule (Rayner et al., 1975; Ito et al.,1977); later, the observation has been confirmed with purified compound (Ishii et al., 1997; Amano et al., 1997; Vale et al., 2006). In addition, it has been already demonstrated that Ca^{2+} plays a crucial role in the mechanism of action of PLTXs in muscle tissue (Ito et al., 1976; Ishii et al., 1997; Bellocci et al., 2011). Here, for the first time, a correlation between the long-lasting phase of the $[Ca^{2+}]_i$ increase induced by PLTXs and their toxicity is described.

In accordance with most quoted mechanism of action on Na^+/K^+ pump and in line with previous reports (Ecault and Sauviat, 1991; Kinoshita et al., 1991), we observed that exposure of skeletal myotubes to PLTXs in an extracellular Na^+-free solution prevented $[Ca^{2+}]_{i.}$ increase, as well as cytotoxicity (Sheridan et al., 2005). However, the presence of TTX only partially reduced the transient phase of the $[Ca^{2+}]_{i.}$ increase induced by PLTX and 42-hydroxyl-derivative. As previously observed for ouabain

(Ciminiello et al., 2009), the effect of 42-OH-PLTX appeared less sensitive to the presence of the blocker than PLTX, confirming that even if the mechanism of action of the two toxins includes the activation of voltage-dependent Na^+ channels, it is somehow different.

The inhibition of PLTXs effects in Ca^{2+}-free conditions seems to be much more complicated to explain. In our experimental model, experiments were performed according to two different protocols: in the first set of experiments the Ca^{2+} chelator EGTA (5 mM) was added to the extracellular solution, in the second, Ca^{2+} was substituted with equimolar concentrations of Mg^{2+}. In the first case, the effect of the toxin on $[Ca^{2+}]_i$ increase was completely abolished whereas, in the second, the effect was visible as inhibition limited to the long-lasting phase. Binding experiments, performed in presence of 5 mM EGTA, revealed a significant decrease of the ability of PLTXs to displace ^{3}H-ouabain only at the higher concentration tested (10 nM). On the contrary, binding affinity of PLTXs at lower concentrations was not significantly altered by the absence of $[Ca^{2+}]_e$. Moreover, binding of ouabain *per se* seemed to be, in some extent sensitive to the presence of extracellular Ca^{2+} making the results obtained in the presence of chelator more difficult to interpret and possibly biased by an effect of free-Ca^{2+} condition on the binding of PLTXs to the Na^+/K^+ pump (Ecault and Sauviat, 1991; Kudo and Shibata, 1980). Very recent data show that PLTXs have high affinity for divalent cations (Ciminiello et al., 2012b). In this light and taking into account our results, it could be hypothesised that the cations are required to stabilize a conformation of PLTXs with high affinity for the molecular targets.

Results of the experiments carried out in the presence of Mg^{2+} are more reliable and helpful in the comprehension of the mechanism of action of the PLTX. Taking into account that in such experimental condition any contribution of Ca^{2+} influx from extracellular compartment was prevented, the persistence of the transient phase strongly suggested that origin of it in the release of Ca^{2+} from intracellular compartments. In addition, and more interestingly, the absence of cytotoxicity when Ca^{2+} was replaced with Mg^{2+} indicated the long-lasting phase of the $[Ca^{2+}]_i$ as the one responsible for the development of the irreversible cell damage. In fact, in the presence of Mg^{2+}, the absence of cytotoxicity cannot be ascribed to the altered binding of PLTX because: *i*) replacing Ca^{2+} with Mg^{2+} maintains the ionic strength of the milieu (Habermann 1983); and *ii*) the role of Ca^{2+} as cofactor for the PLTX binding to its molecular target is guaranteed by the other divalent ion, as already described by other authors (Ecault and Sauviat 1991; Kudo and Shibata 1980).
The effect of the depletion of the intracellular stores on the PLTX-induced response confirmed that the transient phase (affected by cyclopiazonic acid) is mainly sustained by intracellular stores and that the long-lasting phase (unaffected) is responsible for the toxic effect.

According to the accepted molecular mechanism of action of PLTX in excitable cells, the interaction of the toxin with the Na^+/K^+ pump and the consequent massive influx of Na^+ and membrane depolarisation cause opening of the voltage-dependent channels and activation of the reverse mode of the Na^+/Ca^{2+}-exchanger (Rossini and Bigiani 2011; Frelin and Van Renterghem 1995). In view of this, the contribution of voltage-

dependent Ca^{2+} channels and Na^{+}/Ca^{2+}-exchanger in PLTX-induced biphasic $[Ca^{2+}]_i$ increase was evaluated in skeletal muscle cells.

Blockers of voltage-dependent Ca^{2+} channels (verapamil, cadmium and lanthanum) and the reverse mode of the Na^{+}/Ca^{2+}-exchanger (KB-R7943), even combined, inhibited only the transient phase of the PLTX-induced Ca^{2+} response. The transient $[Ca^{2+}]_i$ increase triggered by the 42-OH-PLTX resulted to be even less sensitive to verapamil and KB-R7943, being partially decreased just by the two blockers were applied together. In addition, verapamil and KB-R7943 did not protect skeletal muscle cells from the toxic insult of PLTX. These results ruled out any contribution of voltage-dependent Ca^{2+} channels and Na^{+}/Ca^{2+}-exchanger to the long-lasting increase of $[Ca^{2+}]$ and to myotoxic effect induced by PLTX. The lack of protective effect of verapamil in skeletal muscle cells was in agreement with the results obtained in other excitable cells (Ozaki et al., 1983; Sheridan et al., 2005; Pérez-Gómez et al., 2010).

Since the mechanism sustaining the PLTX-induced $[Ca^{2+}]_i$ increase is still considered "uncertain" (Bellocci et al., 2011), the possibility that the long-lasting phase could be based on voltage-independent channels was considered. At first, the possible role of store-operated channels was explored. Since SKF-96365 did not affect the long-lasting phase elicited by PLTX, and did not prevented cytotoxicity, our data excluded any significant role for those channels in skeletal muscle cells.

Because of the morphological alterations and cell swelling induced by PLTX in our model and observed by others (Louzao et al., 2011; Rossini and Bigiani 2011; Prandi et al., 2011), we also explored the involvement of stretch-activated Ca^{2+} channels. Gd^{3+} abolished the long-lasting phase of the $[Ca^{2+}]_i$ increase induced by PLTX, thus suggesting a possible role

for stretch-activated channels in the mechanism of action of the toxin. It is worth noticing that Gd^{3+}, as trivalent cation of the family of lanthanides, is also known to inhibit voltage-dependent Ca^{2+} conductance in neural cells (Mlinar and Enyard 1993). In our cell system, voltage-dependent Ca^{2+} blockade seems unlikely. In fact, even at the concentration of 100 μM, in the range of those commonly used to investigate stretch-activated channels activity (Molgo et al., 1991; Ducret et al., 2010), Gd^{3+} did not affect the transient phase as verapamil and La^{3+}/Cd^{2+} did.

Beside the reversible inhibition of the long-lasting phase, Gd^{3+} also significantly reduced, although not completely, the toxic effects of PLTX on skeletal muscle cells, confirming a crucial role for the stretch-activated channels in the cascade of events that culminate in cell death. Interestingly, the activation of stretch-activated Ca^{2+} channels triggered by PLTX could be at the basis of the verapamil-insensitive long-lasting (up to 40 minutes) contraction observed in smooth muscle (Ozaki et al., 1983) as well as of the development of symptoms associated with PLTX intoxication, such as muscular spasms and myalgia in humans (Tubaro et al., 2011a) and hind limb paralysis in mice (Sosa et al., 2009; Tubaro et al., 2011b). This novel aspect of the mechanism of action of PLTX represents an intriguing starting point for the further investigation of PLTX effects *in vivo*.

Osmotic stress associated to mechanical stretch of skeletal muscle is known to induce ROS production (Martins et al., 2008), that is supposed to sustain reciprocally Ca^{2+} signalling (Shkryl et al., 2009). Moreover, PLTX itself is known to induce ROS production in human keratinocytes (Pelin et al., 2011) and to induce stress response proteins (Sala et al.,

2009). Since the presence of the radical scavenger Trolox (Jaradat et al., 2006) significantly reduced PLTX-induced toxicity in our cell model, it is likely that the production of ROS could be one of the cellular events that follow the influx of Ca^{2+} and that contribute to the toxin insult in the skeletal muscle tissue. It is worth noticing that the protective effect of Trolox did not last longer than 1 hour. This observation suggests that ROS production is an early event and does not exclude that a non-oxidative damage may follow (Sagara et al., 2011).

The possible role of Cl^- channels was also taken into account. Substitution of the extracellular anion was as effective as the absence of $[Na^+]_e$ in preventing the development of the myotoxic damage after incubation with PLTX. In agreement with a possible role for Cl^- channels, the blocker DIDS partially protected cells from PLTX (see also Pérez-Gómez et al., 2010). Interestingly, both phases of PLTX-induced $[Ca^{2+}]_i$ increase appeared reduced in Cl^--free solution. To test the possible relationship between $[Ca^{2+}]_i$ and Cl^- influx into the cells after incubation with PLTX, a set of experiments were performed to check the possible role of Ca^{2+}-dependent Cl^- channels. In the presence of the specific blocker talniflumate (Walker et al., 2006), the toxicity induced by PLTXs did not change and this exclude a significant role for Ca^{2+}-dependent Cl^- conductances. Thus, the specific mechanisms by which Cl^- channels and/or transporters contribute to the toxicity induced by PLTX in skeletal muscle cells remain to be elucidated.

We have also observed that the $[Ca^{2+}]_i$ increase induced by the analogue OST-D in skeletal muscle cells was less than $1/6^{th}$ of that triggered by parent PLTX. As expected OST-D was also less cytotoxic than PLTX, being the EC_{50} after 24 hours of continuous incubation 5

times lower than that of commercial PLTX. This result is in agreement with those of Bellocci and co-workers (2008), which found the analogue one order of magnitude less cytotoxic than parent PLTX on MCF-7 cells. This data, on the whole suggest that even slight modifications of the structure of the molecule, especially those between C1 and C44, may have a considerable influence on the biological effects of this family of toxins also in the skeletal muscle tissue.

5.2. *In vivo* studies

PLTX and analogues are considered dangerous seafood contaminants and their potential accumulation through the food web suggests that their presence may occur in several edible species of fish, shellfish and echinoderms (Gleibs and Mebs, 1999; Aligizaki et al., 2008; Aligizaki et al., 2011; Tubaro et al., 2011a). Due to the potential wide distribution of PLTX and analogues, exposure assessment should consider that people can come into contact with the toxin several times within a week. Moreover, personal habit must also be taken into account. In this respect, a recent survey of EFSA (EFSA, 2010), aimed to the definition, at European level, of mean consumption values of shellfish for regulatory purposes, considered for Italy maximum shellfish consumption up to 4 times/week. The plausibility of a repeated exposure to this family of toxins becomes stronger, if we consider the delayed occurrence of the symptoms recorded in the study. Obviously, intoxications characterized by a short latency period in the onset of symptoms, such as, for instance, DSP (Diarrheic Shellfish Poisoning)

represent a self-limiting factor for repeated consumption of contaminated seafood.

According to the obtained results, lethality occurred only after the 3rd day of treatment. This result suggests a certain degree of accumulation of the toxin, and/or its toxic metabolites, before appearance of the toxicity. Alternatively, the occurrence of a cumulative damage is also possible. In the latter case, the repeated effect on target tissues may become evident only after reaching a certain threshold. The hypothesis that the toxin and/or its metabolites may cause a damage, persistent also after the end of the treatment, is supported also by the occurrence of lethality during the recovery period. Lethality during recovery period has never been observed during acute oral toxicity studies, performed in our laboratories with the same mouse strain and similar experimental protocol (Sosa et al., 2009; Tubaro et al., 2011), even if the doses were considerably higher (from 300 to 1676 μg/kg). The death of 3/6 animals treated at the dose of 30 μg/kg occurred at a value that is one order of magnitude lower than that proposed as LOAEL (Lowest Observed Adverse Effect Level) by Ito and Yasumoto after acute exposure (Ito and Yasumoto, 2009) and currently used by EFSA for regulatory purposes.

During the period of treatment and also during recovery, general malaise of animals was evident as reduced food consumption and marked decrease of body weight. Congestions and swelling of the gastro-intestinal apparatus, observed during the necropsies, were with high probability correlated with this phenomenon. Another sign related to general malaise and worsening of the animals condition was probably the chromodacryorrhoea.

During the experiment of repeated oral toxicity sever damage of the gastro-intestinal apparatus was observed. During the necroscopic examination intestinal cavity were swollen and occasionally filled with fluids. Slight injuries of stomach and small intestine have been previously observed also after acute oral administration of PLTX (500 μg/kg; Ito and Yasumoto, 2009), whereas more severe involvement small intestine, with bleeding and congestion was described after intra-peritoneal (i.p.) administration (Ito et al.,1996). Later after treatment (16, 24 hours post-injection; 1 μg/kg), Ito and co-workers also described the duodenum to become yellowish and the small intestine to become dilated with a large volume of fluid. These later findings present strong similarities with the data presented in this thesis, suggesting that the peculiar swelling of these abdominal organs could be a phenomenon with slow onset. If we consider similarities despite the different exposure route, it is possible to hypothesize that these signs could be peculiar of PLTX-intoxication. Data describing the involvement of intestinal tract after ingestion of PLTX are in good agreement also with those reported in literature, after the intoxication with PLTX-contaminated seafood. The examination of the intestinal apparatus was rarely performed, but in 1988 Tan and Lee reported a case of intoxication ascribed to PLTX after ingestion of crabs (*Lophozozimus pictor*). Among *post mortem* pathological finding, small and proximal large intestine filled with bloodstained fluid, severe congestion of mucosal lining with areas of hemorrhage were found (Tan and Lee, 1988).

In spite of the appearance of the stomach and intestine at the necropsy, histological analysis revealed erosions just in the non-glandular portion

of the stomach of one the mice treated with the dose of 30 µg/kg. Similar damage was observed more often after acute oral administration of the toxin and of its analogue 42-OH-PLTX (Sosa et al., 2009; Tubaro et al., 2011), suggesting that high turnover of the gastro-intestinal epithelium and limited doses of toxin could hinder the development of inflammatory damage.

In spite of the absence of sites of damage at intestinal level, it is also possible that, as a consequence of the swelling and tension of the intestine, the paracellular absorption of the biotoxin, and/or its metabolites, could have been eased. All the data collected in the study, on the whole, suggest that absorption of the toxin takes place, despite its polar nature. Paralysis of the hind limbs and breathing difficulties were common symptoms of palytoxin treated animals (Munday, 2011), that were recorded both after i.p. (Ito et al., 1996; Riobò et al., 2008b) and oral administration (Munday 2008; Sosa et al., 2009; Tubaro et al., 2011b).

Histological analysis of main tissues and organs, revealed some interesting elements. Inflammatory and necrotic damage at pulmonary level seems to account for severe breathing difficulties observed in animals prior to death. Lung damage, as easily predictable, was previously described also after intra-tracheal installation of PLTX and after oral and sublingual administration of the toxin; in particular in the latter case, interstitial inflammation, bleeding, edema and alveolar destruction were observed (Ito and Yasumoto, 2009). The extreme sensitivity of lung to the toxin may be at the basis of the respiratory problems related to the inhalational exposure to marine aerosol during

proliferation of *O. ovata* (Gallitelli et al., 2005; Durando et al., 2007; Kermarec et al., 2008; Tubaro et al., 2011a).

Depletion of glycogen from hepatocytes was observed also in previous studies performed in our facilities to investigate the acute effects of oral administration of PLTXs in mice (Sosa et al., 2009; Tubaro et al., 2011b). This alteration is likely related to the reduction of body weight that animals underwent prior to death and to the general worsening of their conditions.

In the present thesis, alterations of cardiac muscle structure were observed, visible as fiber separation and cellular vacuolization (mainly at 180 μg/kg). Severe involvement of cardiac muscle was previously observed also by Terao et al. (1992) after acute i.p. administration of the toxin (2 μg/kg). In fact, myofibrillar separation and single cell necrosis, together with rounding of mitochondria were found (Terao et al., 1992). Vacuolization recalls the degenerative process that muscular cells undergoes after incubation with the toxin as shown in the present thesis, as well as in smooth muscle cells (Sheridan et al., 2005). It is difficult to discriminate if the effects of PLTX at cardiac level are the consequence of the direct or secondary effect of the toxin on this tissue. In fact, no kinetic data are available for the description of the ADME (Absorption Distribution Metabolism and Elimination) of the toxin. Till now PLTX effects on the cardiovascular apparatus have been investigated in several animal models, even if the majority of the studies were carried out with semi-purified toxin. The toxin (semi-purified 3300 Da m.w.) had direct effects on heart function inducing ECG alterations after parenteral administration (Kaul et al., 1974; 1981; Vick and Wiles, 1975). In spite of that, the toxin is known to induce

intense vasoconstriction of coronary arteries when administrated intravenously (Vick and Wiles, 1975; Ito et al., 1982). Thus, it is also possible to interpret cardiac muscle degeneration as a consequence of the vasoconstriction and reduced hemoperfusion induced by the toxin.

Increase of cellular elements between skeletal myocytes and the presence of myoblasts on the surface of the fibers of animals treated with the doses of 30 and 90 µg/kg, could be related to regenerative processes of damaged muscle. This hypothesis would explain also why this kind of alteration was not visible in mice treated at the higher dose. In fact, it is likely that, either the damage did not had time to become so evident or the repair mechanisms of the body did not had time to react to the toxic insult. From the epidemiological data that describe the effects of ingestion of PLTX-contaminated seafood, appears clear that a damage of skeletal muscle not only may occurs, as described by Taniyama and co-workers (Taniyama et al., 2002), but it may also take several days to recover. Moreover, to support the idea that skeletal muscle and its regeneration may be affected by the toxin, RT-PCR experiments performed on embryonic and larval stages of development of *Xenopus laevis* revealed that PLTX induced up-regulation of genes related to muscular development, such as myof5 (Franchini et al., 2009).

In the kidneys, the toxin seems to cause increase of erythrocytes content at all dose tested and tubular dilation at the highest dose. As previously described for the heart, it is possible that the renal effects may be due to a direct action of the toxin on the organ or to the vasoconstriction that can be triggered by the toxin. In literature, it is possible to find suggestions in this respect, because a vasoconstriction

particularly intense at renal level has already been reported after parenteral administration of the toxin (Ito et al., 1982). Ultrastructural alterations of the kidney in relation to the i.p. administration of the toxin were also described in literature, with autophagic vacuoles and occasional destruction of the microvilli in the proximal and distal tubules (Terao et al., 1992). Moreover, intra-tracheal administration of the toxin is known to induce glomerular atrophy already at the dose of 1 μg/kg (Ito and Yasumoto, 2009). Reported data, on the whole, strongly suggest the kidneys as target organs for PLTX toxicity.

At spleen level, decrease of lymphoid elements of lymphatic follicles was observed in mice treated with the two lower doses. In this respect, it is worth noticing that that the effects of repeated sub-lethal doses of PLTX on lymphoid tissues have been specifically investigated (Ito et al., 1997). Even if obtained after i.p. administration, this data can give precious suggestions for the comprehension of the alterations observed in our model. After 29 administrations the toxin significantly decreased the weight of spleen and thymus and the recovery of from this damage took one month to occur . Moreover, the ratio between lymphocytes and total leukocytes irreversibly decreased (Ito et al., 1997). On the whole, these data support the idea that PLTXs may have some effect at the level of the immune system that may represent an intriguing starting point for the complete comprehension of the toxic effect of this molecule.

In conclusion, on the whole, from the short-term toxicity study it is possible to identify a LOAEL for the repeated oral administration of 30 μg/kg. Considering the high incidence of lethality recorded during the study at the lower dose, this value has to be considered provisional and

likely to be lowered from further experiments. In spite of that, it is possible to propose a value of short-term reference dose (RfD) that, if respected, should ensure the absence of toxic effects to humans after short term exposure to PLTXs-contaminated seafood. In this case, to the commonly used safety factors (10 for the inter-species differences and 10 for the intra-species difference, EFSA 2009) an additional factor of 10 should be applied to take in consideration that a LOAEL was used for calculation instead of NOAEL. In this way, a RfD of 0.03 µg/kg can be estimated. Thus, for a 60 kg person, the daily amount of toxin ingested within a week should not exceed 1.8 µg. This value is significantly lower than that proposed by EFSA for the acute reference dose (ARfD). If we consider the daily portion size a little smaller than that used for the ARfD, thus 300g instead of 400g, this means that concentration of PLTXs on seafood should not exceed 6 µg/kg of edible meat. This value is 5 times lower than that currently proposed by EFSA (30 µg/kg, EFSA 2009); otherwise if we consider the standard portion, suggested also by food consumption surveys (EFSA, 2010), the concentration of the toxin should not exceed 4,5 µg/kg. According to a recent review that summarizes the concentration of PLTX and analogues in seafood (Aligizaki et al., 2011) the toxin content, during contamination may reach considerable concentration. For instance PLTXs in *M. galloprovincialis* collected in the Adriatic sea were found to reach concentration up to 120-200 µg/kg of toxin (Bellocci et al., 2008; Aligizaki et al., 2011) and octopus up to 971 µg/kg ovatoxin-A and 115 µg/kg pPLTX (Aligizaki et al., 2011). Similarly, Ciminiello and co-workers reported the presence of ovatoxin-A in mussels between 303 and 625 µg/kg (Ciminiello et al., 2011). The consumption

of seafood with this level of contamination will likely results in in the ingestion (for adults of 60 kg b.w.) of toxins in the range of micrograms per kg b.w. Accordingly, EFSA panel reports that consumption of a large portion of shellfish harvested in contaminated areas is likely to result in a dietary exposure of 3 µg/kg b.w. for an adult (EFSA 2009). Even if this data refers to the acute consumption, they can give an idea of the potential exposure to the toxin and therefore rise concern about the more and more frequent presence of PLTX-producing organisms in the Mediterranean area.

6. CONCLUSIONS

In conclusion, the results obtained *in vitro* demonstrate the crucial role of $[Ca^{2+}]_i$ in determining PLTX-induced cytotoxicity also in skeletal muscle cells. Moreover, we show that in skeletal muscle cells, cytotoxicity of PLTXs is strictly related to a long-lasting and irreversible Ca^{2+} influx. The investigation of the mechanisms mediating the long-lasting phase of the Ca^{2+} influx and cytotoxicity suggests a prominent role for the activation of stretch-activated Ca^{2+} channels, possibly related to cytoskeletal disorganization and osmotic swelling that follow PLTX-induced ionic deregulation. The comparison of the effects of PLTX, 42-OH-PLTX and OST-D seems to suggest that small structural differences between the analogues determine considerable variation of biological properties.

The investigation of the toxicity of PLTX and its analogues on primary culture of skeletal muscle cells gave new hints for the comprehension of the mechanism of action of these molecules on their target tissues and could contribute to the knowledge of pharmacological strategies to counteract their effects.

The *in vivo* study revealed high toxicity of PLTX after short-term oral administration. Lethality after repeated administration was observed at doses considerably lower than those causing toxicity after single administration and, for this reason, these data are of crucial importance for the comprehension of the risk associated to the entrance of PLTX into the food chain and the potential threat associated to the entrance of contaminated seafood on the market. The definition of the short-term toxicity of PLTX could also help for the identification of the most sensitive target organ of toxicity and give precious suggestions for the identification/treatment of the intoxications.

Moreover, information for risk characterization reported in the present thesis will also guide toward the definition of the regulatory limits for the presence of PLTXs on commercialized seafood, and, as a consequence they also suggest the sensitivity that screening analytical methods should have for appropriate detection.

7. REFERENCES

Alcala, A.C., Halstead, B.W., 1970. Human fatality due to ingestion of the crab Demania sp. in the Philippines. *J. Toxicol. Clin. Toxicol*. 3, 609-611.

Alcala A. C., Alcala L. C., Garth J. S., Yasumura D., Yasumoto T. 1988. Human fatality due to ingestion of the crab *Demania reynaudii* that contained a palytoxin-like toxin. *Toxicon*. 26, 105-107.

Aligizaki K., Katikou P., Nikolaidis G., Panou A. 2008. First episode of shellfish contamination by palytoxin-like compounds from *Ostreopsis* species (Aegean Sea, Greece). *Toxicon*. 51, 418-427.

Aligizaki K., Katikou P., Milandri A., Diogène J. 2011. Occurrence of palytoxin-group toxins in seafood and future strategies to complement the present state of the art. *Toxicon.* 57, 390-399.

Abboud-Abi Saab M. 1989. Les dinoflagelleés des eaux côtières libanaises-espèces rares ou nouvelles du phytoplankton marin. *Lebanese Science Bulletin*. 5, 5-16.

Amano K., Sato K., Hori M., Ozaki H., Karaki H. 1997. Palytoxin-induced increase in endothelial Ca^{2+} concentration in the rabbit aortic valve. *Naunyn Schmiedeberg's Arch Pharmacol.* 355, 751-758.

Anner B. M., Moosmayer M. 1994. Na,K-ATPase characterized in artificial membranes. 2. Successive measurement of ATP-driven Rb-accumulation, ouabain-blocked Rb-flux and palytoxin-induced Rb-efflux. *Molecular Membrane Biology*. 11, 247-254.

Arakawa O., Hwang D.-F., Taniyama S., Takatani T., 2010. Toxins of pufferfish that cause human intoxications. *In*: Ishimatsu, A., Lie, H.-J.

(Eds.), Coastal Environmental and Ecosystem Issues of the East Dhina Sea, Terrapub and Nagasaki University, Nagasaki, pp. 227-244.

Ares I.R., Cagide E., Louzao M.C., Espina B., Vieytes M.R., Yasumoto T., Botana, L.M. 2009. Ostreocin-D impact on globular actin of intactcells. *Chem. Res. Toxicol*. 22, 374–381.

Artigas P., Gadsby D. C. 2002. Ion channel-like properties of the Na^+/K^+ pump. *Ann. N. Y. Acad. Sci.* 976, 31-40.

Artigas P., Gadsby D. C. 2003a. Ion occlusion/deocclusion partial reactions in individual palytoxin-modified Na/K pumps. *Ann. N. Y. Acad*. 986, 116-126.

Artigas P., Gadsby D. C. 2003b. Na^+/K^+-ligands modulate gating of palytoxin-induced ion channels. *Proc. Natl. Acad. Sci. USA*. 100, 501-505.

Artigas P., Gadsby D. C. 2004. Large diameter of palytoxin-induced Na/K pump channels and modulation of palytoxin interaction by Na/K pump ligands. *J. Gen. Physiol.* 123, 357-376.

Attaway D. H., Ciereszko L. S. 1974. Isolation and partial characterization of Caribbean palytoxin. In: *Proceedings of the Second International Coral Reef Symposium*. 1, 497-504.

Bandi E., Bernareggi A., Grandolfo M., Mozzetta C., Augusti-Tocco G., Ruzzier F., Lorenzon P. 2005. Autocrine activation of nicotinic acetylcholine receptors contributes to Ca^{2+} spikes in mouse myotubes during myogenesis. *J. Physiol*. 568, 171-180.

Barone R. 2007. Behavioral trait of *Ostreopsis ovata* (Dinophyceae) in the Mediterranean rock pools: the spider strategy. *Harmful algal news*. 33, 1-3.

Barroso García P., Rueda de la Puerta P., Parrón Carreño T., Marín Martínez P., Guillén Enríquez J. 2008. Brote con síntomas respiratorios en la provincia de Almería por una posible exposición a microalgas tóxicas. *Gac. Sanit*. 22, 578-584.

Bellocci M., Ronzitti G., Milandri A., Melchiorre N., Grillo C., Poletti R., Yasumoto T., Rossini G. P. 2008. A cytolytic assay for the measurement of palytoxin based on a cultured monolayer cell line. *Anal Biochem*. 374, 48-55.

Bellocci M., Sala G. L. Prandi S. 2011. The cytolytic and cytotoxic activities of palytoxin. *Toxicon*. 57, 449-459.

Béress L., Zwick J., Kolkenbrock H. J., Kaul P. N., Wassermann O. 1983. A method for the isolation of the Caribbean palytoxin (C-PTX) from the coelenterate (zooanthid) *Palythoa caribaeorum*. *Toxicon*. 21, 285-290.

Bignami G. S., Raybould T.J., Sachinvala N.D., Grothaus P. G., Simpson S. B., Lazo C. B., Byrnes J. B., Moore R. E., Vann D. C. 1992. Monoclonal antibody-based enzyme-linked immunoassays for the measurement of palytoxin in biological samples. *Toxicon*. 30, 687-700.

Bignami G. S. 1993. A rapid and sensitive hemolysis neutralization assay for palytoxin. *Toxicon*. 31, 817-820.

Brescianini C., Grillo C., Melchiorre N., Bertolotto R., Ferrari A., Vivaldi B., Icardi G., Gramaccioni L., Funari E., Scardala S. 2006. Ostreopsis ovata algal blooms affecting human health in Genova, Italy, 2005 and 2006. *Euro Surveill.* 11(36), 3040**.**

Cagide E., Louzao M. C., Espiña B., Vieytes M. R., Jaen D., Maman L., Yasumoto T., Botana L. M. 2009. Production of Functionally Active Palytoxin-like compounds by Mediterranean *Ostreopsis* cf.*siamensis*. *Cell. Physiol. Biochem.* 23, 431-440.

Capetanaki Y., Bloch R. J., Kouloumenta A., Mavroidis M., Psarras S. 2007. Muscle intermediate filaments and their link to membrane and membranous organelles. *Experimental Cell Research*. 313, 2063-2076.

Ciminiello P., Dell'Aversano C., Fattorusso E., Forino M., Tartaglione L., Grillo C., Melchiorre N. 2008. Putative palytoxin and its new analogue, ovatoxin-a, in Ostreopsis ovata collected along the Ligurian coasts during the 2006 toxic outbreak. *J. Am. Soc. Mass. Spectrom.* 19, 111-20.

Ciminiello, P., Dell'Aversano, C., Dello Iacovo E., Fattorusso E., Forino M., Grauso L. Tartaglione L., Florio C., Lorenzon P., De Bortoli M., Tubaro A., Poli M., and Bignami G. 2009. Stereostructure and biological activity of 42-hydroxy-palytoxin: a new palytoxin analogue from Hawaiian *Palythoa* subspecies. *Chem. Res. Toxicol*. 22, 1851-1859.

Ciminiello P., Dell'Aversano C., Dello Iacovo E., Fattorusso E., Forino M., Grauso L., Tartaglione L., Guerrini F., Pistocchi R. 2010. Complex palytoxin-like profile of Ostreopsis ovata. Identification of four new

ovatoxins by high-resolution liquid chromatography/mass spectrometry.*Rapid Commun. Mass Spectrom.* 24, 2735-44.

Ciminiello P., Dell'Aversano C., Dello Iacovo E., Fattorusso E., Forino M., Tartaglione L. 2011. LC-MS of palytoxin and its analogues: state of the art and future perspectives. *Toxicon*. 57, 376-389.

Ciminiello P., Dell'Aversano C., Dello Iacovo E., Fattorusso E., Forino M., Grauso L., Tartaglione L., Guerrini F., Pezzolesi L., Pistocchi R., Vanucci S. 2012a. Isolation and structure elucidation of Ovatoxin-a, the major toxin produced by *Ostreopsis ovata*. *J. Am. Chem. Soc.* 134, 1869-1875.

Ciminiello P., Dell'aversano C., Dello Iacovo E., Fattorusso E., Forino M., Grauso L., Tartaglione L. 2012b. High Resolution LC-MS(n) Fragmentation Pattern of Palytoxin as Template to Gain New Insights into Ovatoxin-a Structure. The Key Role of Calcium in MS Behavior of Palytoxins. *J Am Soc Mass Spectrom.* [Epub ahead of print] DOI: 10.1007/s13361-012-0345-7.

Cha J., Christ W. J., Finan J. M., Fujioka H., Kishi Y., Klein L. L., Ko S. S., Leder J., McWhorter W. W. Jr., Pfaff K. P., Yonaga M., Uemura D., Hirata Y. 1982. Stereochemistry of Palytoxin. 4.[1]Complete structure. *J. Am. Chem. Soc.* 104, 7369-7371.

Chia D. G., Lau C. O., Ng P. K., Tan C. H. 1993. Localization of toxins in the poisonous mosaic crab, Lophozozymus pictor (Fabricius, 1798) (Brachyura, Xanthidae). *Toxicon.* 31, 901-904.

Coca R., Soler F., Fernández-Belda F. 2008. Chararacterization of the palytoxin effect on Ca^{2+}-ATPase from sarcoplasmic reticulum (SERCA). *Archives of Biochemistry and Biophysics*. 478, 36-42.

Contreras R. G., Flores-Maldonado C., Lázaro A., Shoshani L., Flores-Benitez D., Larre´I., Cereijido M. 2004.Ouabain Binding to Na^{+},K^{+}-ATPase Relaxes Cell Attachment and Sends a Specific Signal (NACos) to the Nucleus. *J. Membrane Biol*. 198, 147–158.

Deeds J.D.,Schwartz M., 2010. Human risk associated with palytoxin exposure. *Toxicon.* 56, 150-162.

Deeds J. R., Handy S. M., White K. D., Reimer J. D. 2011. Palytoxin Found in Palythoa sp. Zoanthids (Anthozoa, Hexacorallia) Sold in the Home Aquarium Trade. *PLOS one.* 6, 1-9.

Dell'Ovo V., Bandi E., Coslovich T., Florio C., Sciancalepore M., Decorti G., Sosa S., Lorenzon P., Yasumoto T., Tubaro A. 2008. *In vitro* effects of Yessotoxin on a primary culture of rat cardiomyocytes. *Toxicological Sciences.* 106, 392-399.

Deguchi T., Aoshima S., Sakai Y., Takamatsu S., Urakawa N. 1974. Pharmacological actions of palythoatoxin isolated from the zoanthid, *Palythoa tuberculosa*. *Jap. J. Pharmacol.* 24, (suppl.) 116P.

Deguchi T., Urakawa N., Takamatsu S. 1976. Some pharmacological properties of palythoatoxin isolated from the zoanthid, *Palythoa tuberculosa*.*In*: Animal Plant and Microbial Toxins, ed. By A. Ohsaka, K. Hayashi and Y. Sawai, vol, 2, 379-394, Plenum Press, New York.

Di Turi L., Lo Caputo S., Marzano M.C., Pastorelli A.M., Pompei M., Rositani L., Ungaro N., 2003. Ostropsidiaceae (Dynophyceae) presence along the coastal area of Bari. *Biol. Mar. Mediterr*. 10, 675-678.

Dubois J. M., Cohen J. B. 1977. Effect of palytoxin on membrane potential and current of frog myelinated fibers. *J. Pharmac. Exp. Ther.* 201, 148-155.

Ducret T., Vandebrouck C., Cao M. L., Lebacq J., Gailly P.2006. Functional role of store-operated and stretch activated channels in murine adult skeletal muscle fibers. *J. Physiol*. 575, 913-924.

Ducret T., Arrouchi J. E., Courtois A., Quignard J.F., Marthan R., Savineau J. P., 2010. Stretch-activated channels in pulmonary arterial smooth muscle cells from normoxic and chronically hypoxic rats. *Cell Calcium*. 48, 251-259.

Durando P., Ansaldi F., Oreste P., Moscatelli P., Marensi L., Grillo C., Gasparini R., Icardi G., 2007. *Ostreopsis ovata* and human health: epidemiological and clinical features of respiratory syndrome outbreaks from a two year syndromic surveillance, 2005-2006, in north-west Italy. *Euro Surveill.* 12 (23).

Ecault E., Sauviat M. P. 1991. Characterization of the palytoxin-induced sodium conductance in frog skeletal muscle. *Br. J. Pharmacol*. 102, 523-529.

EFSA Panel on Contaminants in the Food Chain (CONTAM); Scientific Opinion on marine biotoxins in shellfish – Palytoxin group.

EFSA Journal 2009; 7(12):1393. [38 pp.]. doi:10.2903/j.efsa.2009.1393.

EFSA Panel on Contaminants in the Food Chain (CONTAM); Statement on further elaboration of theconsumption figure of 400 g shellfish meat on the basis of new consumption data. EFSA Journal 2010; 8(8):1706. [20 pp.]. doi:10.2903/j.efsa.2010.1706.

Faimali M., Giussani V., Piazza V., Garaventa F., Corrà C., Asnaghi V., Privitera D., Gallus L., Cattaneo-Vietti R., Mangialajo L., Chiantore M. 2011. Toxic effect of the harmful benthic dinoflagellate *Ostreopsis ovata* on vertebrate and invertebrate marine organisms. *Marine Environmental Research*. doi:10.1016/j.marenvres.2011.09.010.

Farley R. A., Schreiber S., Wang S. G., Scheiner-Bobis G. 2001. A hybrid between Na^+/K^+ ATPase and H^+/K^+ ATPase is sensitive to palytoxin, ouabain and SCH28080. *The Journal of Biological Chemistr.* 276, 2608-2615.

Faust A. M., Morton S. L., Quod J. P. 1996. Further SEM study of marine dinoflagellates: the genus *Ostreopsis* (Dinophyceae). *J. Phycol.* 32, 1053-1065.

Finney D. J. 1971. Statistical aspects of monitoring for dangers in drug therapy. *Methods Inf. Med.* 10, 1-8.

Fleming L. E., Kirkpatrick B., Backer L. C., Bean J. A., Wanner A., Reich A., Zaias J., Cheng Y. S., Pierce R., Naar J., Abraham W. M., Baden D. G. 2007. Aerosolized red-tide toxins (brevetoxins) and asthma. *Chest*. 131, 187-194.

Flockerzi V., Oeken H. J., Hofmann F., Pelzer D., Cavalié A., Trautwein W. 1986.Purified dihydropyridine-binding site from skeletal muscle t-tubules is a functional calcium channel. *Nature*. 323, 66-68.

Formigli L., Meacci E., Sassoli C., Squecco R., Nosi D., Chellini F., Naro F., Francini F., Zecchi-Orlandini S. 2007. Cytoskeleton/stretch-activated ion channel interaction regulates myogenic differentiation of skeletal myoblasts. *J Cell Physiol*. 211, 296-306.

Franchini A., Casarini L., Malagoli D., Ottavini E. 2009. Expression of the genes *siamois*, *engrailed-2*, *bmp4* and *myf5* during *Xenopus* development in presence of the marine toxins okadaic acid and palytoxin. *Chemosphere*. 77, 308-312.

Frolova G. M., Kuznetsova T. A., Mikhailov V. V., Eliakov G. B. 2000. Immunoenzyme method for detecting microbial producers of palytoxin. *Bioorg. Khim*. 26, 315-320.

Frelin C., Vigne P., Breittmayer J.P. 1990. Palytoxin acidifies chick cardiac cells and activate the Na/H antiporter. *FEBS Lett.* 264,63-66.

Frelin C., Vigne P., Breittmayer J.P. 1991. Mechanism of cardiotoxic action of palytoxin. *Molecular Pharmacology*. 38, 904-909.

Frelin C., Van Renterghem C. 1995. Palytoxin. Recent Electrophysiological and Pharmacological Evidence for Several Mechanisms of Action. *Gen. Pharmac*. 26, 33-37.

Fujioka H., Christ W. J., Cha J. K., Leder J., Kishi Y., Uemura D., Hirata Y. 1982. Stereochemistry of Palytoxin. 3.[1]C7-C51 Segment. *J. Am. Chem. Soc.* 104, 7367-7369.

Fujiki H., Suganuma M., Nakayasu M., Hakii H., Horiuchi T., Takayama S., Sugimura T. 1986. Palytoxin is a non-12-*O*-tetradecanoylphorbol-13-acetate type tumor promoter in two stage mouse skin carcinogenesis. *Carcinogenesis*. 7, 707-710.

Fukui M., Murata M., Inoue A., Gawel M., Yasumoto T. 1987. Occurrence of palytoxin in the trigger fish *Melichtys vidua*. *Toxicon.* 25, 1121-1124.

Fukuio Y., 1981. Taxonomical study of benthic dinoflagellates, collected in coral reef. *Bull. Jap. Soc. Sci. Fish.* 47,967-978.

Fusetani N., Sato S., Hashimoto K., 1985. Occurrence of a water soluble toxin in a parrotfish (*Ypsiscarus ovifrons*) which is probably responsible for parrotfish liver poisoning. *Toxicon.* 23, 105-112.

Gallitelli M., Ungaro N., Addante L. M., Gentiloni Silver M. Sabbà C. 2005. Respiratory illness as a reaction to tropical algal blooms occurring in a temperate climate. *JAMA*. 293, 2599-2600.

Gleibs S., Mebs D., Werding B., 1995. Studies on the origin and distribution of palytoxin in a Caribbean coral reef. *Toxicon*. 33, 1531-1537.

Gleibs S., Mebs D. 1999. Distribution and sequestration of palytoxin in coral reef animals. *Toxicon*. 37, 1521-1527.

Gonzales R. B., Alcala A. C. 1977. Fatalities from crab poisoning on Negros Island, Philippines. *Toxicon*. 15, 169-170.

Granéli E., Vidyarathna N.K., Funari E., Cumaranatunga P.R.T., Scenati R., 2011. Can increases in temperature stimulate blooms of the toxic benthic dinoflagellate Ostreopsis ovata? *Harmful Algae*. 10, 165-172.

Guerrini F., Pezzolesi L., Feller A., Riccardi M., Ciminiello P., Dell'Aversano C., Tartaglione L., Dello Iacovo E., Fattorusso E., Forino M., Pistocchi R. 2010. Comparative growth and toxin profile of cultured Ostreopsis ovate from the Tyrrhenian and Adriatic Seas. *Toxicon*. 55, 211-220.

Geunnoun S., Horisberger J. D. 2000. Structure of the 5^{th} transmembrane segment of the Na,K-ATPase α subunit: a cysteine scanning mutagenesis study. *FEBS Letters*. 482, 144-148.

Habermann E., Chhatwal G. S. 1982. Ouabain inhibits the increase due to palytoxin of cation permeability of erythrocytes. *Naunyn Schmiedebergs Arch.Pharmacol.* 319, 101-107.

Habermann E. 1983. Action and Binding of Palytoxin, as Studied with Brain Membranes.*Naunyn-Schmiedeberg's Arch. Pharmacol.* 323, 269-275.

Habermann E. 1989. Palytoxin acts through Na^+, K^+-ATPase. *Toxicon.* 27, 1175-1187.

Hamill O., McBride D. W. 1996. The pharmacology of mechanogated membrane ion channels. *Pharmacol Rev*. 48, 231-252.

Hirata Y., Uemura D., Ueda K., Takano S. 1979. Several compounds from *Palythoa tuberculosa* (Coelenterata). *Pure appl. Chem.* 51, 1875-1883.

Hoffmann K., Hermanns-Clausen M., Buhl C., Buchler M.W., Schemmer P., Mebs D., Kauferstein S. 2008. A case of palytoxin poisoning due to contact with zoanthid corals through skin injury. *Toxicon.* 51, 1535-1537.

Honsell G., De Bortoli M., Boscolo S., Dell'Aversano C., Battocchi C., Fontanive G., Penna A., Berti F., Sosa S., Yasumoto T., Ciminiello P., Poli M., Tubaro A. 2011. Harmful Dinoflagellate Ostreopsis cf. ovata Fukuyo: Detection of Ovatoxins in Field Samples and Cell Immunolocalization Using Antipalytoxin Antibodies. *Environmental Science and Technology*. 45, 7051-7059.

Hori M., Shimizu K., Nakajyo S., Urakawa N. 1988. Palytoxin-induced K^+ efflux from ileal longitudinal smooth muscle of guinea-pig. *Japan. J. Pharmacol*. 46, 285-292.

Horisberger J. D., Kharoubi-Hess S., Guennoun S., Michielin O. The fourth transmembrane segment of the Na,K-ATPase α subunit. *The Journal of Biological Chemistry*. 279, 29542-29550.

Horisberger J. D. 2004b. Recent insight into the structure and the mechanism of the sodium pump. *Physiology*. 19, 377-387.

Ichida S., Tawada E., Watanebe Y., Minami S., Horiba M., 1988. Two cases of rhabdomyolysis induced by parrotfish liver poisoning. *Kidney & Dialysis (Japan)* 25, 541-544.

Irintchev A., Langer M., Zweyer M., Theisen R., Wernig A. 1997. Functional improvement of damaged adult mouse muscle by implantation of primary myoblasts. *J Physiol*. 500, 775–85.

Ishida Y., Shibata S., Satake N., Habon J., Kitano K. 1981. Inhibitory effects of ouabain on the palytoxin-induced contraction of human umbilical artery. *Blood vessels.* 18, 216.

Ishida Y., Takagi K., Takahashi M., Satake N., Shibata S. 1983. Palytoxin isolated from marine Coelenterates the inhibitory action on the (Na,K)-ATPase.1983. *The Journal of Biological Chemistry*. 258, 7900-7902.

Ishida Y., Kajiwara A., Takagi K., Ohizumi Y.,Shibata S. 1985. Dual effect of ouabain on the palytoxin-induced contraction and norepinephrine release in guinea-pig vas deferens. *Journal of Pharmacology and Experimental Therapeutics*. 232, 551-556.

Ishii K., Ito K. M., Uemura D., Ito K. 1997. Possible mechanism of palytoxin-induced Ca^{2+} mobilization in porcine coronary artery. *Journal of Pharmacology and Experimental Therapeutics*. 281, 1077-1084.

Inuzuka T., Fujisawa T., Arimoto H., Uemura D. 2007. Molecular shape of palytoxin in aqueous solution. *Organic & Biomolecular Chemistry*. 5, 897-899.

Ito E., Ohkusu M., Yasumoto T. 1996. Intestinal injuries caused by experimental palytoxicosis in mice. *Toxicon*. 34, 643-652.

Ito E., Ohkusu M., Terao K., Yasumoto T. 1997. Effects of repeated injections of palytoxin on lymphoid tissues in mice. *Toxicon*. 35, 679-688.

Ito E., Yasumoto T. 2009.Toxicological studies on palytoxin and ostreocin-D administered to mice by three different routes. *Toxicon*. 54, 244-251.

Ito K., Karaki H., Ishida Y., Urakawa N., Deguchi T. 1976. Effects of palytoxin on isolated intestinal and vascular smooth muscles. *Japan. J. Pharmacol*. 26, 683-692.

Ito K., Karaki H., Urakawa N. 1977. The mode of contractile action of palytoxin on vascular smooth muscles. *Japan. J. Pharmacol*. 46, 9-14.

Ito K., Karaki H., Urakawa N. 1979. Effects of palytoxin on mechanical and electrical activities of guinea pig papillary muscle. *Japan. J. Pharmacol*. 29, 467-476.

Ito K., Urakawa N., Koike H. 1982. Cardiovascular toxicity of palytoxin on anesthetized dogs. *Arch. Int. Pharmacodyn.* 258, 146-154.

Ito K., Toyoda I., Higashiyama M., Uemura D., Sato M. H., Yoshimura S. H., Ishii T., Takeyasu K. 2003. Channel induction by palytoxin in yeast cells expressing Na^+,K^+-ATPase or its chimera with sarco/endoplasmic reticulum Ca^{2+}-ATPase. *FEBS Letters*. 543, 108-112.

Jaradat Z. W., Viià B., Marquardt R. R. 2006. Adverse effects of T-2 toxin on chicken lymphocytes blastogenesis and its protection with Vitamin E. *Toxicology*. 225, 90-96.

Jared S. R., Rao J. P., Subramani S. 2009. Action of antidiuretic hormone analogues on intact and nystatin-permeabilized frog skins. *Exp. Physiol.* 94, 1174-1184.

Karaki H., Nagase H., Ohizumi Y., Satake N., Shibata S. 1988. Palytoxin-induced contraction and release endogenous noradrenaline in rat tail artery. *Br. J. Pharmacol*. 95, 183-188.

Kaul P. N., Farmer M. R., Ciereszko L. S. 1974. Pharmacology of palytoxin: the most potent marine toxin known. *Proc. West. Pharmacol. Soc.* 17, 294-301.

Kaul P. N. 1981. Compounds from the sea with actions on the cardiovascular and central nervous system. *Pharmacology of marine natural products federation proceedings*. 40, 10-14.

Kerbrat A. S., Amzil Z., Pawlowiez R., Golubic S., Sibat M., Darius H. T, Chinain M., Laurent D. 2011. First Evidence of Palytoxin and 42-Hydroxy-palytoxin in the Marine Cyanobacterium *Trichodesmium*. *Marine Drugs*. 9, 543-560.

Kermarec F., Dor F., Armengaud A., Charlet F., Kantin R., Sauzade D., de Haro L. 2008. Health risks related to *Ostreopsis ovata* in recreational waters. *Env. Risques Santé.* 7, 357-363.

Kim S. Y., Marx K. A., Wu C. H. 1995. Involvement of the Na,K-ATPase in the induction of ion channels by palytoxin. *Naunyn-Schmiedeberg's Arch. Pharmacol.* 351, 542-554.

Kimura S., Hashimoto Y. 1973. Purification of toxin in a zooanthid *Palythoa tuberculosa*. *Publs. Seto. Mar. biol. Lab.* 20, 713-718.

Kinoshita K., Ikeda M., Ito K. 1991. Properties of Palytoxin induced whole current in single rat ventricular myocytes. *Naunyn-Schmiedeberg's Arch Pharmacol*. 344, 247-251.

Kishi Y. 1989. Natural product synthesis: palytoxin. *Pure & Appl. Chem.* 61, 313-324.

Kockskämper J., Ahmmed G. U., Zima A. V., Sheehan K. A., Glitsch H. G., Blatter L. A. 2004. Palytoxin disrupts excitation-contraction coupling through interactions with P-type ion pumps. *Am. J. Physiol. Cell. Physiol.* 287, 527-538.

Kodama A.M., Hokam, Y., Yasumoto T., Fukui M., Manea S.J., Sutherland N. 1989. Clinical and laboratory findings implicating palytoxin as cause of ciguatera poisoning due to *Decapterus macrosoma* (mackerel). *Toxicon.* 27, 1051-1053.

Kudo Y., Shibata S. 1980. The potent depolarizing action of palytoxin isolated from *Palythoa tubercurosa* on the isolated spinal cord of the frog. *Br. J. Pharmacol.* 71, 575-579.

Kuroki D. W., Bignami G. S., Wattenberg E. V. 1996. Activation of stress-activated protein kinase/c-Jun N-terminal kinase by the non-TPA-type tumor promoter palytoxin. *Cancer Research*. 56, 637-644.

Lau C. O., Tan C. H., Khoo H. E., Yuen R.., Lewis R. J., Corpuz G. P., and Bignami G. S. 1995. *Lophozozymus pictor* toxin: a fluorescent structural isomer of palytoxin. *Toxicon*. 33, 1373-1377.

Lenoir S., Ten-Hage L., Turquet J., Quod P. J., Bernard C., Hennion M. C. 2004. First evidence of palytoxin analogues from an *Ostreopsis mascarenensis* (Dinophyaceae) benthic bloom in southwestern Indian Ocean. *Journal of Phycology*. 40, 1042-51.

Llewellyn L.E., 2001. Human fatalities in Vanuatu after eating a crab (*Daira perlata*). *Med. J. Australia.* 175, 343-344.

Lorenzon P., Bernareggi A., Degasperi V., Nurowska E., Wernig A., Ruzzier F. 2002. Properties of primary mouse myoblasts expanded in culture. *Experimental Cell Research*. 278, 84-91.

Louzao M. C., Vieytes M. R., Yasumoto T., Yotsu-Yamashita M., Botana L. M. 2006. Changes in membrane potential: an early signal triggered by neurologically active phycotoxins. *Chem. Res. Toxicol.* 19, 788-793.

Louzao M. C., Ares I. R., Vieytes M. R., Valverde I., Vieites J. M., Yasumoto T., Botana L. M. 2007. The cytoskeleton, a structure that is susceptible to the toxic mechanism activated by palytoxins in human excitable cells. *The FEBS Journal.* 274, 1991-2004.

Louzao M. C., Espiña B., Cagide E., Ares I. R., Amparo A., Vieytes M., Botana L. M. 2010. Cytotoxic effect of palytoxin on mussels. *Toxicon*. 56, 842-847.

Louzao M. C., Ares I. R., Cagide E., Espiña B., Vilariño N., Alfonso A., Vieites J. M., Botana L. M.2011. Palytoxins and cytoskeleton: an overview. *Toxicon*. 57, 460-469.

Luin E., Ruzzier F. 2007. The role of L- and T-type Ca^{2+} currents during the *in vitro* aging of murine myogenic (i28) cells in culture. *Cell Calcium*. 41, 479-489.

Mahmud Y., Arakawa O., Noguchi T., 2000. An epidemic survey on the freshwater puffer poisoning in Bangladesh. *J. Nat. Toxins*. 9, 319-326.

Mahnir V. M., Kozlovskaya E. P., Kalinovsky A. I. 1992. Sea anemone *Radianthus macrodactylus*_a new source of palytoxin. *Toxicon*. 30, 1449-1456.

Majlesi N., Su M.K., Chan G.M., Lee D.C., Greller H.A. 2008. A case of inhalational exposure to palytoxin. *Clin. Toxicol*. 46, 637.

Malagoli D., Casarini L., Ottavini E. 2008. Effect of the marine toxins okadaic acid and palytoxin on mussel phagocytosis. *Fish and Shellfish Immunology*. 24, 180-186.

Mangialajo L., Bertolotto R., Cattaneo-Vietti R., Chiantore M., Grillo C., Lemee R., Melchiorre N., Moretto P., Povero P., Ruggieri N. 2008. The toxic benthic dinoflagellate *Ostreopsis ovata*: quantification of proliferation along the coastline of Genoa, Italy. *Mar. Poll. Bull.* 56, 1209-1214.

Martins A. S., Shkryl V. M., NowyckyM. C., Shirokova N. 2008. Reactive oxygen species contribute to Ca^{2+} signals produced by osmotic stress in mouse skeletal muscle fibres. *J. Physiol.* 586, 197–210.

Mebs. D. 1998. Occurrence and sequestration of toxins in food chains. *Toxicon*. 36, 1519-1522.

Mlinan B., Enyeart J. J. 1993. Block of current through T-type calcium channels by trivalent metal cations and nickel in neural rat and human cells. *J. Physiol*. 469, 639-652.

Molgó J., del Pozo E., Baños J.E., Angaut-Petit D. 1991. Changes of quantal transmitter release caused by gadolinium ions at the frog neuromuscular junction. *Br. J. Pharmacol*. 104, 133-8.

Monti M., Minocci M., Beran A., Iveša L. 2007. First record of *Ostreopsis* cfr. *ovata* on macroalgae in the Northern Adriatic Sea. *Mar. Poll. Bull.* 54, 598-601.

Moore R.E., Scheuer P.J. 1971. Palytoxin: a new marine toxin from a coelenterate. *Science* , 172, 495-498.

Moore R. E., Bartolini G. 1981. Structure of palytoxin. *J.Am.ChemSoc.*, 103, 2491.

Moore R. E. 1982. Toxins, anticancer agents and tumor promoters from marine prokaryotes. *Pure & Appl. Chem*. 54, 1919-1934.

Moore R.E., Helfrich P., Patterson G.M.L., 1982. The deadly seaweed of Hana. *Oceanus.* 25, 54-63.

Morita K., Teraoka K., Oka M., Levine M. 1996. Inhibitory action of palytoxin on ascorbic acid transport into cultured bovine adrenal chromaffin cells. *The Journal of Pharmacology and Experimental Therapeutics*. 276, 996-1001.

Moshirfar M., Khalifa Y.M., Espandar L., Mifflin M.D. 2010. Aquarium coral keratoconjunctivitis. *Arch. Ophthalmol*. 128, 1360-1362.

Munday, R., 2008. Occurrence and toxicology of palytoxin. *In*: Botana, L.M. (Ed.), Seafood and Freshwater Toxins. Pharmacology, Physiology and Detection. CRC Press, Boca Raton, pp. 693–713.

Munday R. 2011. Palytoxin toxicology: animal studies. *Toxicon*. 57, 470-477.

Muramatsu I., Uemura D., Fujiwara M., Narahashi T. 1984. Characteristics of palytoxin-induced depolarization in squid axons. *The Journal of Pharmacology and Experimental Therapeutics*. 231, 488-494.

Muramatsu I., Nishio M., Kigoshi S., Uemura D. 1988. Single ionic channels induced by palytoxin in guinea-pig ventricular myocytes. *Br. J. Pharmacol*. 93, 811-816.

Naro F., De Arcangelis V., Coletti D., Molinaro M., Zani B., Vassanelli S., Reggiani C., Teti A., Adamo S. 2003. Increase in cytosolic Ca^{2+} induced by elevation of the extracellular Ca^{2+} in skeletal myogenic cells. *Am J Physiol Cell Physiol*. 284, 969-976.

Noguchi T., Hwang D.F., Arakawa O., Daigo K., Sato S., Ozaki H., Kawai N., Ito M., Hashimoto K. 1987. Palytoxin as the causative agent in the parrotfish poisoning. In: Gopalakrishnakone, P., Tan, C.K. (Eds.), Progress in Venom and Toxin Research: Proceedings of the first

Asia-Pacific Congress on Animal, Plant and Microbial Toxins, Faculty of Medicine, National University of Singapore, pp. 325-335.

Nordt S.P., Wu J., Zahller S., Clark R.F., Cantrell F.L., 2011. Palytoxin poisoning after dermal contact with zoanthid coral. *J. Emerg. Med.* 40, 397-399.

Ohizumi Y., Shibata S. 1980. Mechanism of the excitatory action of palytoxin and N-acetylpalytoxin in the isolated guinea-pig vas deferens. *Journal of Pharmacology and Experimental Therapeutics*. 214, 209-212.

Oku N., Sata N. U., Matsunaga S., Uchida H., Fusetani N. 2004. Identification of palytoxin as a principle which causes morphological changes in rat 3Y1 cells in the zoanthid *Palythoa* aff. *margaritae*. *Toxicon*. 43, 21-25.

Okano H., Masuoka H., Kamei S., Seko T., Koyabu S., Tsuneoka K., Tamai T., Ueda K., Nakazawa S., Sugawa M., Suzuki H., Watanabe M., Yatani R., Nakano T. 1998. Rhabdomyolysis and myocardial damage induced by palytoxin, a toxin of blue humphead parrotfish. *Int. Med*. 37, 330-333.

Onuma, Y., Satake, M., Ukena, T., Roux, J., Chanteau, S., Rasolofonirina, N., Ratsimaloto, M., Naoki, H., Yasumoto, T. 1999. Identification of putative palytoxin as the cause of clupeotoxism. *Toxicon.* 37, 55-65.

Ozaki H., Tomono J., Nagase H., Ito K., Urakawa N. 1983. The mechanism of contractile action of palytoxin on vascular smooth muscle of guinea-pig aorta. *Japan J. Pharmacol*. 33, 1155-1162.

Pelin M., Zanette C., De Bortoli M., Sosa S., Della Loggia R., Tubaro A., Florio C. 2011. Effects of the marine toxin palytoxin on human skin keratinocytes: role of ionic imbalance. *Toxicology*. 282, 30-38.

Pelin M., Sosa S., Della Loggia R., Poli M., Tubaro A., Decorti G., Florio C. 2012. The cytotoxic effect of palytoxin on Caco-2 cells hinders their use for *in vitro* absorption studies. *Food Chem. Toxicol.*50, 206-211.

Penna, A., Vila, M., Fraga, S., Giacobbe, M. G., Andreoni, F., Riobò, P., Vernesi, C. 2005. Characterization of Ostreopsis and Coolia (Dinophyceae) isolates in the Western Mediterranean Sea based on morphology, toxicity and internal transcribed spacer 5.8S rDNA sequences. *J. Phycol*. 41, 212-225.

Pérez-Gómez A., Novelli A., Fernández-Sánchez M. T. 2010. .Na+/K+-ATPase inhibitor palytoxin enhances vulnerability of cultured cerebellar neurons to domoic acid via sodium-dependent mechanisms. *J Neurochem*. 114, 28-38.

Pezzolesi L., Guerrini F., Ciminiello P., Dell'Aversano C., Dello Iacovo E., Fattorusso E., Forino M., Tartaglione L., Pistocchi R. 2012. Influence of temperature and salinity on *Ostreopsis* cf. *ovata* growth and evaluation of toxin content through HR LC-MS and biological assays. *Water research*. 46, 82-92.

Plenge-Tellechea F., Soler F., Fernandez-Belda F. 1997. On the inhibition mechanism of sarcoplasmic or endoplasmic reticulum Ca2+-ATPases by cyclopiazonic acid. *J Biol Chem*. 272, 2794-800.

Prandi S., Sala G. L., Bellocci M., Alessandrini A., Facci P., Bigiani A., Rossini G. P. 2011. Palytoxin Induces Cell Lysis by Priming a Two-Step Process in MCF-7 Cells. *Chem. Res. Toxicol.* 24, 1283-1296.

Rayner M. D., Sanders B. J., Harris S.M., Lin Y. C., Morton B. E. 1975. Palytoxin: effects on contractility and $^{45}Ca^{2+}$ uptake in isolated ventricle strips. *Research Communications in Clinical Pathology and Pharmacology*. 11, 55-64.

Redondo J., Fiedler B., Scheiner-Bobis G. 1996. Palytoxin-induced Na^{+} influx into yeast cells expressing the mammalian sodium pump is due to the formation of a channel within the enzyme. *Molecular pharmacology*. 49, 49-57.

Rhodes L., Towers N., Briggs L., Munday R., Adamson J. 2002. Uptake of palytoxin-like compounds by shellfish fed *Ostreopsis siamensis* (Dinophyceae). *New Zealand Journal of Marine and Freshwater Research*. 36, 631-636.

Riobò P., Paz B., Franco J. M. 2008a. Analysis of palytoxin-like in *Ostreopsis* cultures by liquid chromatography with precolumn derivatization and fluorescence detection. *Analytica Chimica Acta*. 566, 217-223.

Riobò P., Paz B., Franco J. M., Vázquez J. A., Murado M. A., Cacho E. 2008b. Mouse bioassay for palytoxin. Specific symptoms and dose

response against dose-death time relationship. *Food and Chemical Toxicology*. 46, 2639-2647.

Riobò P., Franco J. M. 2011. Palytoxins: biological and chemical determination. *Toxicon*. 57, 368-375.

Robinson C. P., Franz D. R. 1991. Effects of palytoxin on guinea pig tracheal strips. *Pharm. Res*. 8, 859-864.

Robinson C. P., Franz D. R., Bondura M. E.1992. Effects of palytoxin on porcine coronary artery rings. *J. Appl. Toxicol.*12, 185-189.

Rossi R, Castellano V, Scalco E, Serpe L, Zingone A, Soprano V. 2010. New palytoxin-like molecules in Mediterranean Ostreopsis cf. ovata (dinoflagellates) and in *Palythoa tuberculosa* detected by liquid chromatography-electrospray ionization time-of-flight mass spectrometry. *Toxicon*. 56, 1381-1387.

Rossini G.P. and Bigiani A. 2011. Palytoxin action on the Na(+),K(+)-ATPase and the disruption of ion equilibria in biological systems. *Toxicon*. 57, 429-439.

Sala G. L., Bellocci M., Rossini G. P. 2009. The Cytotoxic Pathway Triggered by Palytoxin Involves a Change in the Cellular Pool of Stress Response Proteins. *Chem. Res. Toxicol*. 22, 2009–2016.

Sagara T., Nishibori N., Itoh M., Morita K., Her S. 2011. Palytoxin causes non oxidative necrotic damage to PC12 cells in culture. *Journal of Applied Toxicology*. DOI 10. 1002/jat.1728.

Sansoni G., Borghini B., Camici G., Casotti M., Righini P., Rustighi C. 2003. Fioriture algali di *Ostreopsis ovata* (Gonyaulacales: Dinophyceae): un problema emergente. *Biologia ambientale*. 17, 17-23.

Sauviat M. P., Pater C., Berton J. 1987. Does palytoxin open a sodium-sensitive channel in cardiac muscle? *Toxicon*. 25, 695-704.

Sauviat M. P. 1989. Effect of PLTX on the calcium current and the mechanical activity of frog heart muscle. *Br. J. Pharmacol.* 98, 773-780.

Schmidt J. 1901. Peridiniales. *Bot. Tidsskr*. 24, 212-221.

Scheiner-Bobis G. Meyer zu Heringdorf D., Christ M., Habermann E. 1994. Palytoxin induces K^+ efflux from yeast cells expressing the mammalian sodium pump. *Molecular pharmacology*. 45, 1132-1136.

Scheiner-Bobis G. 1996.The sodium pump. *Eur. J. Biochem.* 269, 2424-2433.

Scheiner-Bobis G., Schneider H. 1997. Palytoxin-induced channel formation within the Na^+/K^+-ATPase does not require a catalytically active enzyme. *Eur. J. Biochem.* 248, 717-723.

Scheiner-Bobis G., Hübschle T., Diener M. 2002. Action of palytoxin on apical H^+/K^+ ATPase in rat colon. *Eur. J. Biochem*. 269, 3905-3911.

Seemann P., Gernert C., Schmitt S., Mebs D., Hentschel U. 2009. Detection of hemolytic bacteria from *Palythoa caribaeorum* (Cnidaria, Zoantharia) using a novel palytoxin-screening assay. *Antonie van Leeuwenhoek*. 96, 405–411.

Sheridan R. E., Deshpande S. S., Adler M. 2005. Cytotoxic action of palytoxin on aortic smooth muscle cells in culture. *J. Appl. Toxicology*. 25, 365-373.

Shinazato T., Furusu A., Nishino T., Abe K., Kanda T., Maeda T., Kohno S., 2008. Cowfish (Umisuzume, *Lactoria diaphana*) poisoning with rhabdomyolysis. *Int. Med.* 47, 853-856.

Shimizu Y., 1983. Complete structure of palytoxin elucidated. *Nature*. 302, 212.

Shkryl V. M., Martins A. S., Ullrich N. D., Nowycky M. C., Niggli E., Shirokova N. 2009. Reciprocal amplification of ROS and Ca^{2+} signals in stressed mdx dystrophic skeletal muscle fibers. *Pflugers Arch - Eur J Physiol*. 458, 915–928.

Skou J.,C. 1957. The influence of some cations on adenosinetriphosphatase from peripheral nerves. *Biochim. Biophys. Acta*. 23, 394–401.

Sosa S., Del Favero G., De Bortoli M., Vita F., Soranzo M. R., Beltramo D., Ardizzone M., Tubaro A. 2009. Palytoxin toxicity after acute oral administration in mice. *Toxicology Letters*. 191, 253-259.

Tabata H., Nanjo K., Kokuoka H., Machida K., Miyamura K. 1989. Two cases of fish poisoning caused by ingesting parrot fish. *Int. Med.* 64, 974-977.

Tan C.T.T., Lee E.J.D., 1988. A fatal case of crab toxin (*Lophozozymus pictor*) poisoning. *Asia Pacific J. Pharmacol.* 3, 7-9.

Taniyama S., Mahmud Y., Tanu M. B., Takatani T., Arakawa O., Noguki, T. 2001. Delayed haemolytic activity by the freshwater puffer *Tetraodon* sp. Toxin. *Toxicon.* 39, 725-727.

Taniyama S., Mahmud Y., Terada M., Takatani T., Arakawa O., Noguki, T. 2002. Occurrence of a food poisoning incident by PLTX from a serranid *Epinephelus sp.* in Japan. *J. Nat. Toxins.* 11, 277-282.

Taniyama S., Arakawa O., Terada M., Nishio S., Takatani T., Mahmud Y., Noguchi T. 2003. *Ostreopsis* sp., a possible origin of palytoxin (PTX) in parrotfish *Scarus ovifrons*. *Toxicon*. 42, 29-33.

Taylor F. J. R. 1979. A description of the benthic dinoflagellate associated with maitotoxin and ciguatoxin, including observations on Hawaiian material. *In*: Taylor, D.L., Seliger, H.H. (Eds.), *Toxic Dinoflagellate Blooms*. Elsevier/North-Holland, New York, pp. 71–76.

Taylor T. J., Parker J. W., Fajer A. J., Mereish K. A. 1991. Non-specific binding of palytoxin to plastic surfaces. *Toxicology letters*. 57, 291-296.

Terao K., Ito E., Yasumoto T. 1992. Light and electron microscopic observation of experimental palytoxin poisoning in mice. *Bull. Soc. Path. Ex.* 85, 494-496.

Tichadou L., Glaizal M., Armengaud A., Grossel H., Lemée R., Kantin R., Lasalle J.-L., Drouet G., Rambaud L., Malfait P., De Haro L. 2010. Health impact of unicellular algae of the *Ostreopsis* genus blooms in the Mediterranean Sea: experience of the French Mediterranean coast surveillance network from 2006 to 2009. *Clin. Toxicol*. 48, 839-844.

Tognetto L., Bellato S., Moro I., Andreoli C. 1995. Occurrence of*Ostreopsis ovata* (Dinophyceae) in the Tyrrhenian Sea during summer
1994. *Bot. Mar.* 38, 291–295.

Totti C., Cucchiari E., Romagnoli T., Penna A. 2007. Bloom of *Ostreopsis ovata* on the Conero riviera (NW Adriatic Sea). *Harmful Algae News*. 33, 12–13.

Traub P., Nelson W. J. 1981. Occurrence in various mammalian cells and tissues of the Ca^{2+} activated protease specific for the intermediate-sized filament proteins vimentin and desmin. *Eur. J. Cell. Biol*. 26, 61-67.

Tubaro A., Durando P., Del Favero G., Ansaldi F., Icardi G., Deeds J. R., Sosa S. 2011a. Case definitions for human poisonings postulated to palytoxins exposure. *Toxicon*. 57, 478-95.

Tubaro A., Del Favero G., Beltramo D., Ardizzone M., Forino M., De Bortoli M., Pelin M., Poli M., Bignami G., Ciminiello P., Sosa S. 2011b. Acute oral toxicity in mice of a new palytoxin analog: 42-hydroxy-palytoxin. *Toxicon*. 57, 755-763.

Uemura D., Ueda K. , Hirata Y., Naoki H. and Iwashita T. 1981. Structure of palytoxin *Tetrahedron Letters*. 22, 2781.

Uemura D., Hirata Y., Iwashita T., Naoki H. 1985. Studies on palytoxins. *Tetrahedron*. 41, 1007-1017.

Uemura D. 2006. Bioorganic studies on marine natural products-Diverse chemical structures and bioactivities. *The chemical record*. 6, 235-248.

Usami M., Satake M., Ishida S., Inoue A., Kan Y. and Yasumoto T. 1995. Palytoxin analogs from the dinoflagellate Ostreopsis siamensis. *J. Am. Chem. Soc*. 117, 5389–5390

Ukena T., Satake M., Usami T., Oshima Y., Fujita T., Kan Y., Yasumoto T. 2001. Structure elucidation of Ostreocin-D, a palytoxin analog isolated from the dinoflagellate *Ostreopsis siamensis*. *Bioscience, Biotechnology and Biochemistry*. 65, 2585-2588.

Vale C., Alfonso A., Suñol C., Vieytes M. R.., Botana L. M. 2006. Modulation of calcium entry and glutamate release in cultured cerebellar granule cells by palytoxin. *Journal of Neuroscience Research*. 83, 1393-1406.

Vale-Gonzáles C., Gómez-Lima B., Vieytes M. R.., Botana L. M. 2007. Effects of the marine phycotoxin palytoxin in neuronal pH in primary cultures of cerebellar granule cells. *Journal of Neuroscience Research*. 85, 90-98.

Valverde I., Lago J., Reboreda A., Vieites J. M. Cabado A. G. 2008. Characteristics of palytoxin-induced cytotoxicity in neuroblastoma cells. *Toxicology in Vitro.* 22, 1432-1439.

Valverde I., Lago J., Vieites J. M. Cabado A. G. 2008. *In vitro* approaches to evaluate palytoxin-induced toxicity and cell death in intestinal cells. *J. Appl. Toxicol.* 28, 294-302.

Van Renterghem C., Frelin C. 1993. 3,4-Dichlorobenzamil-sensitive, monovalent cation channel induced by palytoxin in cultured aortic myocytes. *Br. J. Pharmacol.* 109, 859-865.

Vasconcelos V., Azevedo J., Silva M., Ramos V. 2010. Effects of Marine Toxins on the Reproduction and Early Stages Development of Aquatic Organisms. *Marine Drugs*. 8, 59-79.

Vick J. A., Wiles J. S. 1975. The mechanism of action and treatment of palytoxin poisoning. *Toxicology and applied pharmacology*. 34, 214-223.

Vila M., Garcés E., Masò M., 2001. Potentially toxic epiphytic dinoflagellate assemblages on macroalgae in the NW Mediterranean. *Aq. Microb. Ecol*., 26, 51–60.

Wachi K. M., Hokama Y., Haga L. S., Shiraki A., Takenaka W.E., Bignami G.S., Levine L. 2000. Evidence for palytoxin as one of the sheep erythrocyte lytic in lytic factors in crude extracts of ciguateric and non-ciguateric reef fish tissue.*J. Nat. Toxins*. 9, 139-146.

Walker N. M., Simpson J. E., Levitt R.C., Boyle K. T., Clarke L. L. 2006. Talniflumate increases survival in a cystic fibrosis mouse model of distal intestinal obstructive syndrome.*J Pharmacol Exp Ther*. 317, 275-83.

Wang Y. C., Huang R. C. 2006. Effects of the sodium pump activity on spontaneous firing in neurons of the rat suprachiasmatic nucleus. *J. Neurophysiol.* 96, 109-118.

Wattenberg E. 2007. Palytoxin: exploiting a novel skin tumor promoter to explore signal transduction and carcinogenesis. *Am. J. Physiol. Cell. Physiol.* 292, 24-32.

Wiles J. S., Vick J. A., Christenson M. K. 1974. Toxicological evaluation of palytoxin in several animal species. *Toxicon*. 12, 427-433.

Wu C. H. 2009. Palytoxin: membrane mechanism of action. *Toxicon*. 54, 1183-1189.

Yasumoto T., Yasumura D., Ohizumi Y., Takahashi M., Alcala A. C., Alcala L. C. 1986. Palytoxin in two species of xanthid crab from the Philippines. *Agric. Biol. Chem.* 50, 163-167.

Yoshimine K., Orita S., Okada S., Sonoda K., Kubota K., Yonezawa T. 2001. Two cases of parrotfish poisoning with rhabdomyolysis. *J. Jap. Soc. Int. Med.* 90, 1339-1341.

Zingone A., Siano R., D'Alelio D., Sarno D. 2006. Potentially toxic and harmful microalgae from coastal waters of the Campania region (Tyrrhenian Sea, Mediterranean Sea*). Harmful Algae*. 5, 321–337.

Giorgia Del Favero: peer reviewed publications (2009-2011)

Tubaro A., **Del Favero G.**, Beltramo D., Ardizzone M., Forino M., De Bortoli M., Pelin M., Poli M., Bignami G., Ciminiello P., Sosa S. Acute oral toxicity in mice of a new palytoxin analog: 42-hydroxy-palytoxin. *Toxicon*. 57 (5): 755-63 (2011).

Tubaro A., Durando P., **Del Favero G.**, Ansaldi F., Icardi G., Deeds J. R., Sosa S. Case definitions for human poisonings postulated to palytoxins exposure. *Toxicon*. 57 (3): 478-95 (2011).

Sosa S., **Del Favero G.**, De Bortoli M., Vita F., Soranzo M.R., Beltramo D., Ardizzone M., Tubaro A. Palytoxin toxicity after acute oral administration in mice. *Toxicol Lett.* 191(2-3):253-9 (2009).

Ringraziamenti ***Acknowledgments***

Nello sviluppo di questa tesi sono stata guidata da tanti preziosi consigli e supportata da importanti collaborazioni, per questo desidero ringraziare:

Le mie due relatrici, la Prof.ssa Aurelia Tubaro e la Prof.ssa Paola Lorenzon.

Il Dr. Silvio Sosa e la Dr. Chiara Florio del Dipartimento di Scienze della Vita, Università degli Studi di Trieste.

Il Dr. Dario Beltramo dell'Istituto di Ricerche Biomediche "Antoine Marxer" RBM (Colleretto Giacosa).

Il Prof. Orfeo Sbaizero e la Dr. Barbara Codan del Dipartimento di Ingegneria Industriale e dell'Informazione, Università degli Studi di Trieste.

La Dr. Emanuela Testai dell'Istituto Superiore di Sanità (Roma).

La Prof.ssa Patrizia Ciminiello, il Prof. Ernesto Fattorusso e il loro gruppo di ricerca del Dipartimento di Chimica delle Sostanze Naturali dell'Università di Napoli "Federico II".

Il Prof. Jordi Molgo del Laboratoire Neurobiologie et Développement, C.N.R.S., Institut Fédératif de Neurobiologie Alfred Fessard.

Il Dr. Mark Poli della Integrated Toxicology Division, U.S. Army Medical Research Institute of Infectious Diseases (Fort Detrick).

Il Prof. Takeshi Yasumoto del Japan Food Research Laboratories, Tama Laboratory (Tokyo).

Un ringraziamento particolare va alle persone che in questi tre anni hanno condiviso con me la vita di laboratorio, considero un onore potervi chiamare "Amici" e non semplicemente "colleghi".